DOE/MC/29248 -- 5595
(DE97002242)

Kinetic Inhibition of Natural Gas Hydrates in Offshore Drilling, Production and Processing

Annual Report
January 1 - December 31, 1992

Work Performed Under Contract No.: DE-FG21-92MC29248

For
U.S. Department of Energy
Office of Fossil Energy
Morgantown Energy Technology Center
P.O. Box 880
Morgantown, West Virginia 26507-0880

By
Center for Hydrate Research
Colorado School of Mines
Golden, Colorado 80401

Disclaimer

II. Table of Contents

III. INTRODUCTION

III.A. Statement of the Problem

Natural gas hydrates are solid crystalline compounds which form when molecules smaller than n-butane contact molecules of water at elevated pressures and reduced temperatures, both above and below the ice point. Because these crystalline compounds plug flow channels, they are undesirable, so that every attempt is made to prevent hydrates from forming large masses.

In pipeline and processing operations the ambient operating conditions (low temperature and high pressure) are very conducive to hydrate formation. In the history of hydrate prevention, four classical means have been used to prevent hydrate formation:

1. Removal of free and dissolved water from the hydrocarbon.
2. Increasing the temperature above the formation point.
3. Reducing the pressure below the formation point.
4. Injection of inhibitors (typically methanol or ethylene glycol) to shift the thermodynamic equilibrium formation conditions.

Frequently the above four traditional (thermodynamic) approaches may not be viable due to extreme conditions or high cost, such as offshore or remote multiphase production systems, or those systems where environment/safety concerns mitigate methanol disposal/storage. In this project we proposed an alternate approach of controlling hydrate formation by preventing hydrate growth into a sizeable mass which could block a flow channel. We call this new technique kinetic inhibition, because

while it allows the system to exist in the hydrate domain, it prevents the kinetic agglomeration of small hydrate crystals to the point of pluggage of a flow channel. → go to p. 6.

During project DEA-30, we modified 1 echanism for hydrate formation from ice, (Sloan ar l) to define a mechanism for hydrate formation from liquid water. During the final year of the DEA-30 project, particularly in the thesis work of Müller-Bongartz (1990), we made measurements on hydrates which support the hypothesized mechanism described below.

Figure 1 is a depiction of the progress of molecular species from water [A], to unstable species [B] and [C], to stable nuclei [D] which will grow to larger crystal masses. A thorough explanation of Figure 1 is given in Sloan and Fleyfel (*AIChE J*, 37(9), 1281, (1991)) provided in Appendix A of the previous DEA-62/CEA-20 Annual Report; only a brief overview is given here. When the nucleation period starts, liquid water and gas are in the system. These two phases interact with each other and form clusters of both large and small hydrate-like cages in structures I and II ([B]). At this point the structures are long-lived but unstable. The cages may either dissipate or grow to hydrate unit cells or agglomerations of unit cells ([C]), thus forming metastable nuclei. Since these metastable unit cells are of subcritical size, they may grow or shrink. The metastable nuclei are in equilibrium with the cages until the nuclei reach the critical radius, thus becoming stable. The stable crystals ([D]) indicate the onset of catastrophic growth, or agglomerations which could cause the pluggage of a flow channel.

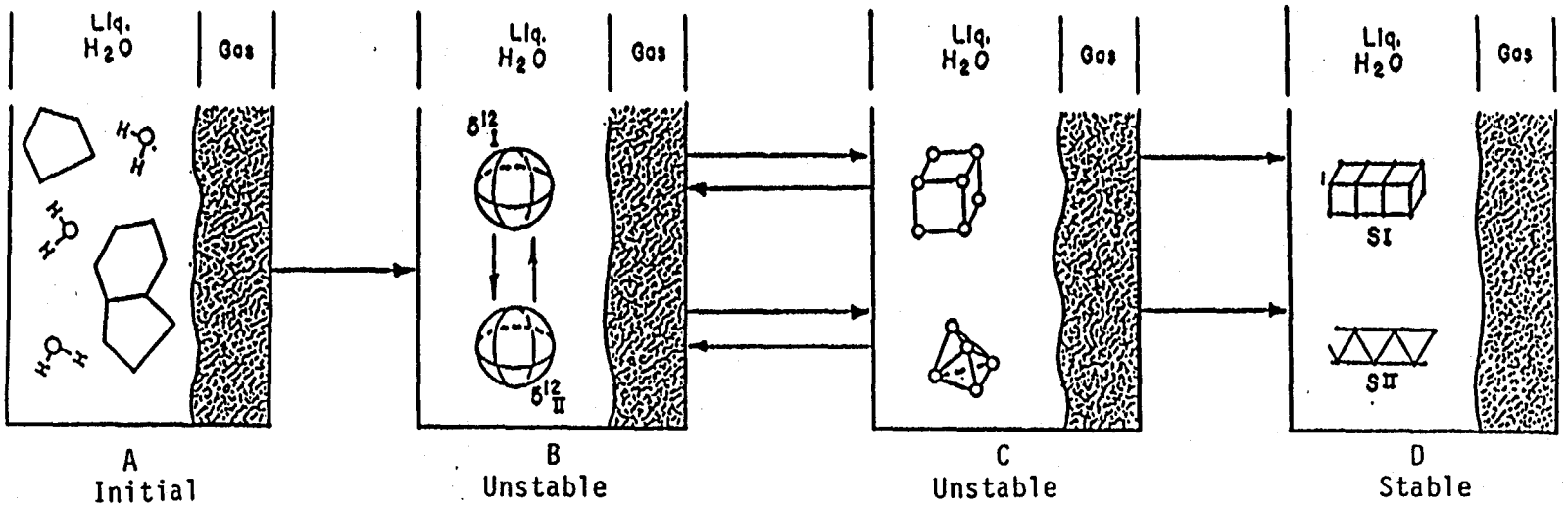

Physics of a Mechanism for Hydrate Formation from Water

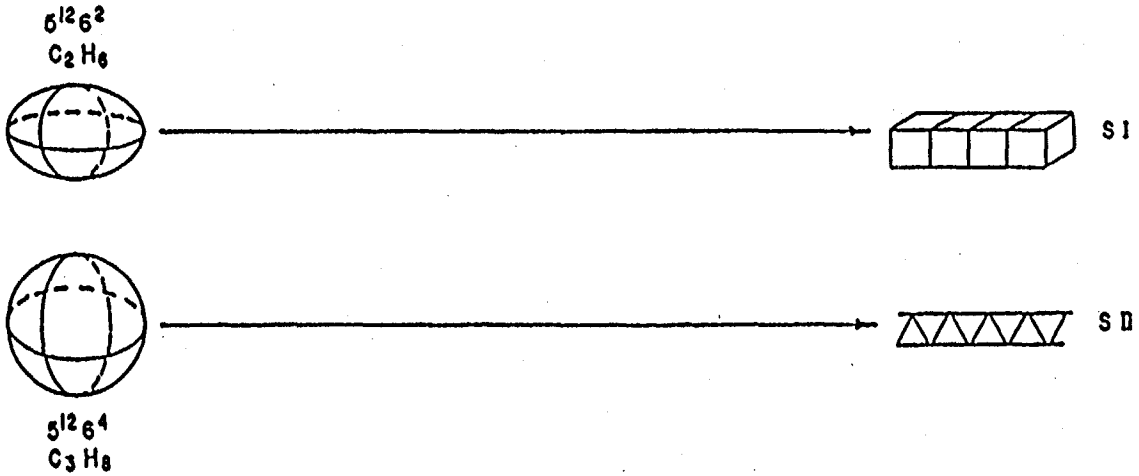

During DEA-30 in our laboratory, Müller-Bongartz determined fundamental variables which control the hydrate formation process as well as the variables which did not affect hydrate formation. Further we were able to determine two spectroscopic means of identifying molecular species such as those in the above mechanism. However, the above mechanism must still be regarded as tentative, pending further refinement.

The real importance of such a molecular mechanism is that it allows the proposal of new means of hydrate prevention. For example, if hydrate formation is the joining of cavities, such as those shown in Figure 1b, then an inhibition mechanism might involve the prevention of that joining. Since the cavities themselves are of very small size (≤ 10Å), they should flow freely in any fluid phase without obstructing flow channels.

The logical extension of the hypothesized mechanism would suggest that a surfactant or a polymer may be effective in hydrate prevention. For example, if a surfactant or polymer attached to the hydrate crystal surface, such attachments might block a preferred growth direction of the hydrate crystal or prevent the attachment of two small crystals. Such ideas are new and outside of the four classical thermodynamic prevention means on the previous page of this report. The new ideas however form the foundation of the work on this project.

III.B. What Was Proposed?

In order to investigate the kinetic means of inhibiting hydrate formation, we held two consortium meetings, on June 1,

1990 and on August 31, 1990. As a result of those first meetings the following companies became participants in the project: ARCO, Amoco, BP America, Chevron, Conoco, Department of Energy, Exxon, Mobil, Oryx, Petrobras, Shell and Texaco. At subsequent meetings, we determined the following four stages of the project, necessary to reach the goal of determining a new hydrate field inhibitor:

1. A rapid screening method was to be determined for testing the hydrate kinetic formation period of many surfactants and polymer candidates (both individually and combined). The present report presents the success of two screening apparatuses: a multi-reactor apparatus which is capable of rapid, high volume screening, and the backup screening method - a viscometer for testing with gas at high pressure.
2. The construction of two high, constant pressure cells were to experimentally confirm the success of the chemicals in the rapid screening apparatus. At the same time we were to perform a hydrate computer simulation and Raman spectroscopic study of formation with the objective of formulating a molecular hydrate formation model which would perhaps lead to a mathematical description of inhibition.
3. In the third phase of the work, Exxon volunteered to evaluate the performance of the best chemicals from the previous two stages in their 4 inch I.D. multiphase flow loop in Houston.
4. In the final phase of the work, our intention was to take the successful kinetic inhibition chemicals from the previous three stages and then test them in the field in gathering lines and wells from member companies.

I.B.1. What are the Deliverables?

There are three deliverables from the project:

A. Measurements and Modelling. The object of the study is to provide data on the best hydrate formation kinetic inhibitors. All of the data obtained in the study will be made available in both hardcopy and ASCII files (if appropriate) to each participating company. We will provide each participant with computer codes and videotapes of hydrate formation generated in this work.

B. Reports and Proprietary Agreements. Each year we provide member companies with annual reports of the work. We have obtained permission from the CSM faculty to have a proprietary agreement for non-exposure of this work for one year after its completion.

C. A Common Basis for Examining Results and Field Tests. We hold consortium meetings at least twice each year to review the work and to propose the next stages of work. For new company representatives, we invited attendance at our normal semi-annual consortium meetings at least one-half day early, to provide an understanding of phenomena to be held common by participants. When the consortium members hold a similar understanding of hydrates, it should enable the sharing of information determined in field tests, on Exxon's flow loop with our suggestions of chemicals, as well as the determinations of our laboratory.

While the project was intended for research in the laboratory, it can also be the basis for a forum of sharing results from field tests of the best chemical inhibitors.

III.C. What Was Done in 1990/1991?

During the first 15 months of the project (September 1, 1990 to December 31, 1991) we had the following five major accomplishments:

1. We tried three means to rapidly screen hydrate kinetic inhibitors, with success in the final, viscometer method.
2. We generated a multiple reactor rapid-screening technique which will allow testing ≤ 1000 hydrate inhibitors per year.
3. We tested approximately 50 hydrate kinetic inhibitor combinations, and we determined several likely candidates.
4. We modified our two high pressure apparatuses, determined some principal operating variables, and established the water baseline on one apparatus.
5. We simulated the first stages of hydrate formation on the computer, as water clusters around apolar molecules.

III. D. What was Projected for 1992?

In the 1990-1991 "First 15 Months" Report, we reported the following goals for 1992:

1. Screen 1000 inhibitor variations of inhibitor chemicals including various combinations, concentrations, etc.
2. Determine the reproducibility of the two high pressure apparatuses and the transferability from the screening

apparatus.

3. Measure the rate of hydrate formation (on the high pressure apparatus) with and without inhibitors.

4. Simulate the ice-water interface and the hydrate-water interface, in preparation for inserting a computer-simulated surfactant or polymer at that interface. A video was to be be made of molecular motion in the simulation.

5. During the winter of 1992, testing of several inhibitors was to be done on pipelines operated by member companies.

IV. WHAT WAS ACCOMPLISHED IN 1992?

IV.A. Inhibitor Screening Methods

IV.A.1. Multiphase Viscometer: A Backup Screening Method

A high pressure apparatus was constructed to screen hydrate inhibitors using the viscometer shown in Figure 2. The viscometer contained a piston which was impelled through the measurement chamber via magnetic coils. The time for the piston to move up and down in the measurement chamber was an indication of viscosity. The hydrate formers used were carbon dioxide and the Green Canyon gas whose composition is given in the High Pressures Apparatus (Section IV.B.) of this report. Carbon dioxide was used initially to develop the experimental procedure.

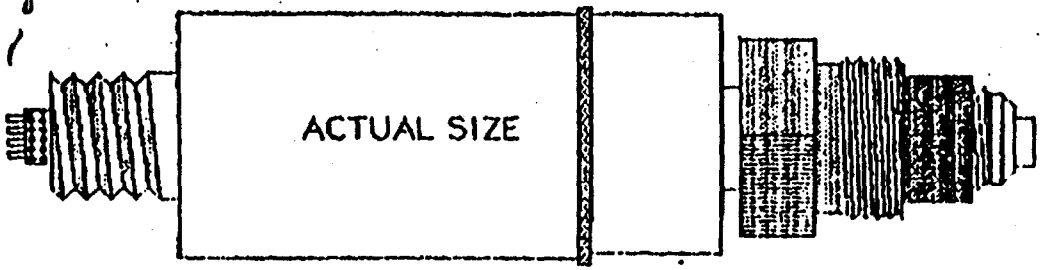

Figure 2. Viscometer Used as Backup Screening Apparatus

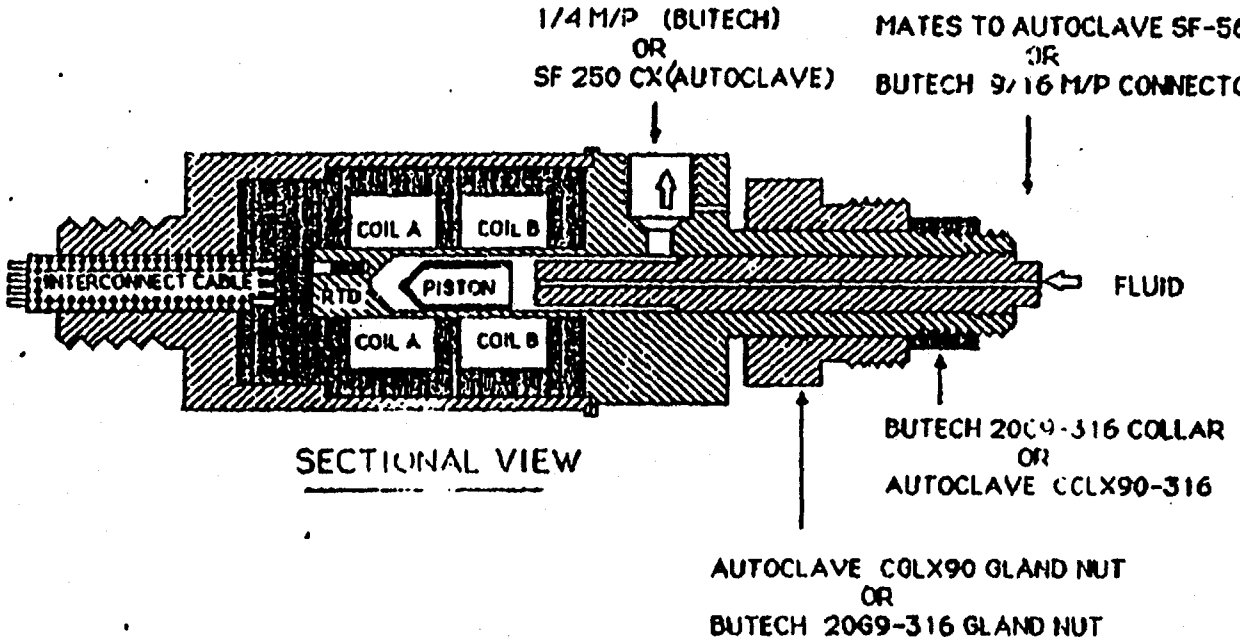

SECTIONAL VIEW

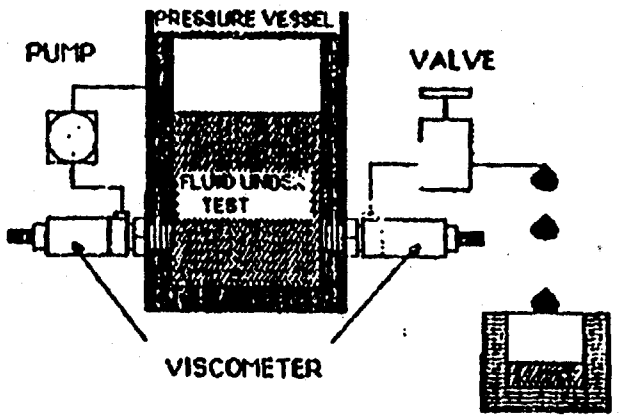

UNSPECIFIED TOLERANCES MECHANICAL X +-.015 XX +-.010 XXX +-.005 ANGLES +-1DEG INTERNAL RADII .010" DIMENSIONS IN INCHES ELECTRICAL RESISTORS +-10%,1/8W CAPACITORS +-10%	SCALE: 1:1 DRAFTER: DATE: 4MAY89 CHECKER: DATE: ENG: DATE: MFG: DATE: QC: DATE: MATERIAL: 11 [illegible] 718	Cambridge Applied Systems Incorporated 57 Smith Place, Cambridge, MA 02138 (617) 576-7700 TITLE: PISTON SENSOR MODEL SPL-340 SMALL SAMPLE VOLUME, HIGH PRESSURE ELECTROMAGNETIC VISCOMETER NUMBER: 91241 REV FILE P340ILLUS

Hydrate formation was indicated by a sharp rise in viscosity.

For this experiment the viscometer was mounted vertically as depicted in Figure 3. Fluid was then added to the measurement chamber at a level so that the piston would disrupt the liquid-gas interface at the top of its stroke. To begin the experiment the viscometer is kept above 80°F until the circulation system is activated. Once circulation is begun, the temperature will drop to a low value, either 32.5°F for carbon dioxide, or to 40.5°F for the Green Canyon Gas. Viscosity and temperature are recorded as the viscometer cools, and hydrate formation is noted by a sharp increase in viscosity and a small temperature rise, as shown in Figure 4 at approximately 1200 seconds for Green Canyon Gas and ASTM sea water.

Reproducibility of hydrate formation for carbon dioxide and de-ionized water is shown in Figure 5 and for Green Canyon gas and ASTM sea water in Figure 6; Figure 7 demonstrates the inhibition of hydrate formation for the same gas when 0.5 wt% PVP is added to ASTM sea water. At around 3200 seconds the viscosity begins a slow rise indicating initial nucleation, and at about 18,000 seconds the viscosity rises sharply indicating rapid growth of hydrates. The viscosity rise probably represents solids forming in the gas around the piston. At times we have observed some unusual viscosity traces which we believe could be more certainly interpreted with a transparent viscometer chamber. Comparisons of induction times for the viscometer, the screening apparatus and the high pressure apparatus are shown in Table 1. The results for the inhibitors show good agreement among the

Figure 3.

VISCOSITY EXPERIMENT FOR SENSING HYDRATE FORMATION KINETICS

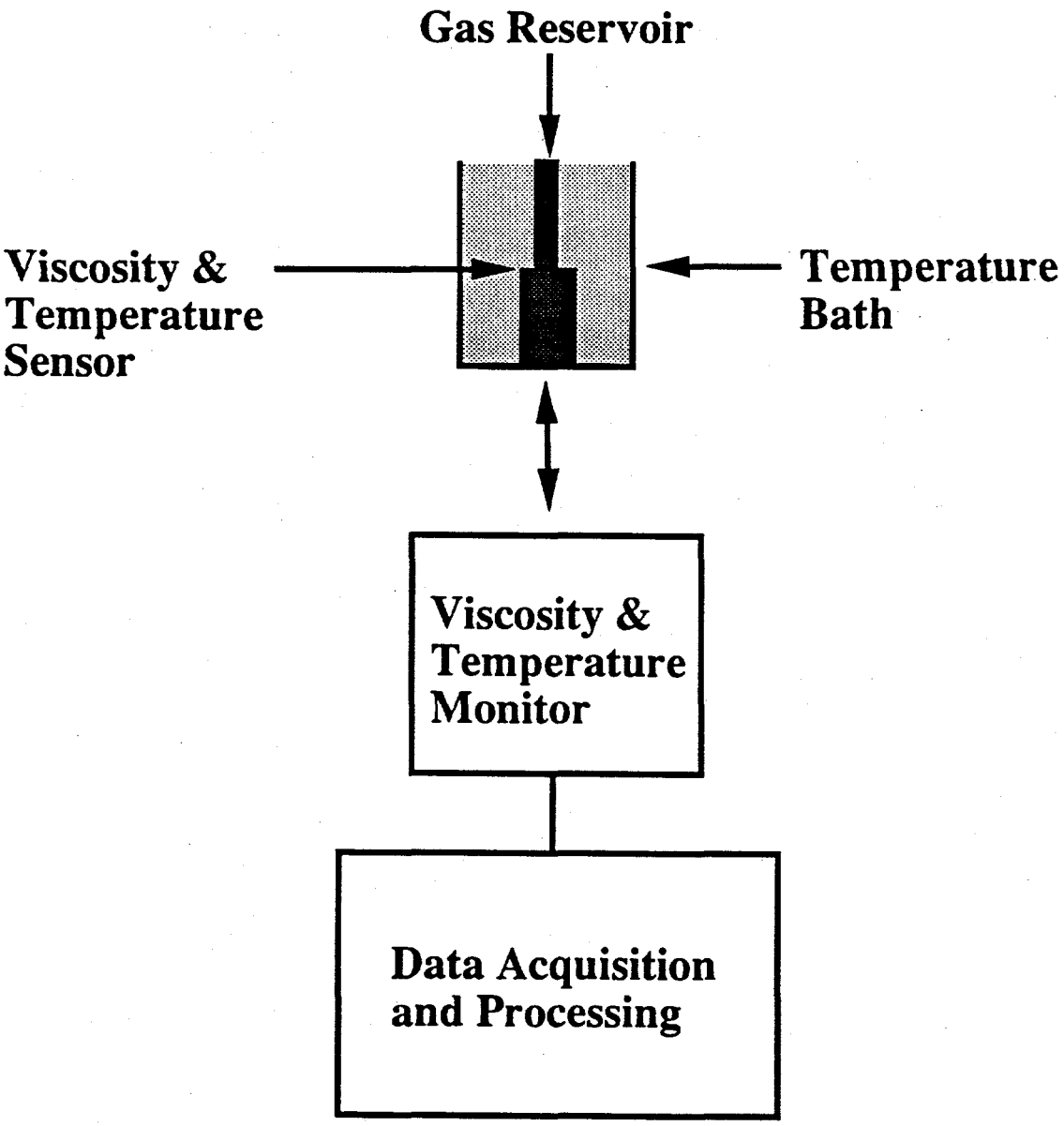

Figure 4. Viscosity and Temperature Changes Upon Hydrate Formation in Viscometer

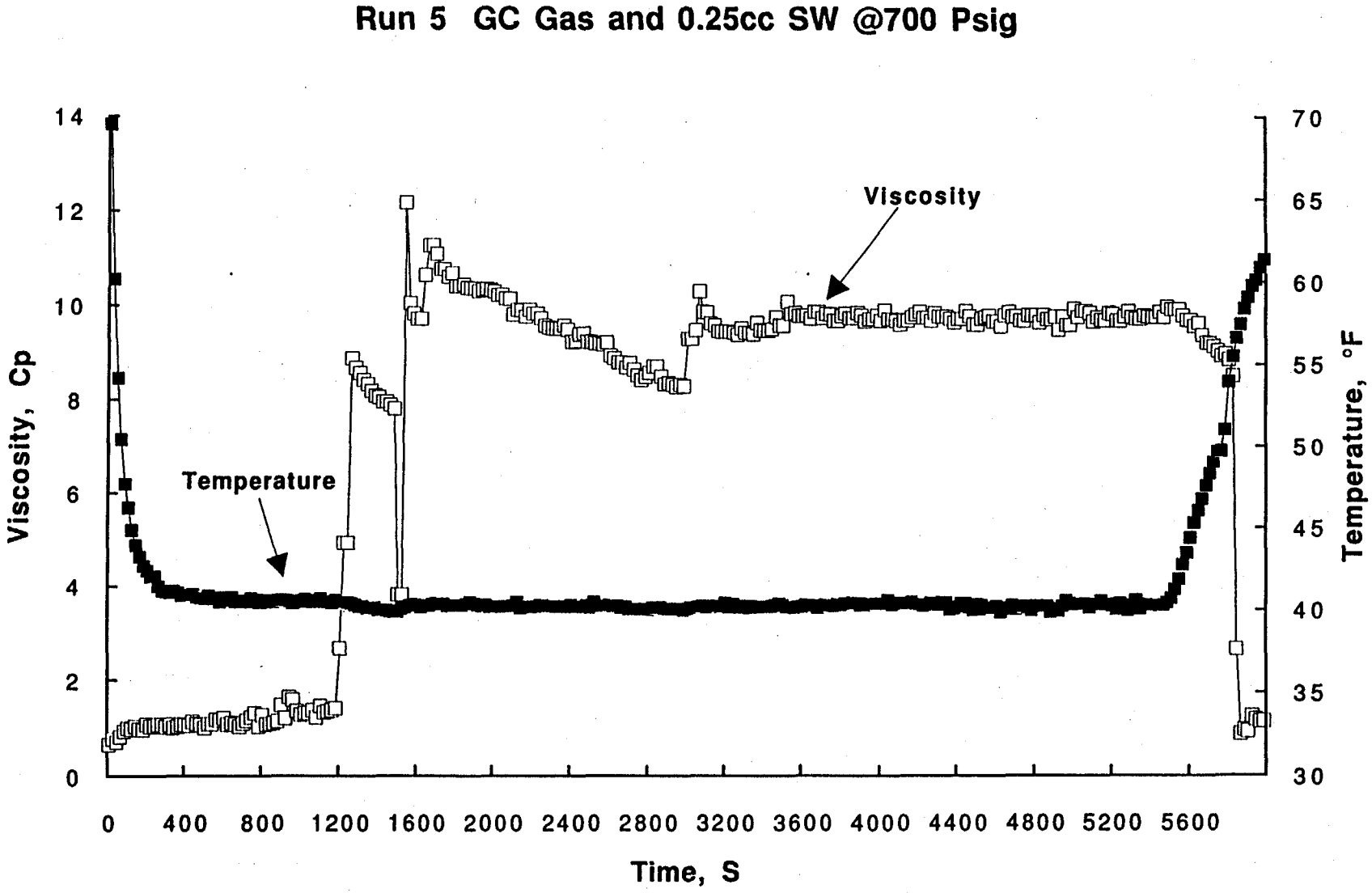

Figure 5. Viscometer Hydrate Formation for Carbon Dioxide and De-Ionized Water

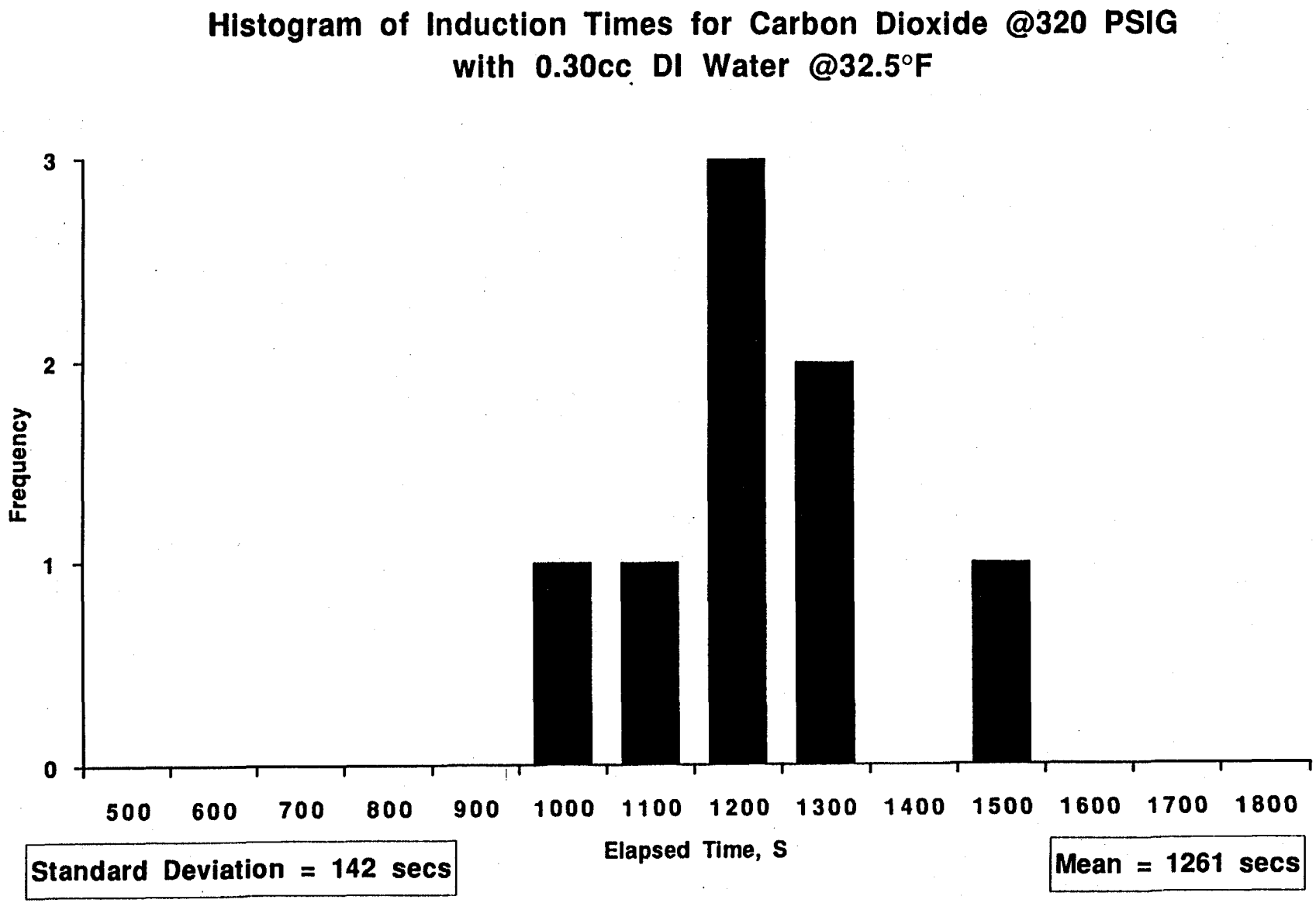

Figure 6. Viscometer Hydrate Formation for Green Canyon Gas with ASTM Sea Water

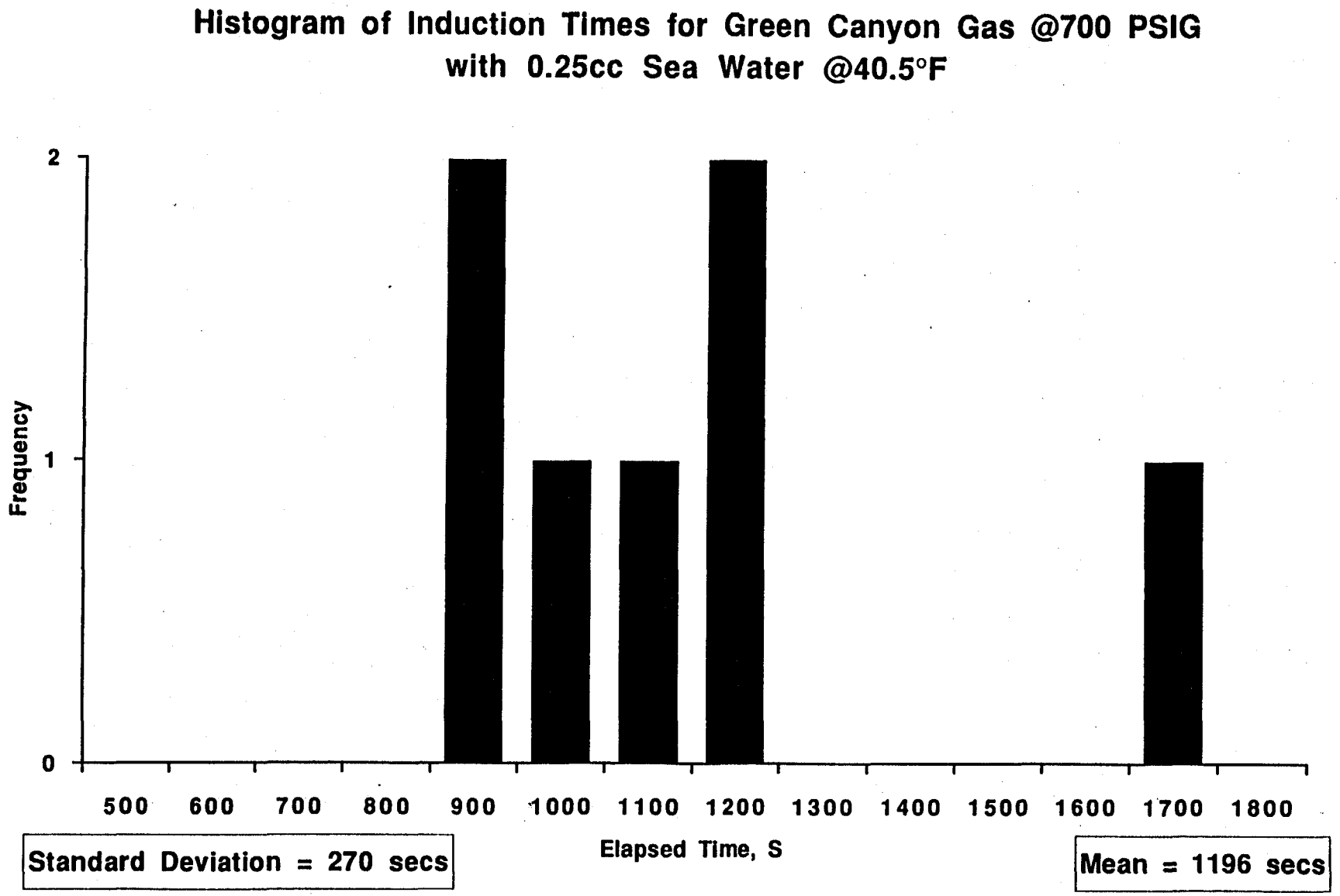

Figure 7. Viscometer Hydrate Formation for Green Canyon Gas with 0.5 wt% PVP

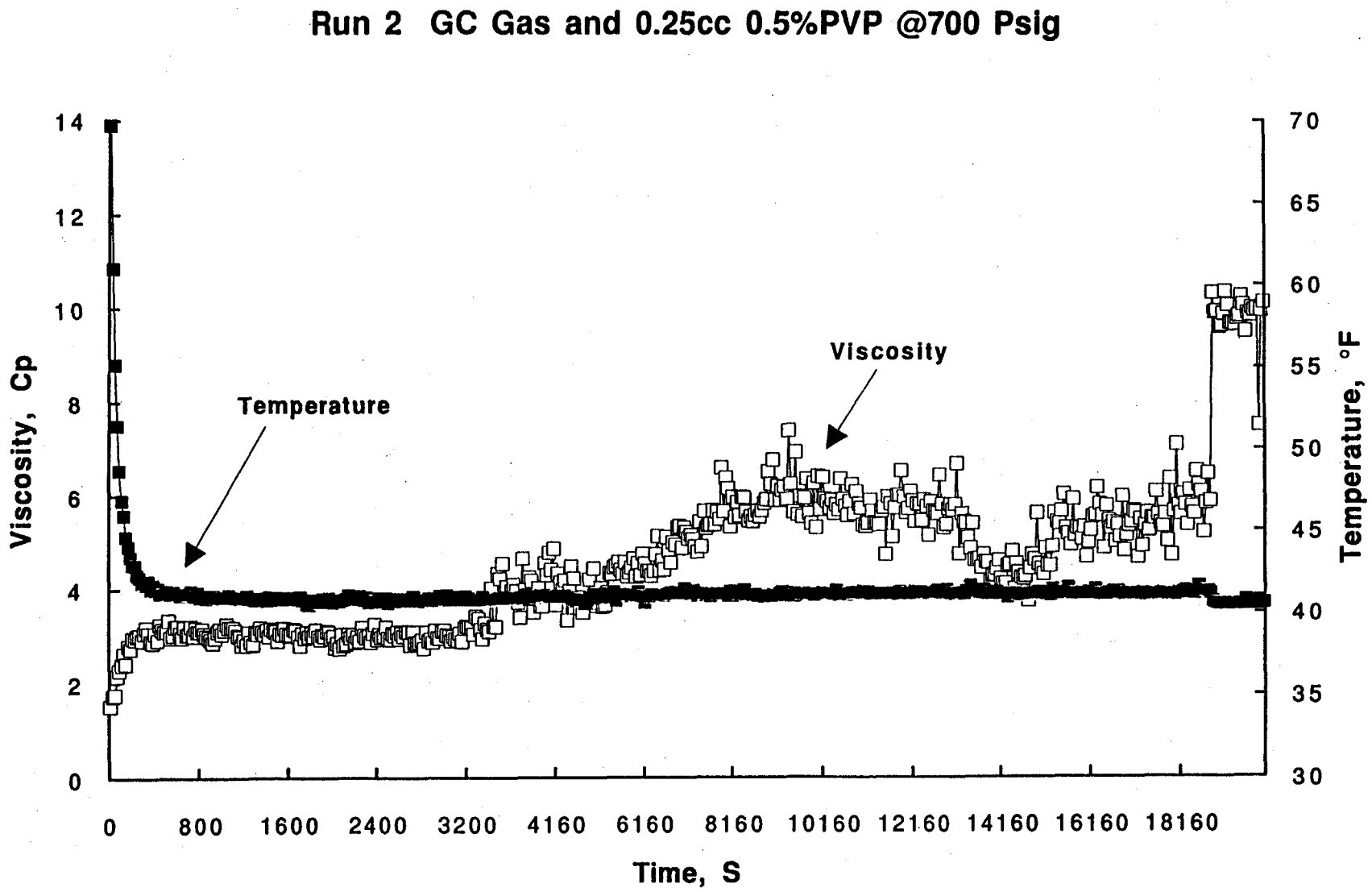

Table 1.

Comparisons with Other Apparatus

	CAS Viscometer	Screening Apparatus	High Pressure Apparatus
Systems	GC gas/SW	THF/SW	GC gas/SW
Pressure(psig)	700	0	1150
Temperature °F	40.5	32	54.86
Hydrate Formation Indicators	Viscosity/ Temperature	Induction Time/Ball Stop Time	Rising Gas Consumption/ Temperature
Inhibitors - at 0.5wt%			
none	20 minutes	10 minutes	< 7 minutes
PVP	330 minutes	>360 minutes	420 minutes
Alcodet 218	40 minutes	20 minutes	N/A
QP 100MH	600 minutes	>360 minutes	N/A

different apparatuses.

Based upon evidence such as the above, we judge that the viscometer can be used for measurement of induction times for gas-liquid experiments. For rapid evaluation of inhibitors, multiple viscometers could be operated in parallel. Table 2 provides itemized costs for four operational units with a total cost of approximately $40,000.

IV.A.2. The Multiple Reactor Screening Apparatus

IV.A.2.a. Equipment and Procedures. The rationale for this apparatus was the application of principles learned in the 1991 work with the above viscometer to construct a device to screen as many as 1000 combinations of inhibitors per year. This rate is an order of magnitude greater than that obtainable in either the viscometer or the high pressure apparatus (see the following description). We also wished to use the apparatus to examine the influence of different variables (e.g. pH, hydrate former concentration, ball types, etc.) on hydrate kinetics.

Our basic idea was to bypass the major experimental difficulties (mass transfer, surface renewal) associated with hydrate formation from an immiscible former such as natural gas. One of the simplest miscible hydrate formers is the four-carbon member of the furan family, tetrahydrofuran (THF), which forms hydrates from a 20wt% solution of THF in water at 4°C.

A schematic diagram of the multiple screening apparatus for THF hydrate formation is shown in Figure 8. The apparatus is submersed in a glass temperature bath, one third filled with ice,

Table 2.

Estimate for Viscometer Experiment (4 units)

Quantity	Equipment	Unit Cost	Total Cost($)
1	Temperature Bath Neslab RTE 210D	2400	2400
4	CAS Viscometers SPL 340	3350	13400
4	Viscometer Displays N4S500	2300	9200
4	Pressure Transducer DP15	450	1800
1	Carrier Demodulator CD280-4	950	950
4	Cables 12457-10	50	200
3	Pumps	200	600
1	Computer Mac IIsi	3400	3400
1	Data Aquisition System Strawberry Tree & Workbench	2200	2200
		Total	34150
	Misc. Costs		5850
		Estimated Cost	$ 40,000

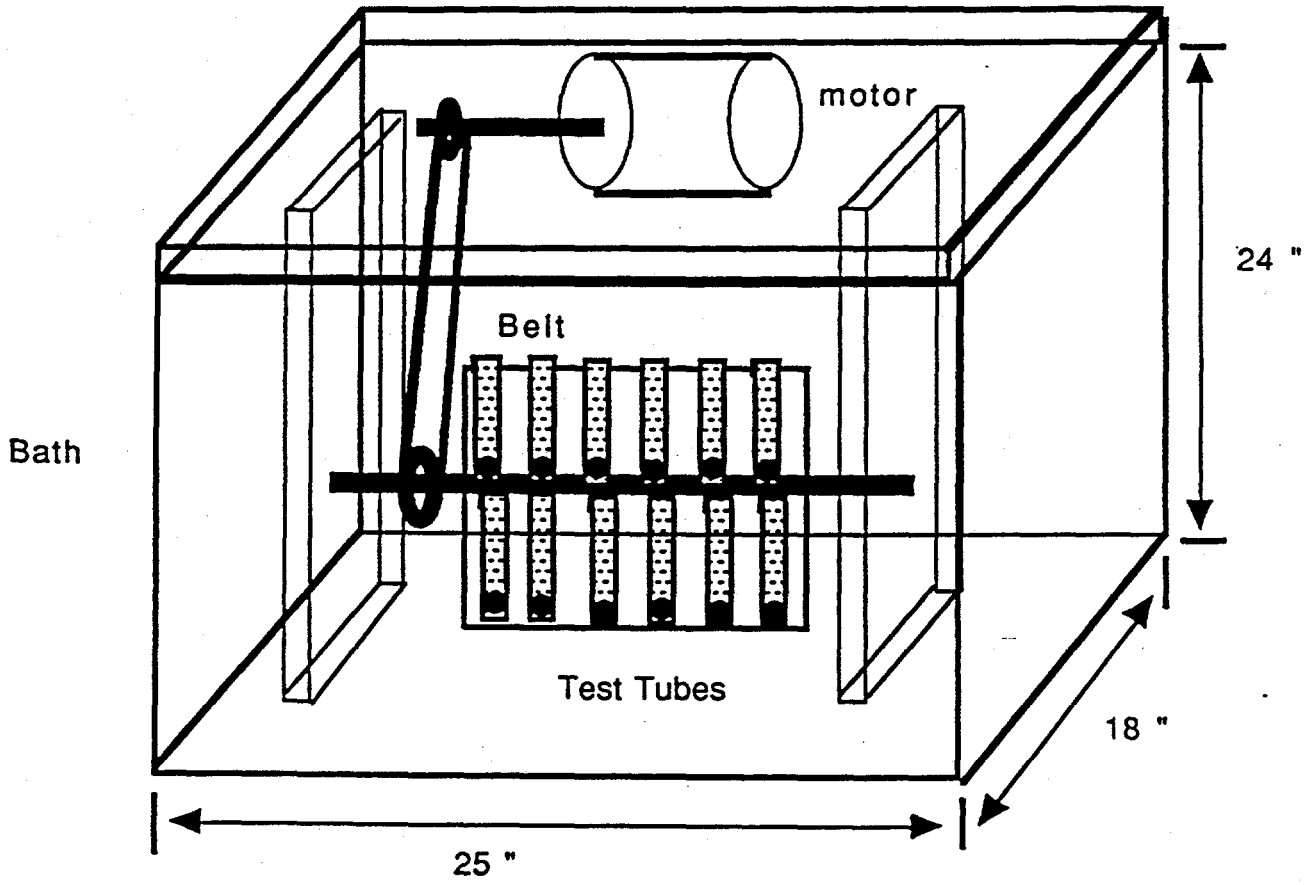

Schematic Diagram of Multiple Reactor Apparatus

Figure 8.

and two-thirds filled with water, so that the experimental temperature is 0°C.

In the experiment 12 test tubes, each with a volume of 8 ml, are mounted on a rack. Each of the tubes is filled with the test inhibitor solution and THF in the correct ratio for hydrate formation which is always 6 ml of water solution (e.g. ASTM sea salt solution in de-ionized water) and 2 ml of THF, to obtain a mixture molar ratio (water:THF) close to 17:1 for hydrate formation. A 3/8 inch stainless steel ball serves to initiate hydrate formation.

The test tube rack is rotated at 15 rpm via a motor with a ladder chain belt to prevent slippage. After the test tubes are filled and mounted on the rack, the rack is loaded into the bath at 0°C, and we begin timing the induction period required for hydrate formation. The rack rotation provides bath agitation.

Two results can be obtained from this experiment. The end of induction is indicated when hydrates (or a cloud point) are visually observed. The time for hydrate induction can be determined along with how long it takes for hydrates to grow to a substantial size, i.e. the "ball stop time". The "ball stop time" is determined as the time at which ball motion ceases.

Tests solutions are made from 700-800 gram of concentrated synthetic sea salt solution (ASTM) which has been mixed for 4 hours, before filtering it through a 0.45 micron filter. Concentrated polymer and/or surfactants solutions are made in 200 gram batches and mixed for 24 hours. The above two solutions are combined to make a specified concentration of polymer and or

surfactant. In this work, concentrations of 0.5wt% are used for each inhibitor, unless otherwise specified; that is, if two inhibitors chemicals are used each has a concentration of 0.5 wt% relative to the total solution.

IV.A.2.b. Results: Chemicals as Good Inhibitors This year we have tested 700 different combinations of solutions. Each screening apparatus data point represents an average of data from six test tubes. A few chemicals did not have a ball stop time within six hours; we tested such chemicals longer than 24 hours and still did not observe the ball to stop.

We labelled chemicals which had a ball stop time longer than six hours as good candidates for hydrate inhibition. In contrast, poor inhibitors always had ball stop times less than an hour after immersion. Similarly, good inhibitors had an induction time longer than one hour while bad inhibitors had induction times of only a few minutes.

Appendix A presents the major portion of the chemicals tested (all known structures) during this year together with the structures of each. When we compared the structure of bad chemicals with good chemicals, we found that many good inhibitors were polymers with five or six member rings attached to a long polymer chain. This seems to be a necessary but not sufficient requirement; performance of hydrate inhibitors also seems to depend on the substitution on the ring and the length of the chain.

Polyvinylpyrrolidone (PVP) was rated as a good hydrate

inhibitor from the screening results. Figure 9 indicates that higher molecular weights (via viscometry) of PVP provide better results. The PVP with a high molecular weight (360,000) has a long induction time, and the ball never stopped within 6 hours. On the other hand, Figure 10 shows that when the PVP concentration was reduced to 0.1wt%, high molecular weight PVP showed a shorter induction time than that for 0.5wt%, but the ball never stopped for either concentration.

We also obtained good inhibition results for PVP copolymers, as shown in the lower portion of Table 3. For example PVP-PVA (polyvinylacetate) provided good inhibition in low concentration (several hundred ppm by weight) and low molecular weight (ca. 40,000). These results suggest that a copolymer can increase inhibitor effectiveness relative to PVP. These results have yet to be tested in the high pressure apparatus (see Section IV.B which follows) and therefore only preliminary, but encouraging screening results are reported here.

Some types of HEC solutions provided good inhibition results, i.e. the ball never stopped within 6 hours. Figure 11 shows that the HEC ball stop times for QP-4400 and QP-100MH are comparable to PVP and both QP4400H and QP100MH yield better results than QP09-L. This suggests that the substitution of the ring and molecular weight play important roles providing long ball stop times. However, the induction times for the best HEC solutions are significantly shorter than that of PVP, suggesting that chemicals with five member rings such as PVP work better than those with six member rings (HEC).

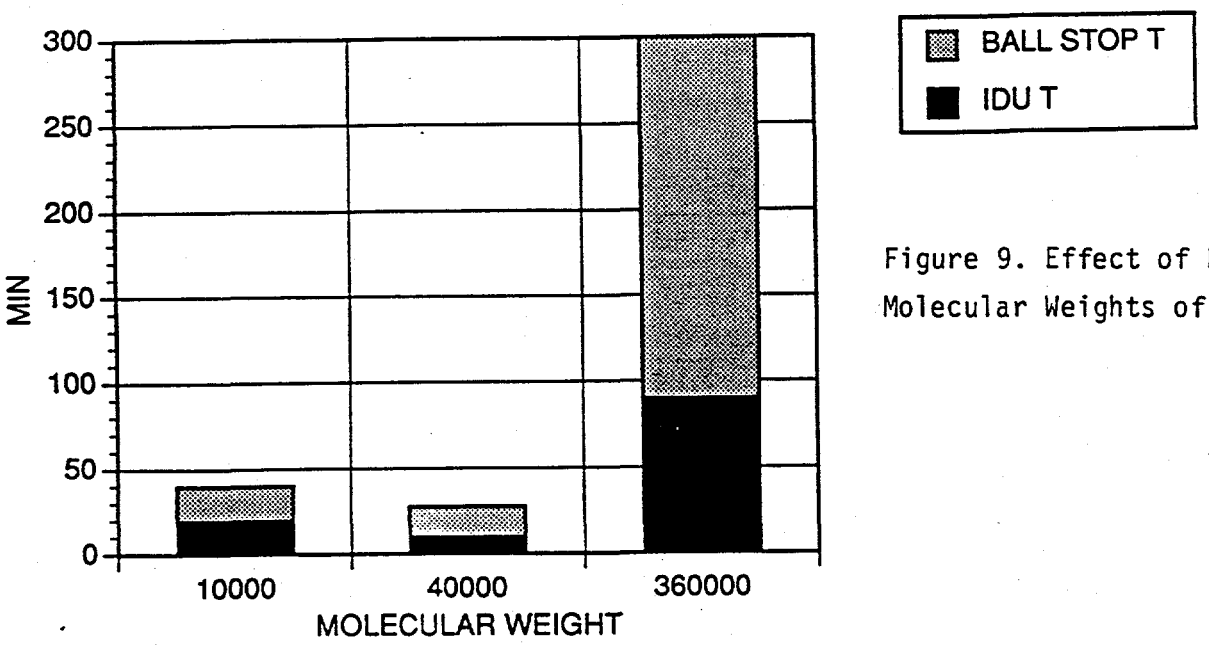

Figure 9. Effect of Different Molecular Weights of PVP

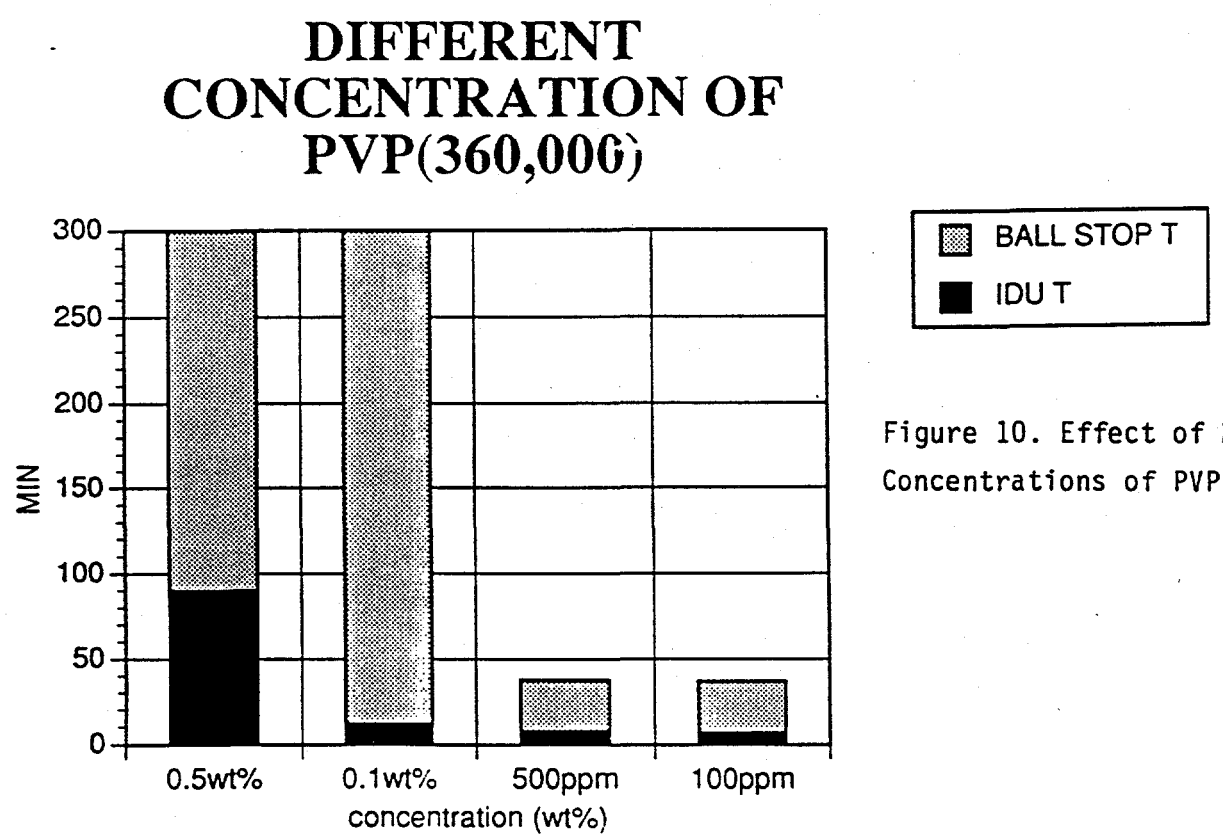

Figure 10. Effect of Different Concentrations of PVP

TABLE 3

THE RESULTS OF COPOLYMER

CHEMICALS FROM POLYSCIENCE	TIME INDUCTION T./BALL STOP T. (MIN.)
POLY(N-VINYLPYRROLIDONE) M.W. 1,000,000	10/>3hr
POLY(N-VINYPYRROLIDONE-VINYL ACETATE) 60:40 M.W. 100,000	7/35
POLY(N-VINYLPYRROLIDONE-VINYL ACETATE) 30:70 50% ISOPROPANOL SOLUTION	3/28
POLY(VINYLPYRROLIDONE-DIMETHYLAMIONETNYL METHACRYLATE QUATERNIZED HIGH MW 20% POLYMER IN WATER	3/4.5hr
POLY(4-VINYLPYRIDINE-N-OXIDE)	4/28
POLY(VINYLPYROLIDONE STYRENE 40% SOLID IN WATER	3/4.5hr
CHEMICALS FROM BASF	
VA 55E (PVP VINYL-ACETATE COPOLYMER) 50:50	7/6hr
VA 73E (PVP VINYL-ACETATE COPOLYMER 70:30 50% ethanol solution	4/6hr
COPOLYMER 845	5/35
COPOLYMER 937	3/>4hr
COPOLYMER 958	7/>4hr
(VISCOCITY 854<937<958)	

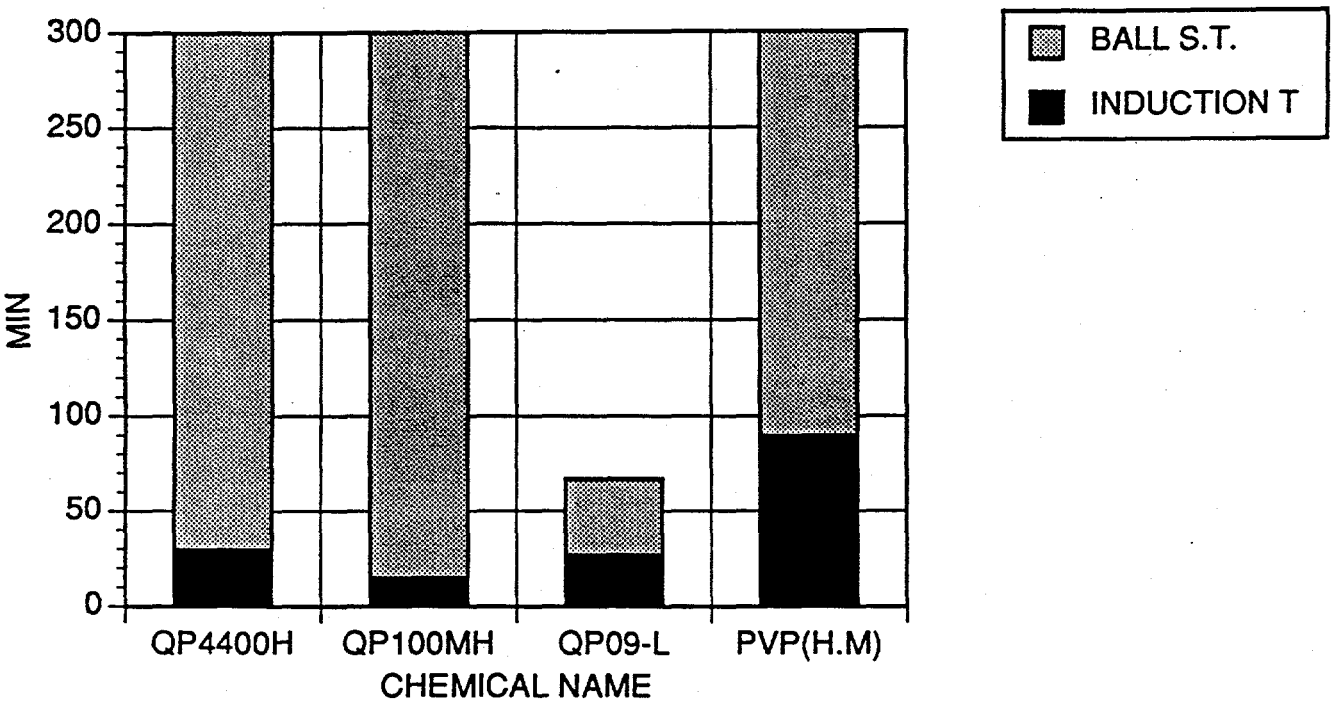

Figure 11. Comparisons of Ball Stop Times and Induction Times for HEC and PVP Used as Single Inhibitors

Generalized characteristics of good inhibitors are given here. All good inhibitors are non-ionic polymers; cationic or anionic polymers like polyacrylamide are not good. Polymeric substances provided better inhibition than simple surfactants (with low molecular weight). PO/EO block copolymer series are not good hydrate inhibitors (except for one batch of F-127 which could not be reproduced). Different EO/PO ratios in copolymer structure were not significantly different for either induction times or ball stop times. Many modified starches have been tested but we found no encouraging results with this class of chemical.

Figure 12a shows that some types of surfactants mixed with PVP prolonged the induction time while others (shown in Figure 12b) gave a shorter induction time than that of PVP. In Figure 12a note that when HEC and PVP are combined (each at 0.5wt%) the solution mixture gave a very long induction time (about five hours) and the ball never stopped within the experimental period.

IV.A.2.c. Sensitivity to Different Variables. In 1991 we found that a precipitation occurred when we used sea salt solution with THF for hydrate formation. After we finished the experiments to compare the sea salt results and NaCl results we found that the precipitation did not effect either aspect of hydrate formation (induction time or ball stop time). In order to more closely mimic industrial situations we chose sea water solutions for our screening apparatus in 1992.

Also as a result of our 1991 work, different ball materials

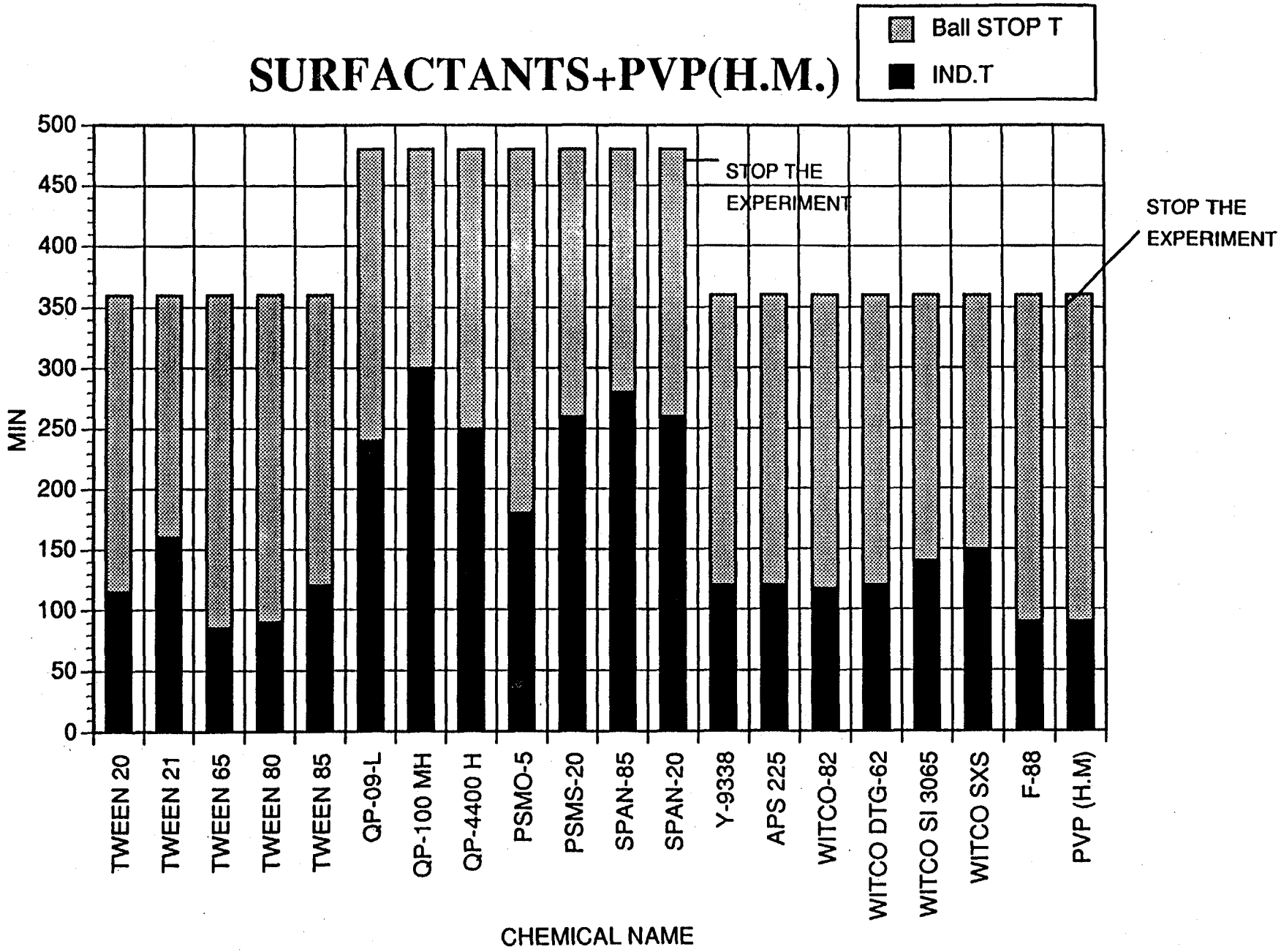

Figure 12 a Surfactants Which, Combined with PVP, Gave Better Inhibition Results

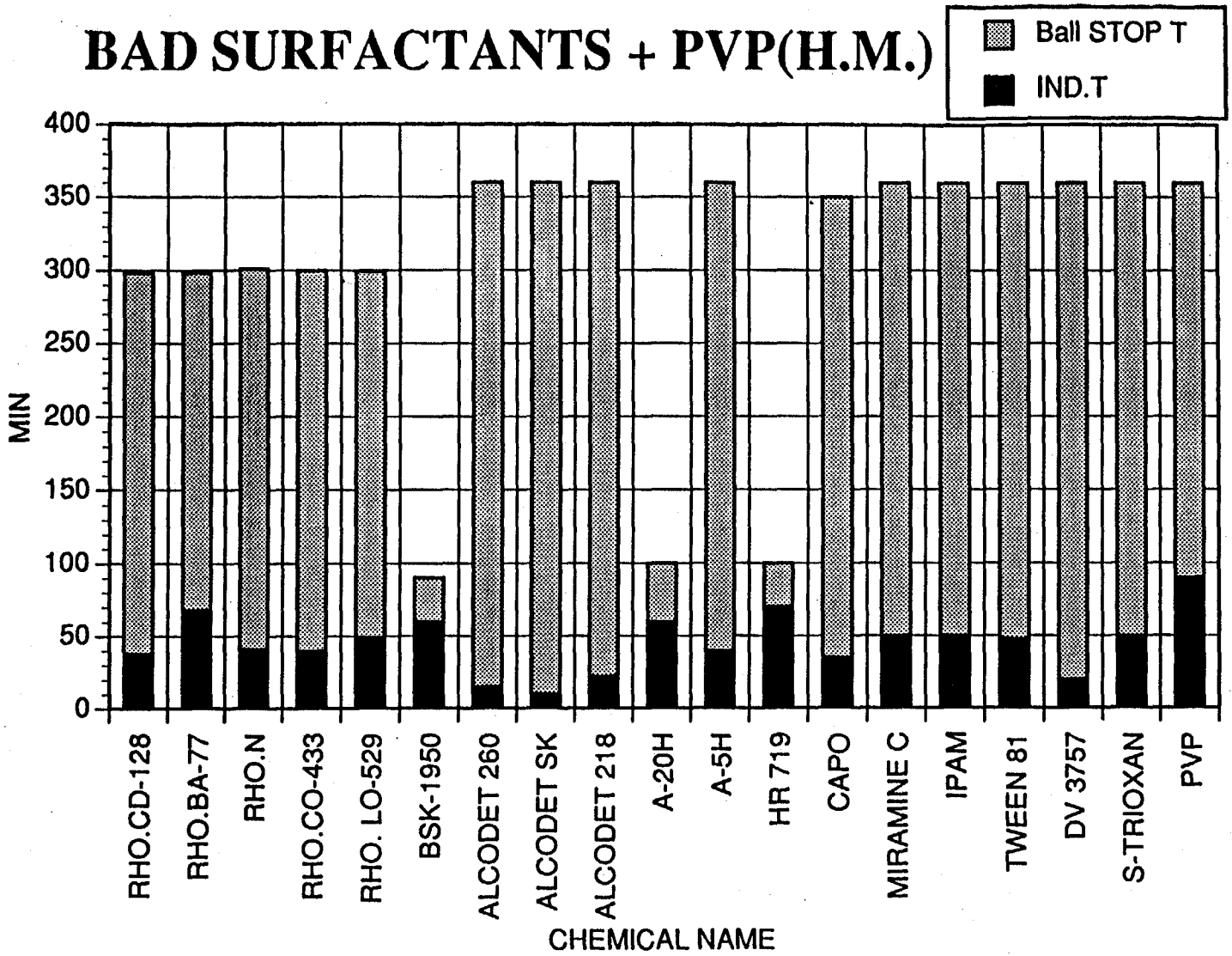

Figure 12b. Surfactants Which, Combined with PVP, Gave Shorter Induction Times Than PVP Alone

were tested to determine their effect as hydrate initiators. Table 4 shows that different ball materials do not significantly affect induction time. Exceptions in these tests were nylon balls which never initiated hydrate formation, wooden balls, and Teflon balls (and stirrer coatings) which initiated hydrate formation only in de-ionized water. We were unable to explain these exceptions, but continued our screening experiments with 440 stainless steel balls.

Figure 13 presents the results of a pH sensitivity test, indicating that pH did not have a big effect on the results of either induction time or ball stop time. From such results on pH, it is difficult to say that the hydrate surface is anionic, cationic or non-ionic related to charge. In addition, Table 5 illustrates that neither induction time nor ball stop time are sensitive to THF concentration, when it was varied from 13.7wt% to 37wt%.

IV.B. High Pressure Apparatus Check on Screening Results

IV.B.1. Equipment, Materials, and Procedure

The experimental equipment used in the construction of this apparatus is essentially the same as that described in the 1990 DEA-30 Annual Report with the exception of nine new pieces of equipment as noted below. Initially constructed as an isochoric apparatus in 1988, the system was completely disassembled and reconstructed in 1991 to achieve constant pressure operation. A

TABLE- 4 DIFFERENT SCREENING BALL MATERIALS

MATERIAL NAME (SOLUTION)		INDUCTION TIME (min)
CERAMIC BALL	(NaCl)	3
GLASS BALL	(NaCl)	5
TEFLON BALL	(NaCl)	>2 h
COATED STIRRER	(NaCl)	>2 h
WOOD BALL	(NaCl)	>2 h
NYLON BALL	(NaCl)	>2 h
COATED STIRRER	(D.I.WATER)	2
TEFLON BALL	(D.I WATER)	5
NYLON BALL	(D.I.WATER)	>2 h
440 S.S.	(D.I.WATER)	3
316 S.S	(D.I.WATER)	3.5
BRASS	(D.I.WATER)	3

Figure 13.

pH did not have big effects on either induction time or ball stop time

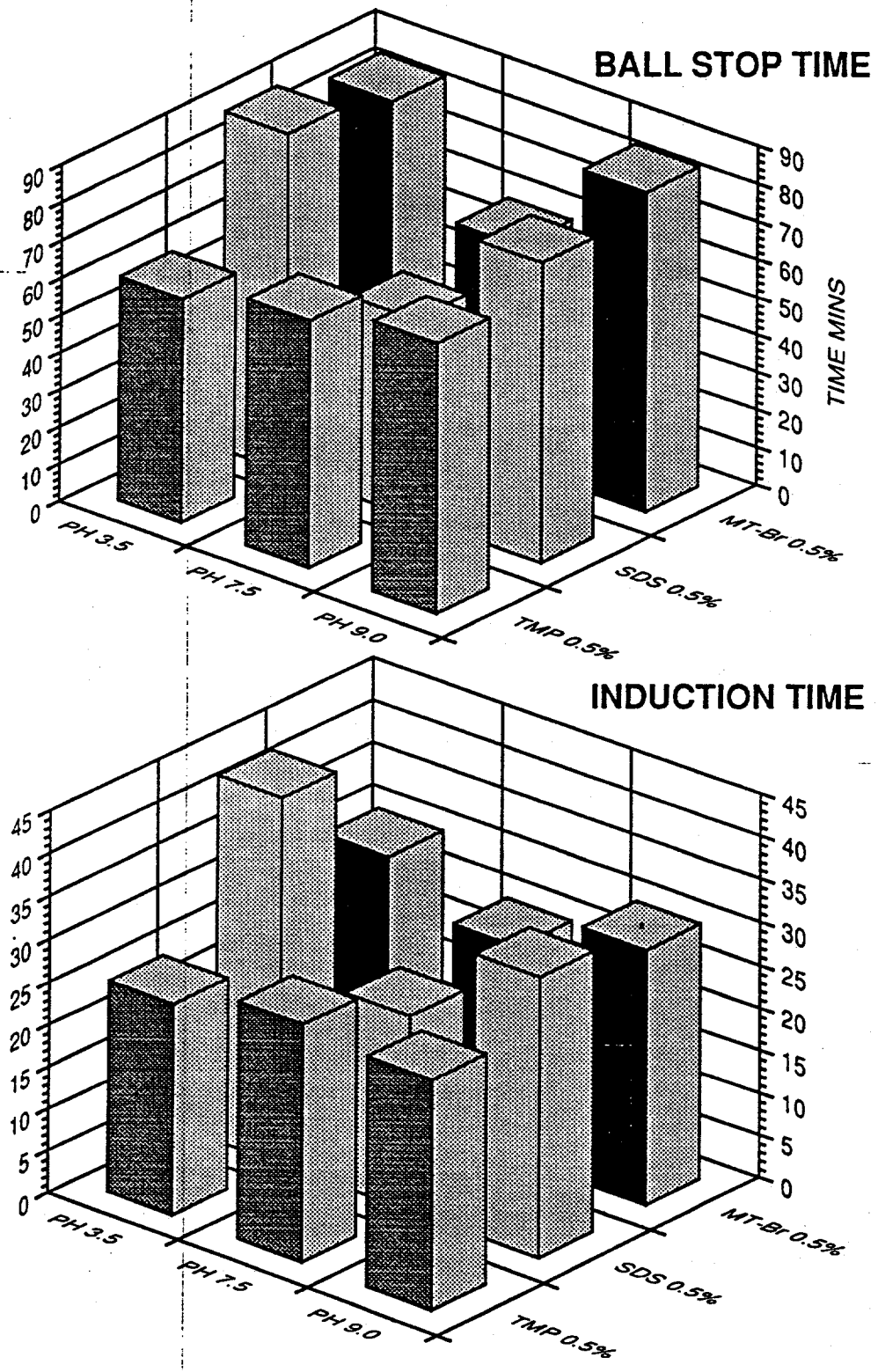

Table 5.

Both induction time and ball stop time are not sensitive to the THF concentration when THF concentration varies from 13% to 35%.

THF Sensitivity

H2O:THF (Mol.)	THF W.C%.	H2O:THF ml	IND.T mins.	Ball S.T. mins.
7: 1	37%	2.9 : 2	2	5
10 : 1	28.8%	4.2 : 2	2	6
13.5 : 1	22%	6 : 2	1	3
15 : 1	21.1%	6.35 : 2	2	5
17 : 1	19.1%	7.2 : 2	1.5	4
20 : 1	16.7%	8.45 : 2	1	3.5
25 : 1	13.8%	10.58 : 2	1.2	4

schematic of the new constant pressure apparatus is given in Figure 14. A brief description of the apparatus is outlined below.

The heart of the apparatus consists of a 300 cc magnetically stirred autoclave with a removable cover (16). The stirrer torque is monitored by a Keithley 500 data acquisition system (1). The autoclave is submerged in a temperature-controlled bath (14) filled with ethylene glycol-water solution. In the previous DEA-30 project, the bath temperature could only be controlled within 0.7°F. For the isothermal kinetics work, a separate temperature controller was added to the system to maintain the bath temperature to within 0.05°F.

The constant pressure in the autoclave is controlled through new installations of both pressure reducing (12) and back pressure (13) regulators, connected respectively to a high pressure supply reservoir (4) and a low pressure discharge reservoir (9). The bath, autoclave, and ambient temperatures are recorded by the data acquisition system. Pressures in the autoclave and both pressure reservoirs are also recorded by the data acquisition system. In addition, the pressure is measured via a Heise dial gauge. An IBM XT personal computer, linked to the Keithley 500 data acquisition system, controls and stores data readings through a software program developed in this laboratory.

With the exception of the second gas used in the sensitivity tests (Section IV.B.3) and liquid condensate experiments (Section IV.B.4) all of the high pressure work was done with a simulated

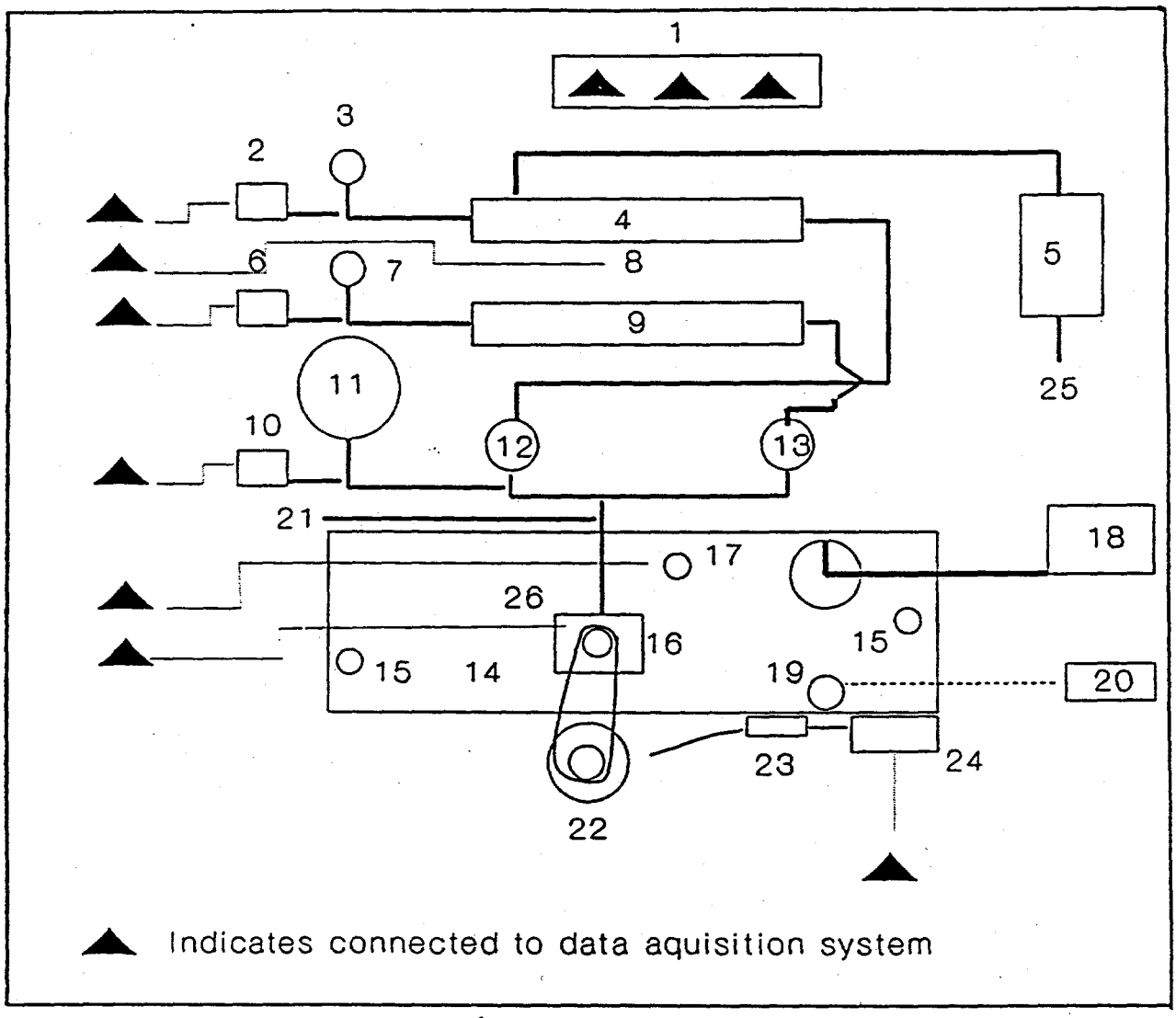

1. Keithley
2. Pressure Transducer
3. Pressure Gauge
4. High Press. Reservior
5. Gas Booster
6. Pressure Transducer
7. Pressure Gauge
8. Ambient Thermistor
9. Low Press. Reservior
10. Pressure Transducer
11. Reactor Press. Gauge
12. Press. Reducing Regulator
13. Back Press. Regulator
14. Glycol-Water Bath
15. Bath Mixer
16. Autoclave Reactor
17. Bath Thermistor
18. Bath Cooling Unit
19. Bath Heaters
20. Neslab Temp. Controler
21. System Vent
22. Motor
23. Transformer
24. Beckman
25. Gas Bottle
26. Cell Thermistor

Figure 14. High Pressure Apparatus Schematic

Green Canyon Gas supplied by Matheson Gas Products, of the composition listed below:

Component	mol fraction
Methane	0.872
Ethane	0.076
Propane	0.031
N-Butane	0.008
I-Butane	0.005
Nitrogen	0.004
I-Pentane	0.002
N-Pentane	0.002

All of the inhibitor solutions were composed as indicated in the screening apparatus (Section IV.A.2.a). Quantities of the same solution was used for multiple reactor screening tests and for the high pressure kinetic tests. Concentrations of all inhibitors were at 0.5 wt% unless otherwise indicated.

The kinetic experiments in the high pressure apparatus are completed under isothermal and isobaric conditions. A detailed explanation of the kinetic experimental procedures is given below; they will help the reader to understand the physical quantities we measured during the run.

(1) Cleaning Procedures. From previous work, we found that an impurities, (e.g. dust, small particles, residual inhibitors, etc.) present in the reactor dramatically alters the kinetics of hydrate formation. A thorough cleaning procedure was adopted in our experiments. First, the reactor was initially cleaned by rinsing with tap water several times, then 120ml of methanol was put into the cell and sealed; the reactor mixer was then started to agitate the cell interior for 15-20 minutes. Finally, the cell was rinsed with deionized water several times, and then thoroughly dried with tissue.

(2) Charging Procedures. With the completion of the cleaning, 120 grams of test solution is placed in the 300ml reactor which was then sealed and placed into isothermal bath. While the autoclave was being cleaned and prepared, the high pressure reservoir was charged to approximately 3 times the operating pressure, using a gas booster. The reactor was then connected to the apparatus and then purged with the test gas.Then the reactor was charged with natural gas after the temperature of the solution inside the reactor reached a steady-state value. During the equilibration period, the agitator was activated about 15-20 minutes to enhance the heat transfer rate.

After the temperature had equilibrated, the agitator was turned off. A small temperature decrease was observed due to the mechanical energy of mixing. After the temperature of the cell had reached a new steady-state (10-15 minutes), the cell was charged to the operating pressure. Since the gas enters the system with higher thermal energy, the temperature of the cell rises a few degrees, requiring another 15-20 minutes to reach the new thermal equilibrium. The pressure was maintained constant by back pressure regulator during the run.

(3) Kinetic Run Procedure. After the system reaches a new steady-state, the mixer and the run clock were simultaneously started. Small temperature increases were observed due to mixing. The start of the mixer is considered as the starting time for hydrate kinetic run. In this part of the work, we determine the induction time for initiation of hydrate formation. The induction time is defined as the time between commencing cell

agitation and the rise in gas consumption, as well as the rise in cell temperature due to the exothermic heat of hydrate formation. The induction time was used as one of the criteria to check inhibitor performance from the screening apparatus.

The gas consumption was monitored continuously and correlated against other variables at 10 hours and at 15 hours during the run, to give us information about the hydrate growth domain. The duration of each run was about 15-20 hours.

Another quantity measured was the difference between the cell temperature and the bath, with the cell agitator on and off. This temperature difference is due to the viscous heat dissipation caused by mixing after hydrate formation, and is directly related to the rate of agitation, and fluid viscosity for heterogeneous fluids.

IV.B.2. Confirming Screening Results at High Pressure

Both induction time and gas consumption are used as criteria to check the performance of the inhibitors. Illustrative figures for gas consumption during the run and are depicted in Figure 15.

IV.B.2.a. Induction Time Confirmation. The inhibitor induction times were comparable in both the high pressure apparatus and the screening apparatus as shown in Figures 16 and 17. As can be seen there is a marked difference between low (< 30 minutes) induction times in both apparatuses and high (> 70 minutes) induction times. From both figures one can see that while there in not an absolutely linear translation for induction times, a clear, quantitative relationship between the induction

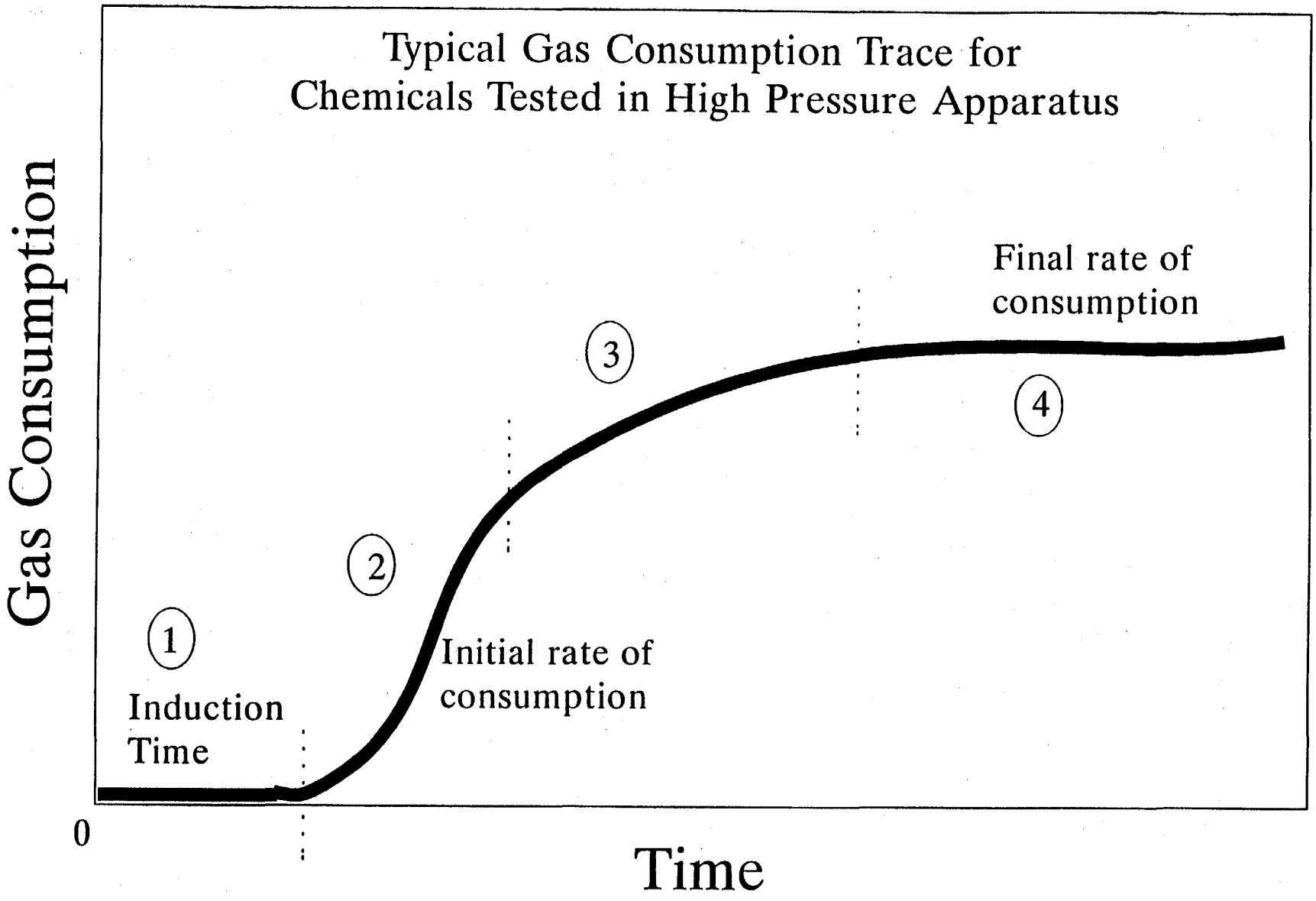

Figure 15. Schematic Diagram for Gas Consumption on High Pressure Apparatus

RSTA AND HPA
A QUALITATIVE ANALYSIS

Figure 16. Qualitative Comparison of Induction Times on Rapid Screening Test Apparatus and on the High Pressure Apparatus

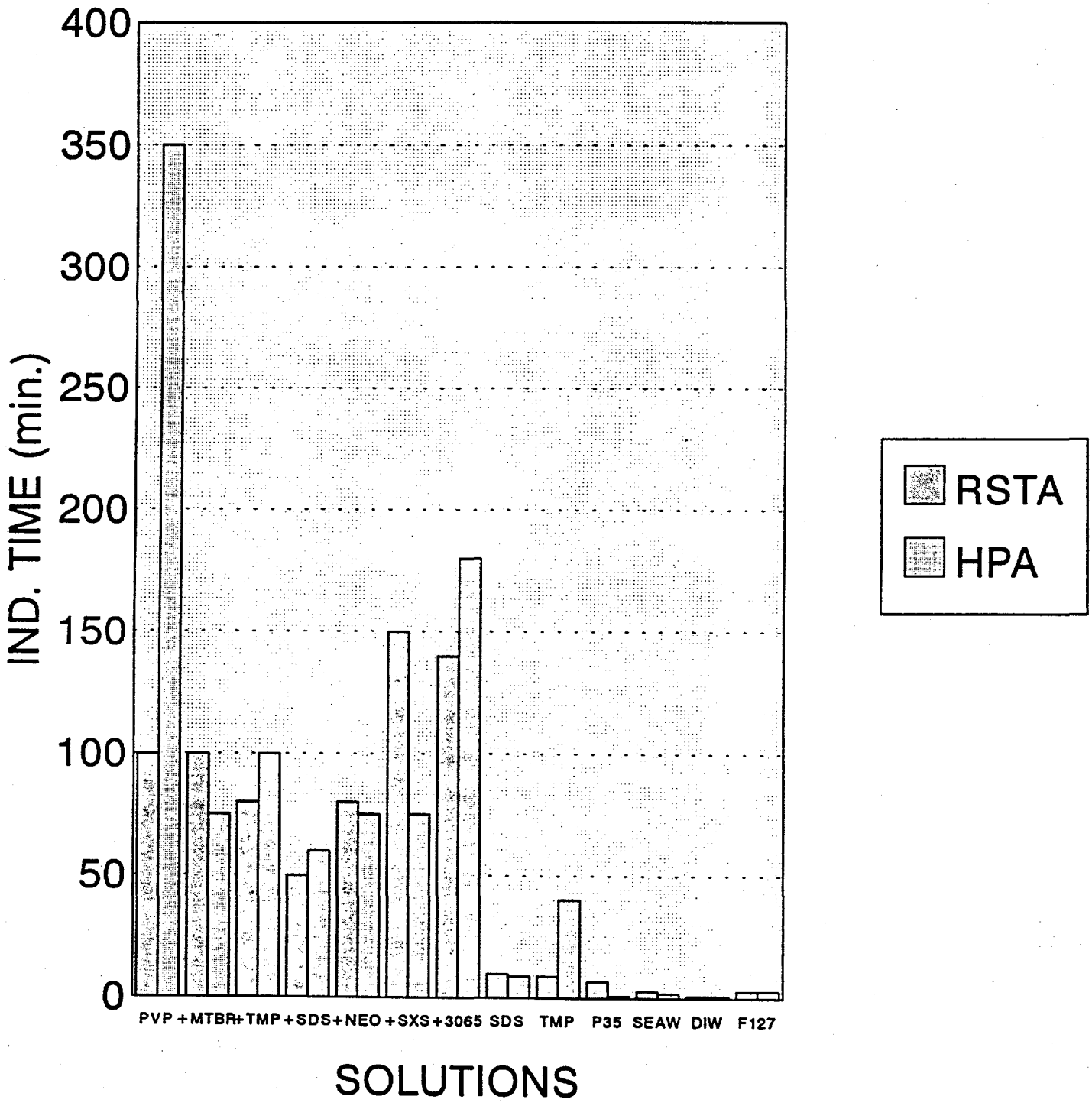

RSTA (Rapid Screening Test Apparatus)
HPA (High Pressure Apparatus)

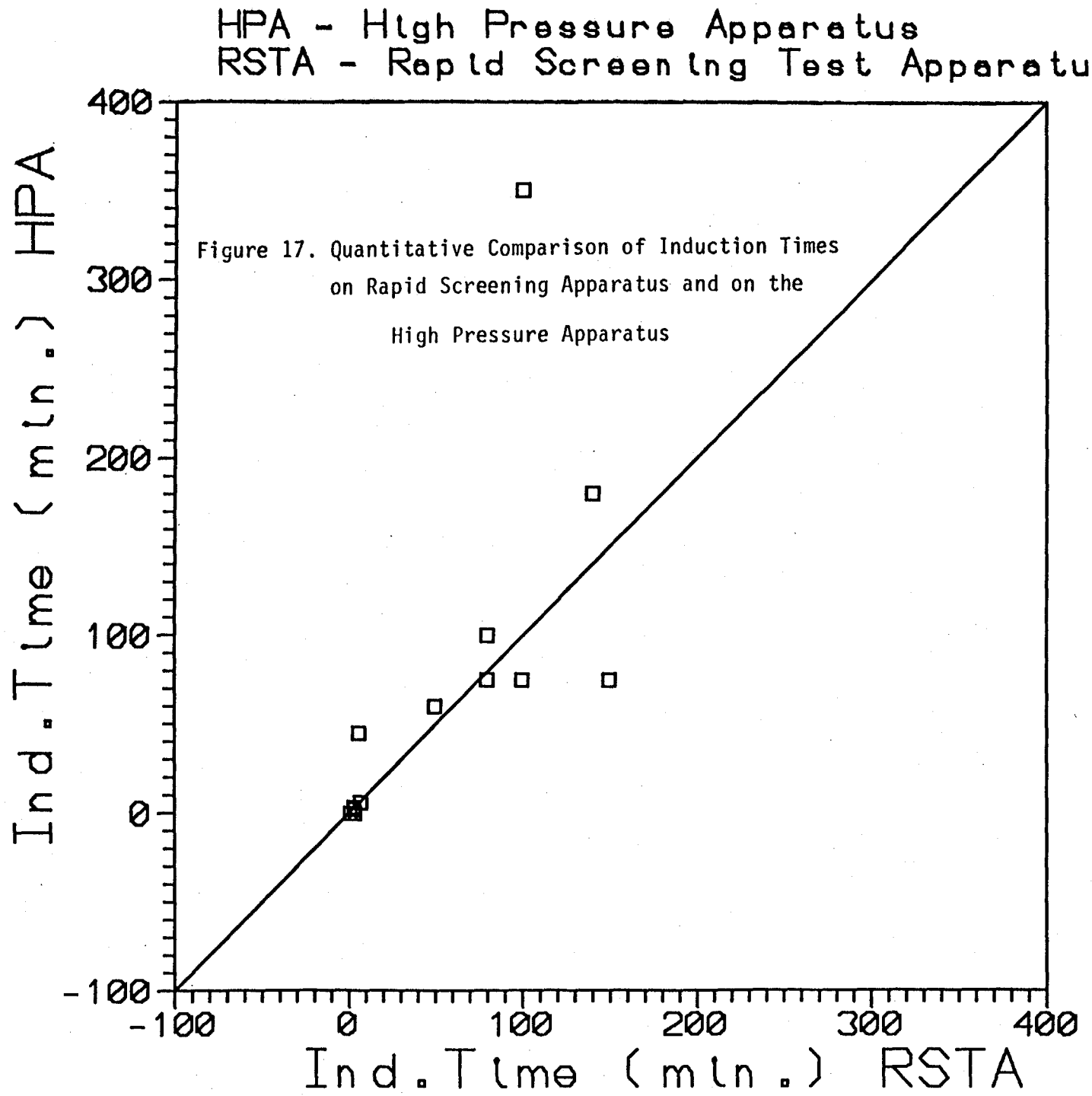

Figure 17. Quantitative Comparison of Induction Times on Rapid Screening Apparatus and on the High Pressure Apparatus

times observed on both apparatuses so that one may easily distinguish between poor and good inhibitors.

However, a correlation was not observed in every instance; very occasionally there was a chemical provided a good induction time on the screening apparatus, yet the high pressure performance of the same chemical was disappointing. For example, while they performed well on the screening apparatus, Sorbitan and Span did not show acceptable high pressure performance in terms of either induction time or gas consumption. One possible reason for their poor performance is their high insolubility in water. Both Sorbitan and Span solutions appeared very cloudy at 0.5% (wt) indicating incomplete dissolution of the chemical.

The converse was never true; we never found a good inhibitor in the high pressure which had not first provided good results on the screening apparatus. Such results led us to believe that good performance in the screening apparatus was "necessary but not sufficient" to declare a chemical a good inhibitor.

Yet because induction time was visually observed on the screening apparatus, some member companies believed induction time to be somewhat less reliable in that apparatus. As a result we also tried to find variables in the high pressure apparatus which correlated with observations of ball stop times in the screening apparatus.

<u>IV.B.2.B. Ball Stop Time Confirmation</u>. One of our primary goals was to obtain a pumpable solution, even with the presence of hydrates in the system. The rheological properties of the solution after hydrate formation are very important. In the

screening apparatus, there is a very good indicator for such properties, that is the motion of the metal ball inside the tube. The ball stop time is thus used as one criterion to determine the best chemical inhibitors. In the high pressure apparatus however, it is very difficult to obtain the rheological properties. We decided to try to correlate the ball stop time with various quantities measurable in our high pressure apparatus.

Ten different inhibitor solutions were chosen for such a study. The ball stop time for these ten solutions are listed in Table 6, covering a substantial range of ball stop times. Five different correlating quantities were obtained from the high pressure apparatus. They were: (1) gas consumption at 10 hours, (2) initial rate, (3) the rate at 10 hours, (4) final cell temperature difference, and (5) the slope intercepts of the initial rate and the rate at 10 hours. A schematic illustration of each of these seven variables is in Figure 18.

The correlation results are duplicated in Figure 19-22. The best quantitative correlation is the gas consumption at 10 hours shown in Figure 19. While this correlation is clearly imperfect, it is better than the remainder in Figure 20-22, and gas consumption does show general trends for good inhibitors.

IV.B.2.c. Both Long Induction and Ball Stop Times. Since the PVP gives a very long induction time (sample results shown in Figure 23) and HEC compounds provide very low gas consumption (sample results shown with a change in scale in Figures 24 and 25) their combination was thought to be a potentially good candidate for hydrate kinetic inhibition. Preliminary results

TABLE - 6

CORRELATION BETWEEN SCREENING RESULTS AND HIGH PRESSURE RESULTS

	Ball Stop	Gc(@10hr) (mol)	I. Rate(mol/hr)	F. Rate(mol/hr)	FT. Diff.	Slope Int. (min)
D.I Water	1.5	0.2127	0.08295	0.00368	0.305	120
Sea Water	11	0.1788	0.06055	0.00508	0.14	195
Quat 3	10	0.18986	0.05085	0.00607	0.11	555
OD410	17	0.2032	0.07475	0.00735	0.1	285
APG 600	20	0.283845	0.1167	-0.00155	0.285	180
NARTEX	35	0.16775	0.089	-0.0005	0.085	97.5
WI 3065	35	0.2353	0.06225	0.00925	0.17	310
Witco 82	40	0.211365	0.096	0.01	0.12	200
A20+PVP	100	0.1308	0.01865	0.0132	0.15	375
HR719+PVP	100	0.071865	0.01025	0.288	0.13	360

Figure 18. **SCHEMATIC DIAGRAM OF CORRELATION WITH BALL STOP TIME AND HIGH PRESSURE RESULTS**

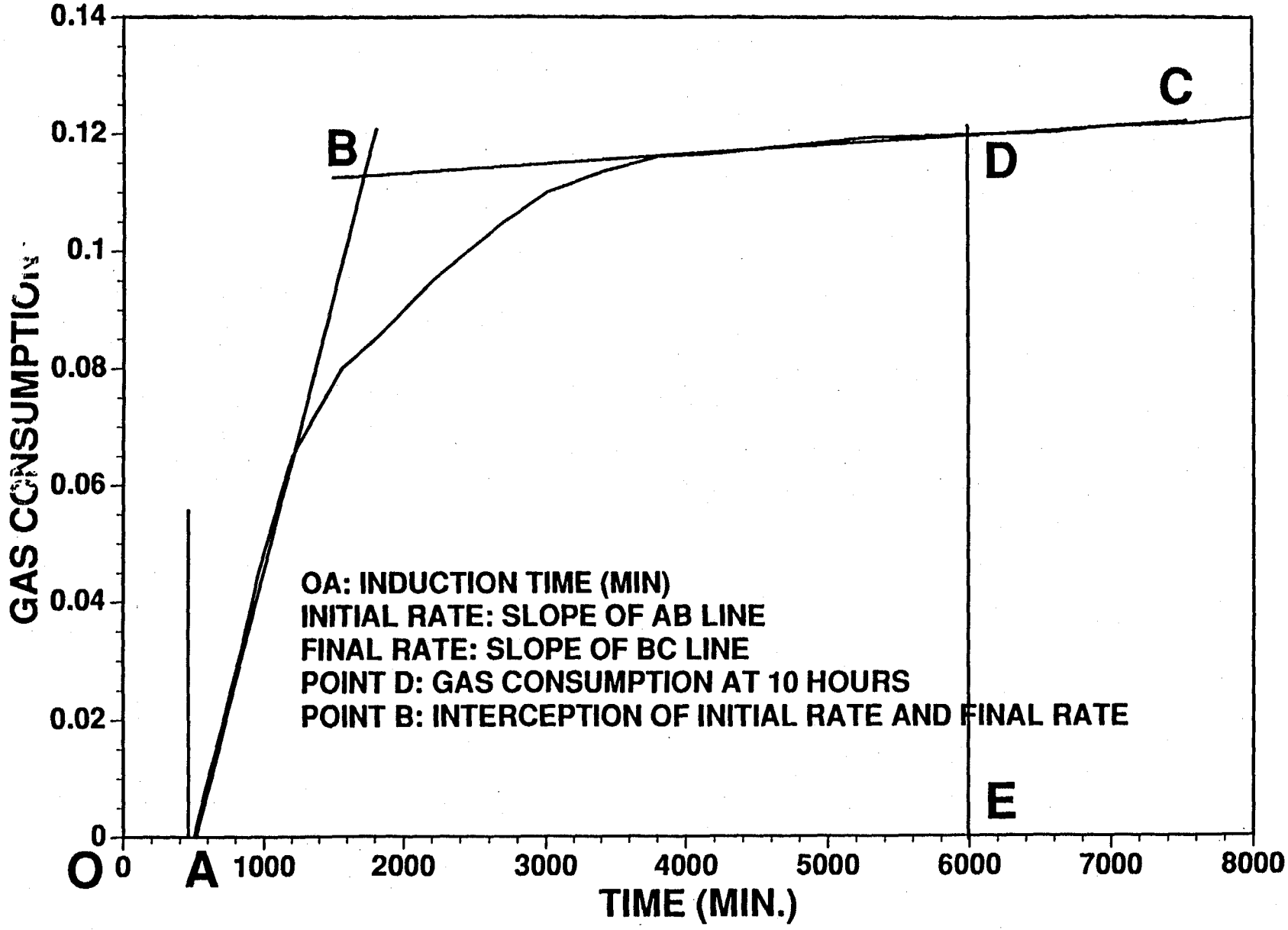

FIGURE-18

Figure 19. The correlation of Ball Stop Time vs. High Pressure Results

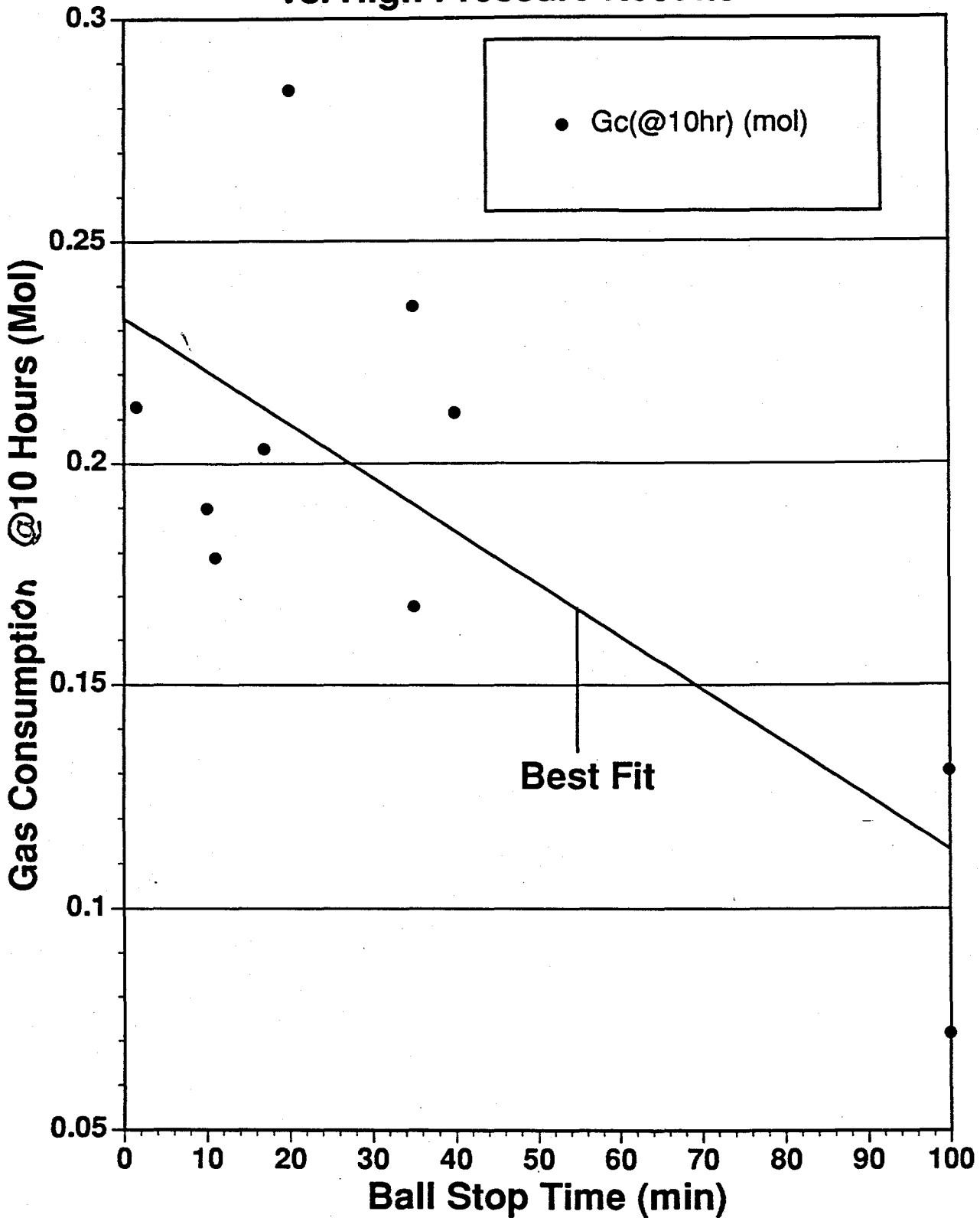

Figure 20. The correlation of Ball Stop Time vs. High Pressure Results

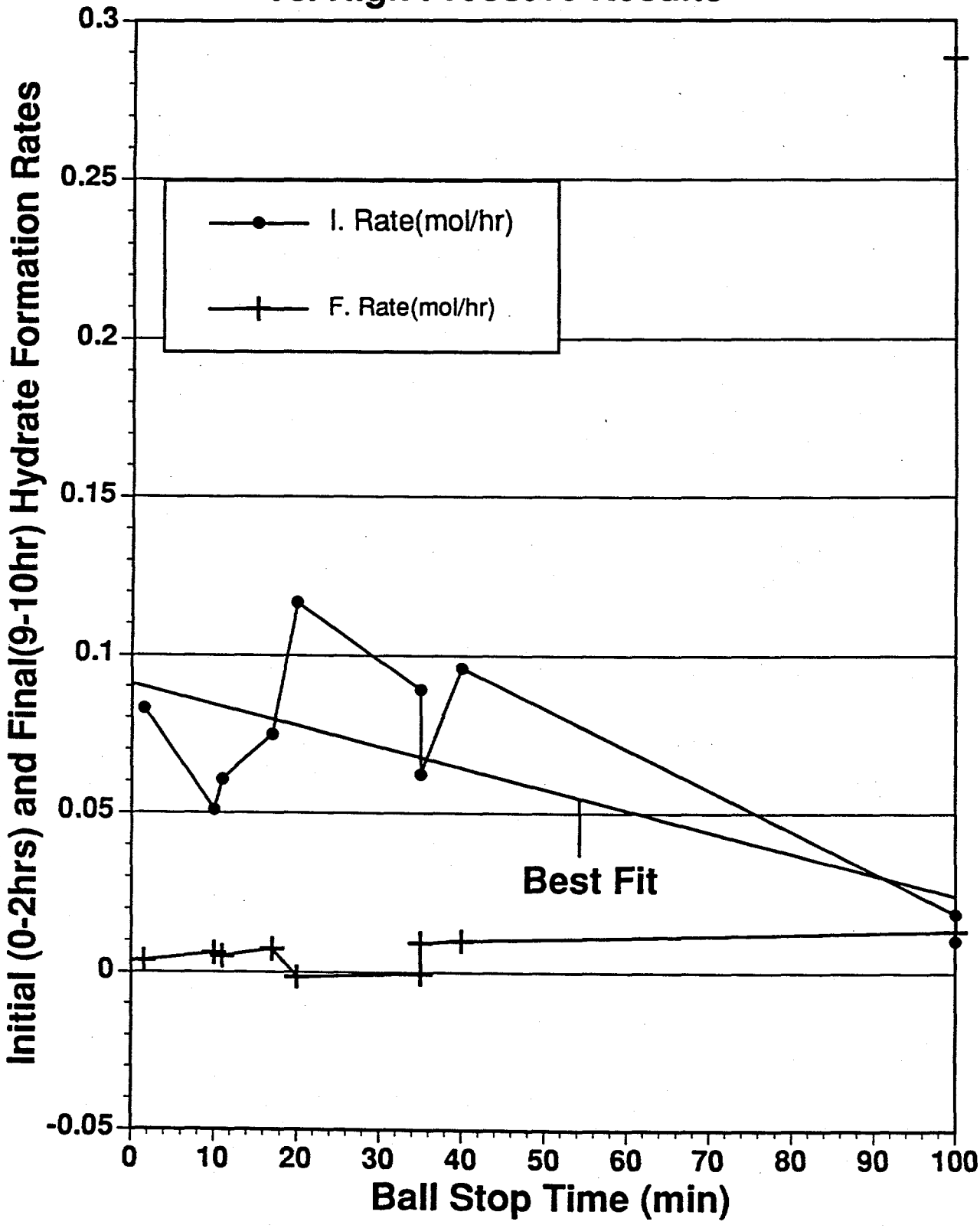

Figure 21. The correlation of Ball Stop Time vs. High Pressure Results

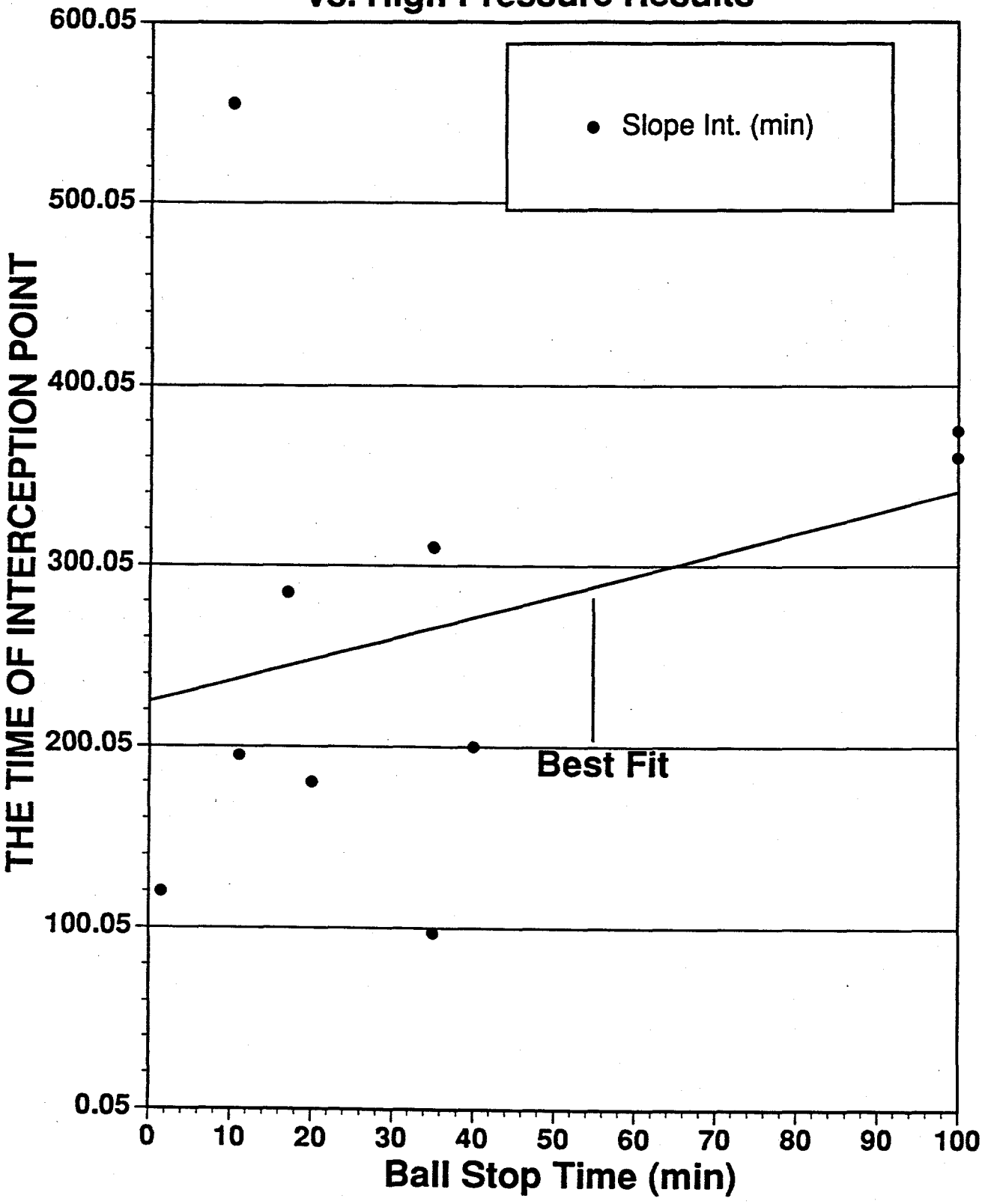

Figure 22. The correlation of Ball Stop Time vs. High Pressure Results

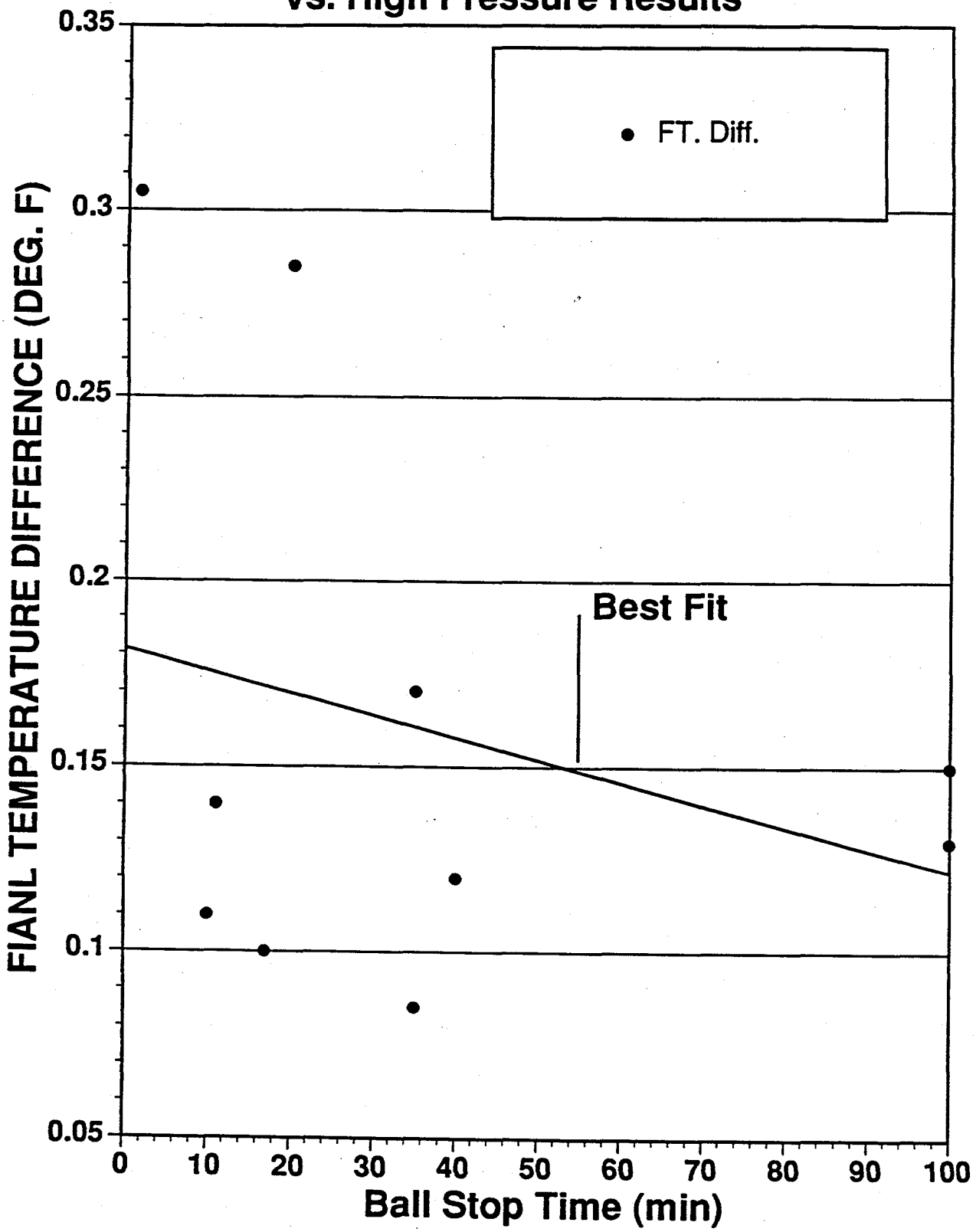

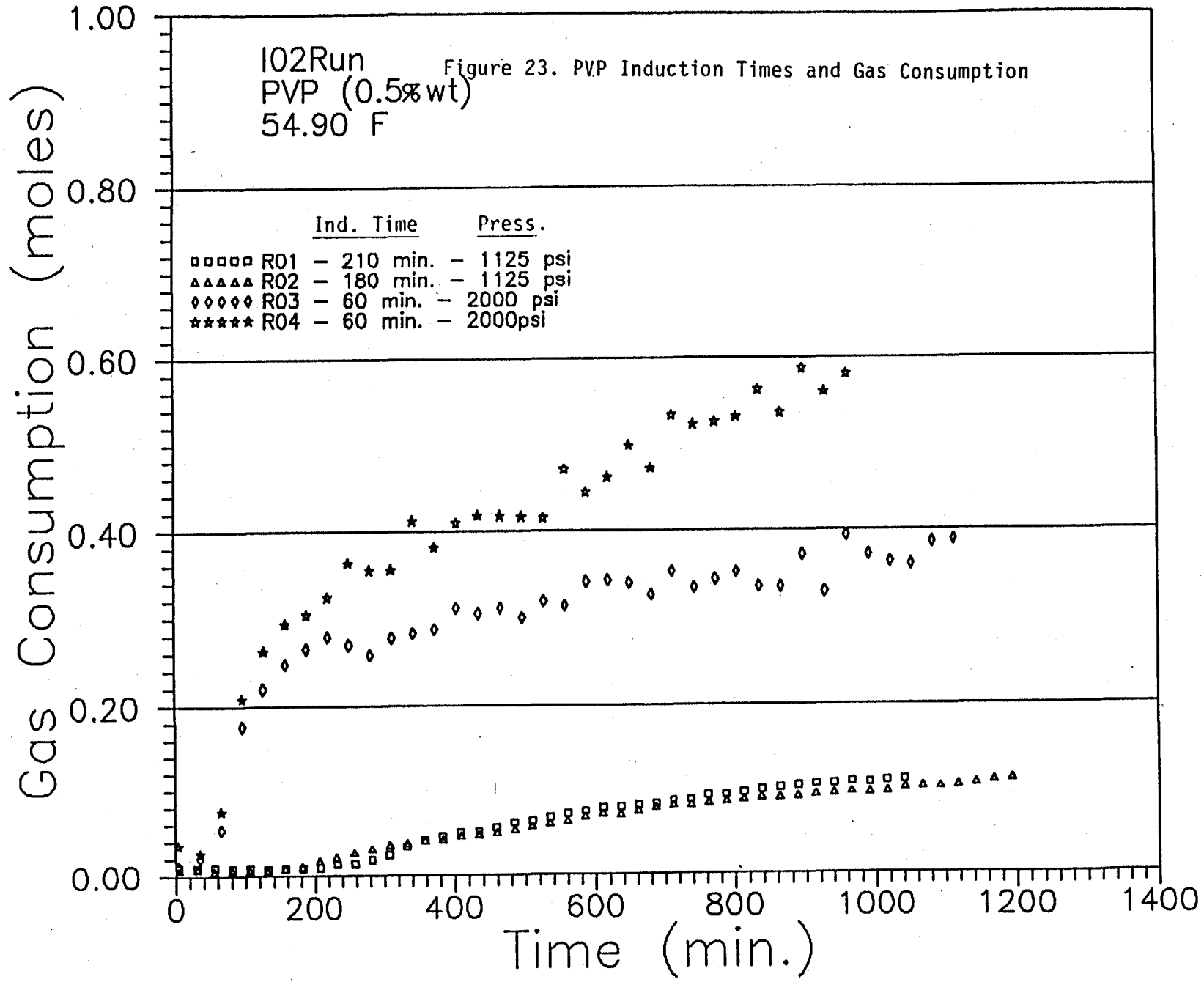

Figure 23. PVP Induction Times and Gas Consumption

Fig 23

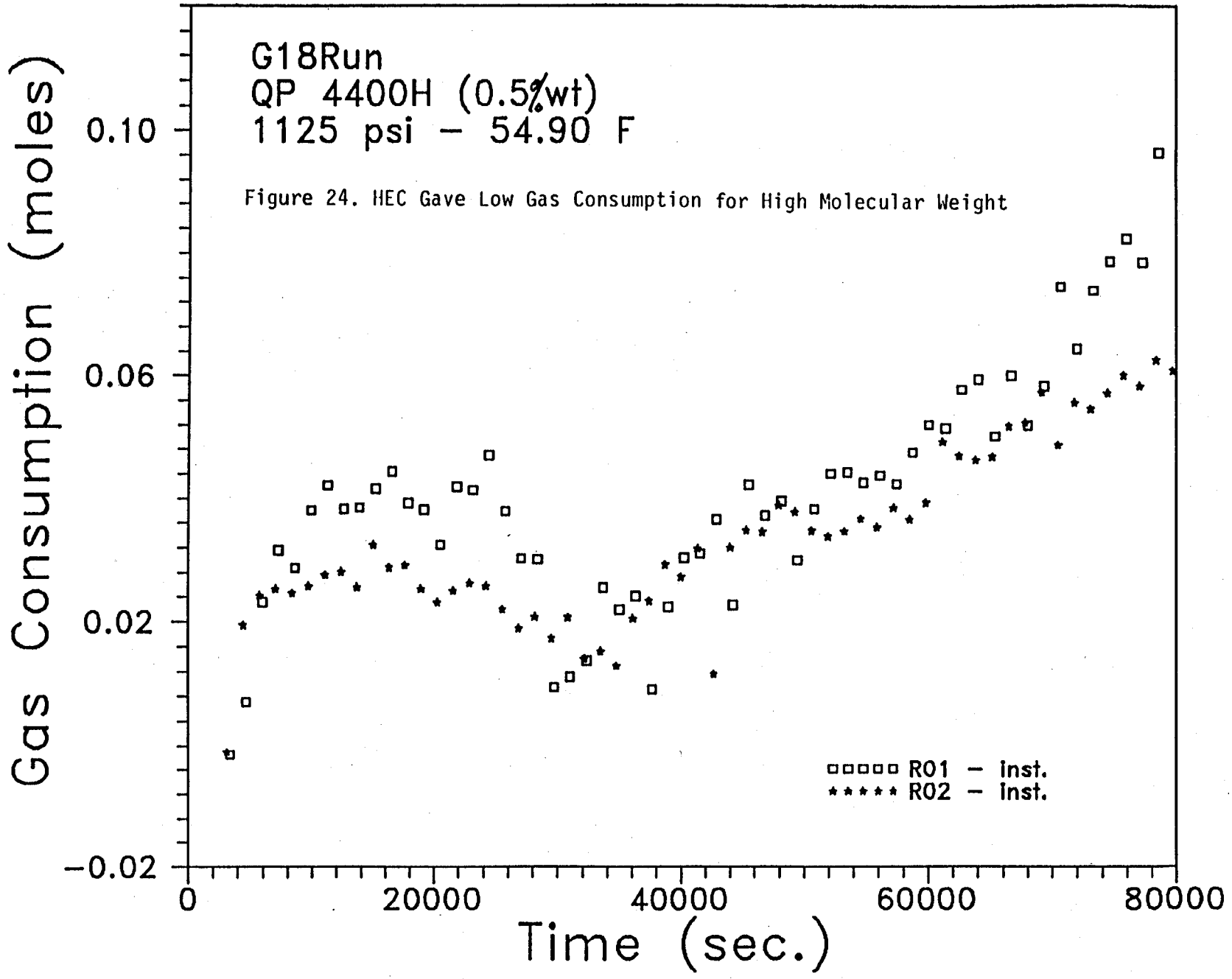

Figure 24. HEC Gave Low Gas Consumption for High Molecular Weight

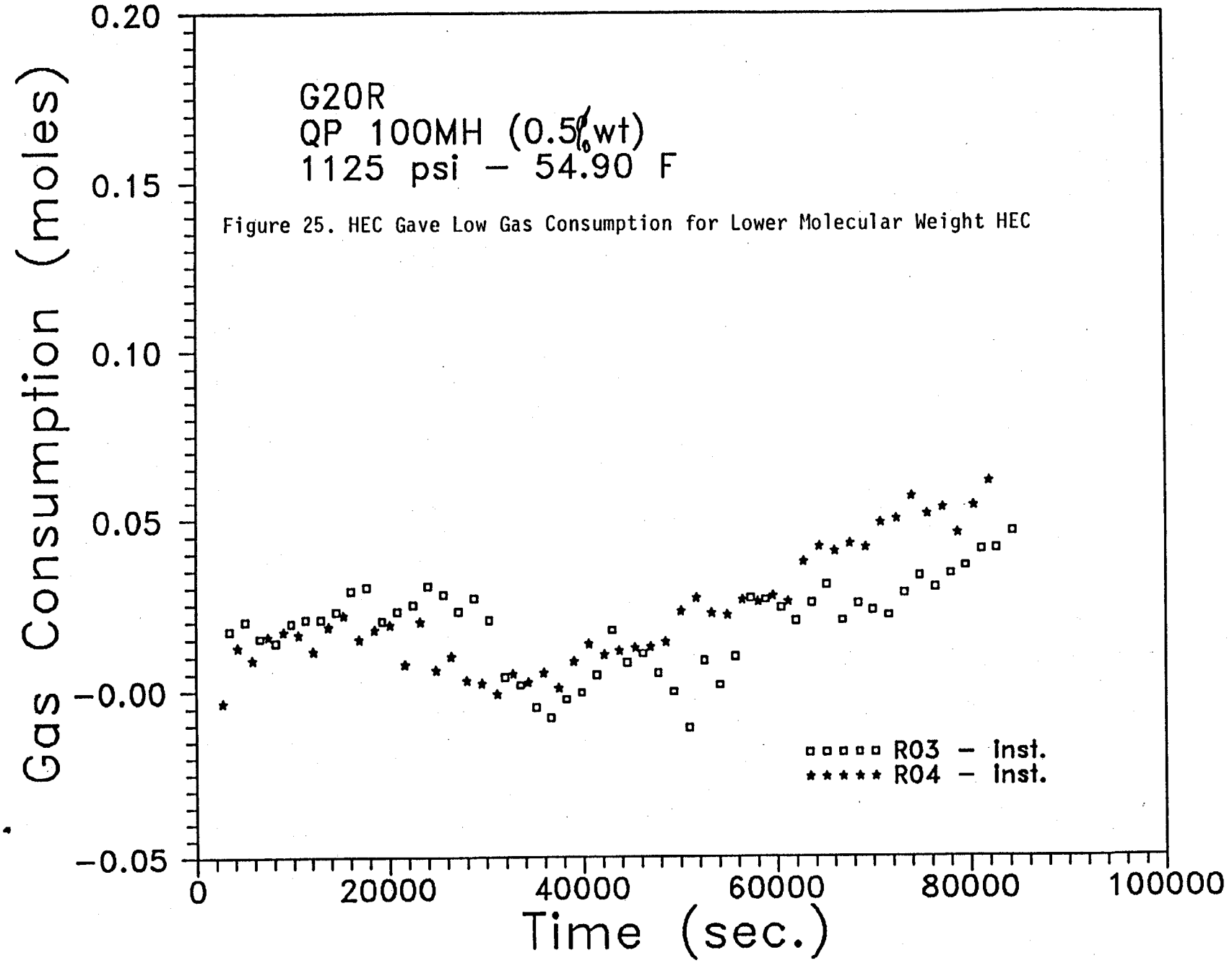

Figure 25. HEC Gave Low Gas Consumption for Lower Molecular Weight HEC

are promising as shown in Figure 26a,b, and 27 for tests at the 1150 psig, and 54.9°F, with duplicate runs given in each figure.

Figure 26a shows extremely low gas consumption and long induction times for mixtures containing 0.5 wt% PVP and 0.5% wt% of HEC-4400 and HEC-100MH. Figure 26b shows the effect deteriorates for a lesser concentrations (0.25%) of low (4400H) molecular weight HEC, but is promising for the high mol. wt. HEC. In Figure 27 at a higher pressure of 2000 psia, the gas consumption rate was higher, indicating more hydrate growth.

It should be noted however that solutions of HEC-4400 and HEC-100MH at 0.5% (wt) have very high viscosity. Such viscosity effects might be decreased by lower molecular weights of HEC in future research.

While the above promising results hold for high molecular weight HEC (HEC4400 and HEC 100 MP) they are not true for lower molecular weight species (QP 09). In the immediate future more experiments will be performed to determine the effects of pressure, temperature, concentration and molecular weight on these promising results.

IV.B.3. Sensitivity Tests at High Pressure

IV.B.3.a. PVP Molecular Weight Sensitivity. Table 7 shows the sensitivity of induction time and gas consumption to PVP molecular weight. High mol. wt. PVP was a good kinetic inhibitor.

More than 5 different types of PVP was obtained from BASF. Differences were with regard to molecular weight and molecular weight distribution. As can be seen, the best inhibitors were

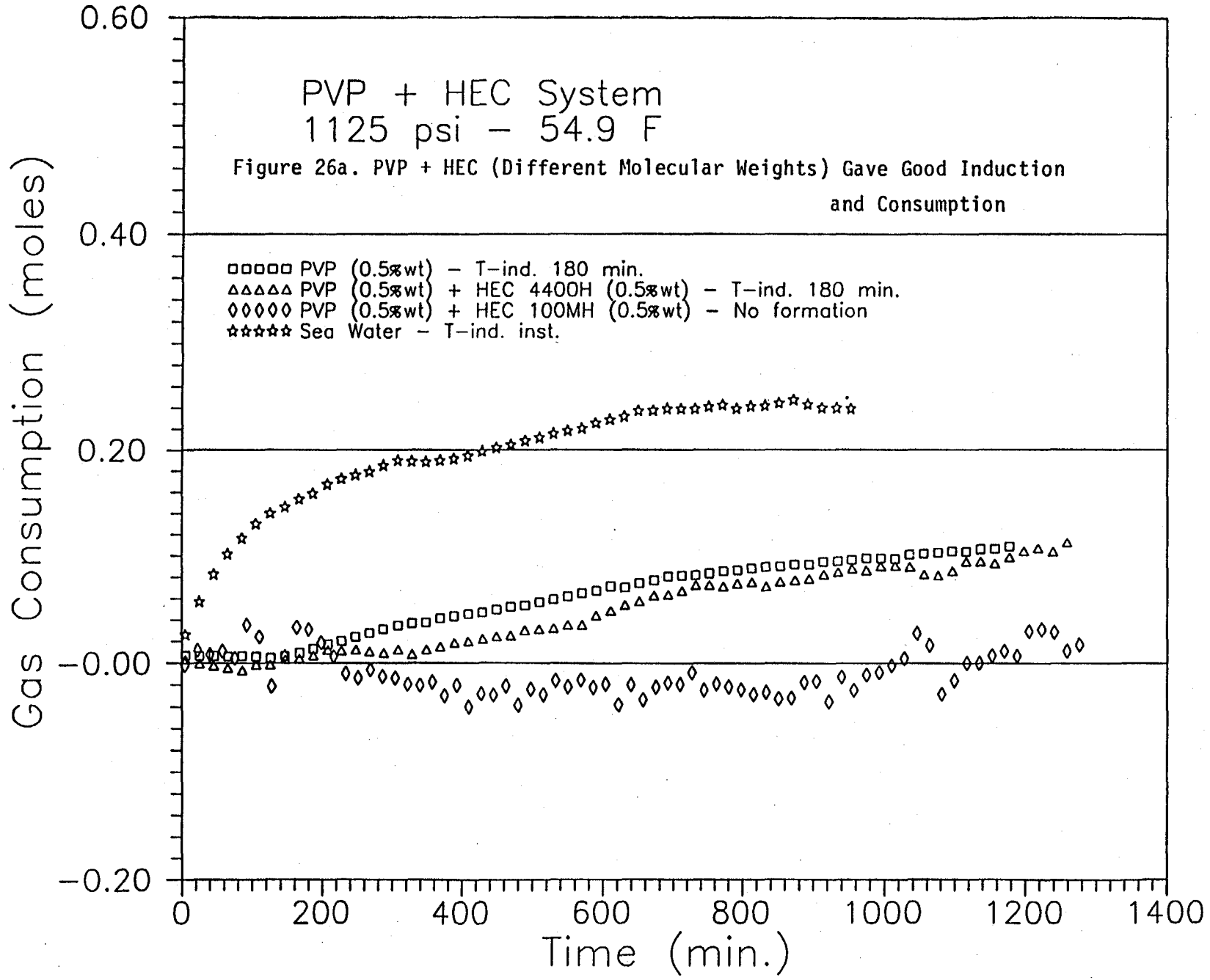

Figure 26a. PVP + HEC (Different Molecular Weights) Gave Good Induction and Consumption

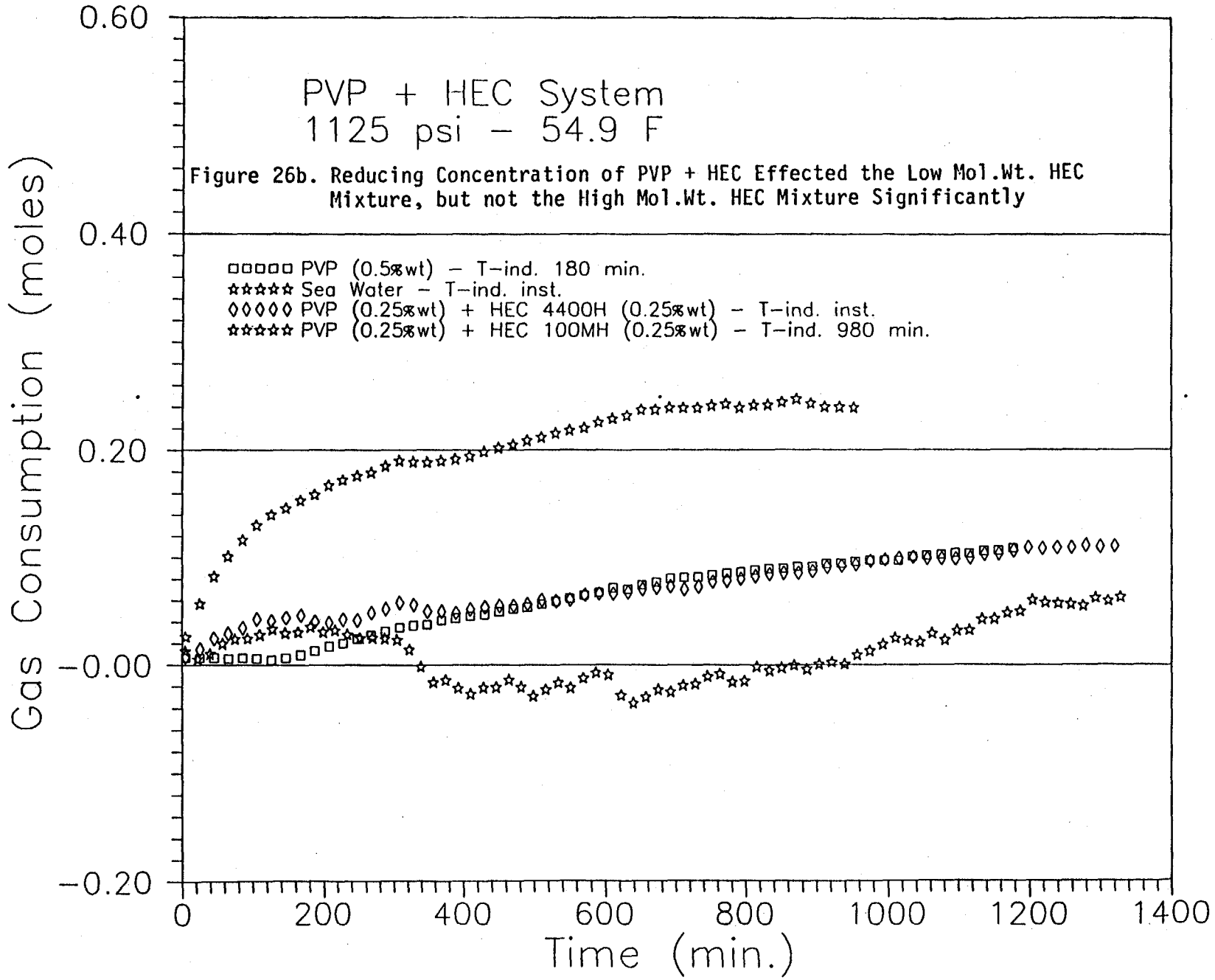

Figure 26b. Reducing Concentration of PVP + HEC Effected the Low Mol.Wt. HEC Mixture, but not the High Mol.Wt. HEC Mixture Significantly

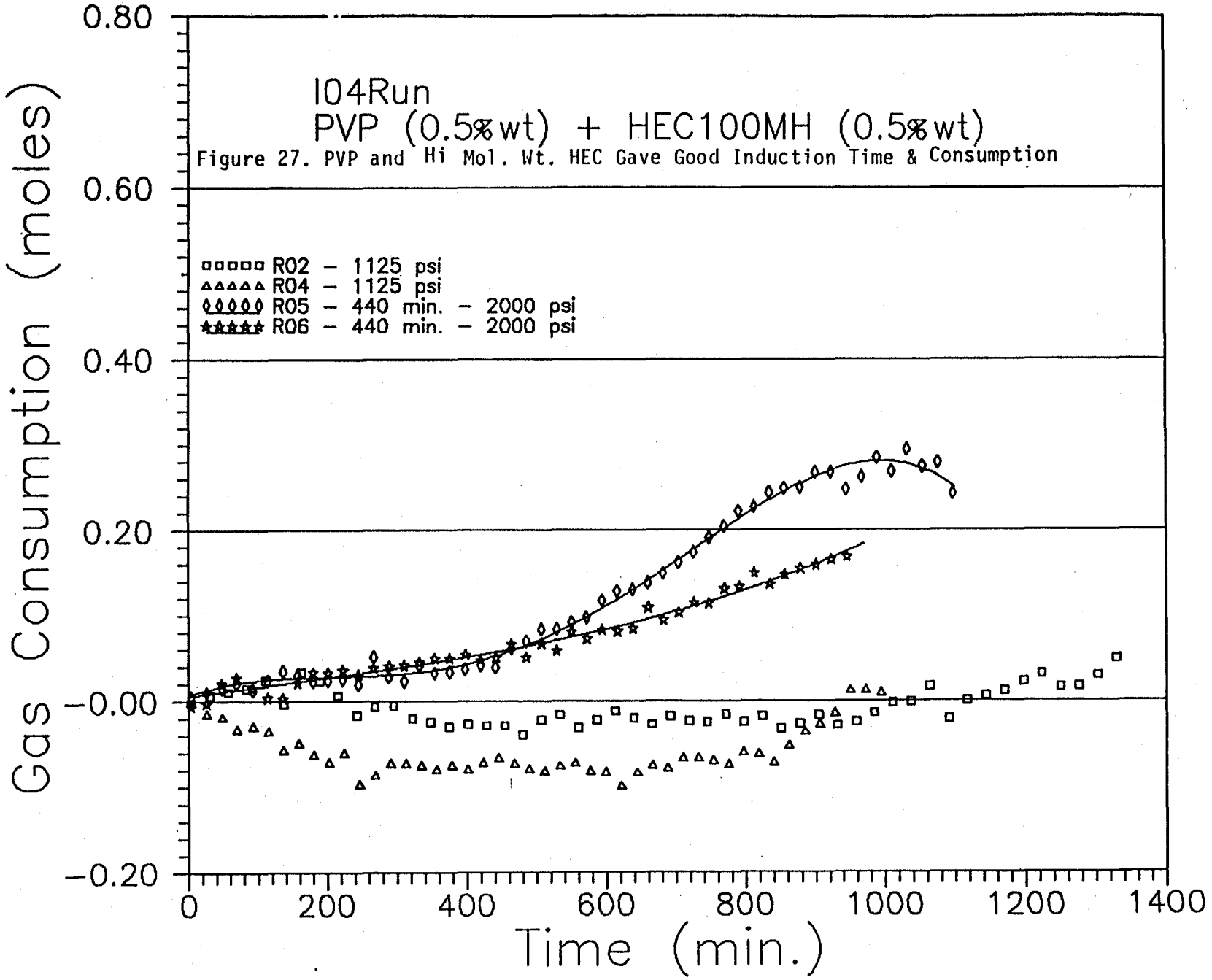

Figure 27. PVP and Hi Mol. Wt. HEC Gave Good Induction Time & Consumption

TABLE-7 PVP SENSITIVITY TEST AT HIGH PRESSURE

SOURCE: BASF **OPERATION CONDITIONS: 1125 PSI, 55 DEG. F**

TRADE NAME	MOL. WEIGHT	IND. TIME (MIN)	GAS CON. @10	COMMENTS
PVP-K17	LOW	100+/-17	0.13282	WE DO NOT HAVE THE QUANTITATIVE NO.
PVP-K30	MID. LOW	295+/-4	0.0903	FOR MOLECULAR WEIGHT
PVP-K60	MID.	300+/-10	0.11886	K60 HAS WIDE RANGE OF MOLECULAR
PVP-K90	HIGH	567+/-1	0.10275	WEIGHT DISTRIBUTION.

determined to have high molecular weights.

IV.B.3.b. Pressure, Concentration, and pH Sensitivity. A PVP concentration sensitivity test was performed on the high pressure apparatus. The lowest concentration of PVP which gave similar induction times to the 0.5wt% solution (at 1150 psig and 54.9°F) was 0.2wt% PVP. Gas consumption results suggest that PVP can only delay the nucleation period and slow down the growth period; at long times the observed gas consumption attained the same level as that in sea water without kinetic inhibition.

Sensitivity of hydrate induction times to pressure, inhibitor concentration, and pH are listed in Table 8; all experiments were performed at 54.9°F. In parentheses in the leftmost column are the designations for the polymer type (e.g. "PVP(360)" designates the 360,000 molecular weight PVP), together with the polymer concentration and the pH of the solution. The second column denotes the surfactant used in each induction test. Within each of the blocks under the heading marked "PRESSURE (psi)" in the table, repeated tests for induction time are separated with a slash "\".

In every case, the induction time decreased with increasing pressure. The second through the sixth rows of the table indicate that pH does not have a substantial effect on the induction time. In general, the lower molecular weight PVP(40) provided lower induction times than the higher weight PVP(360).

The effects of surfactant addition are shown in rows 6-21. The addition of either MT-Br, or WIT.SXS, or WIT.3065 to the polymer PVP(360) provided an increase of induction time at 2000

Table 8.

Summary of Pressure, Concentration and pH Sensitivity Tests

POLYMER	SURFACTANT		PRESSURE (psi)			
		1100	1500	2000	2500	3000
PVP (360) C=0.5%wt	None	N.O.	98/124	9/18	30/33	10/10
PVP (360) C=1.0%wt	None			40/41		
PVP (360) C=1% pH=8.5	None			54		
PVP (360) C=1% pH=2.5	None			82		
PVP (360) C=.5% pH=6	None					17
PVP (360) C=.5% pH=8	None					9
PVP (360)	MT-Br			28/38	7/8	0/0
PVP (360)	WIT.SXS		N.O..	41/47	0/6	0/0
PVP (360)	WIT. 3065		115/120	66/68	13/20	2/2
PVP (360)	WIT. 3065 C=1.0%wt					17/11
PVP (360)	Neo.45-7	90/95		5/6		
PVP (360)	TMP(B)	N.O.		0/0		
PVP (40)	None	N.O.			18/20	
PVP (40)	TMP	N.O.				
PVP (40)	TMP(B)	N.O.				
PVP (40)	MT-Br	N.O.		31	11	7
PVP (40)	SDS	N.O.		0/0		
PVP (40)	Neo.45-7	63/93		5/23		
F 127 C=0.1%wt	None	4/5				
F 127	None	3/3				
None	SDS	4/6				
None	TMP(B)	44/16				

F 127 - Bad Batch

All Induction Times in minutes

Bath Temperature = 54.86 F

Solutions Concetrations is 0.5%wt, except where noted

N.O. = Never observed during the Run Time

Base Line - DI Water at all pressures, Induction Time = 0

psig, relative to the base case (first row of table) of PVP(360). However at higher pressures of 2500 and 3000 psig, the presence of the above three surfactants appeared to decrease the induction time, relative to the base case. Similar results may be observed for PVP(360) with TMP(B) and with Neo.45-7.

It should be noted that the suite of tests indicated in Table 8 were completed prior to the discovery of the advantageous effects of HEC (Section IV.B.2.c.).

A second note is that the effects of temperature, while not tested, are anticipated to be qualitatively similar to those of pressure; that is, in every case we anticipate that lowering the temperature would cause a lower induction time at the same pressure. Preliminary sensitivity tests at lower temperatures indicated that we would have to decrease the pressure below our controllable limit, in order to achieve induction times greater than zero. Temperature sensitivity tests are yet to be done.

IV.B.3.c. Sensitivity to Gas Composition. To determine the effects of gas composition, a series of runs were performed with a second gas (herein named the Bicudo gas). The composition of the Bicudo gas differed from that of the Green Canyon gas as seen in the below table composition comparisons:

Component	Bicudo mol fraction	Green Canyon mol fraction
Methane	0.8132	0.872
Ethane	0.0884	0.076
Propane	0.0612	0.031
N-Butane	0.0061	0.008
I-Butane	0.0103	0.005
Nitrogen	0.0035	0.004
I-Pentane	0.0035	0.002
N-Pentane	0.0000	0.002
Carbon Dioxide	0.0133	0.000

Figure 28 gives the thermodynamic (pressure versus temperature) hydrate equilibrium curves for the above Bicudo gas and the standard Green Canyon gas (used for all other tests in this report). The equilibrium curves for the Bicudo gas is several degrees higher than that of the Green Canyon gas, so that the driving forces for the rate of hydrate formation should be greater for the Bicudo gas than for the Green Canyon gas at a given temperature and pressure.

Figures 29 and 30 compare three of the most interesting kinetic runs for the two gases at the normal temperature of 54.9°F but at a higher pressure of 2000 psia. Figure 29 provides a comparison of results obtained from (1) de-ionized water and (2) PVP (0.5wt%), while Figure 30 shows a comparison of (3) PVP (0.5wt%)+ HEC 100MH (0.5wt%). According to the results seen in the two figures, we conclude that composition differences between these two gases had little effect on the hydrate formation.

IV.B.3. Results With Liquid Condensate

In most industrial situations, there is always some kind of hydrocarbon condensate present in the pipeline. Therefore natural gas hydrate formation kinetics in the presence of hydrocarbon condensates should be examined. This study serves two purposes:

(1) to investigate the influence of liquid hydrocarbon on kinetics of hydrate formation, and

(2) to establish the baseline for future research with inhibitors in the system.

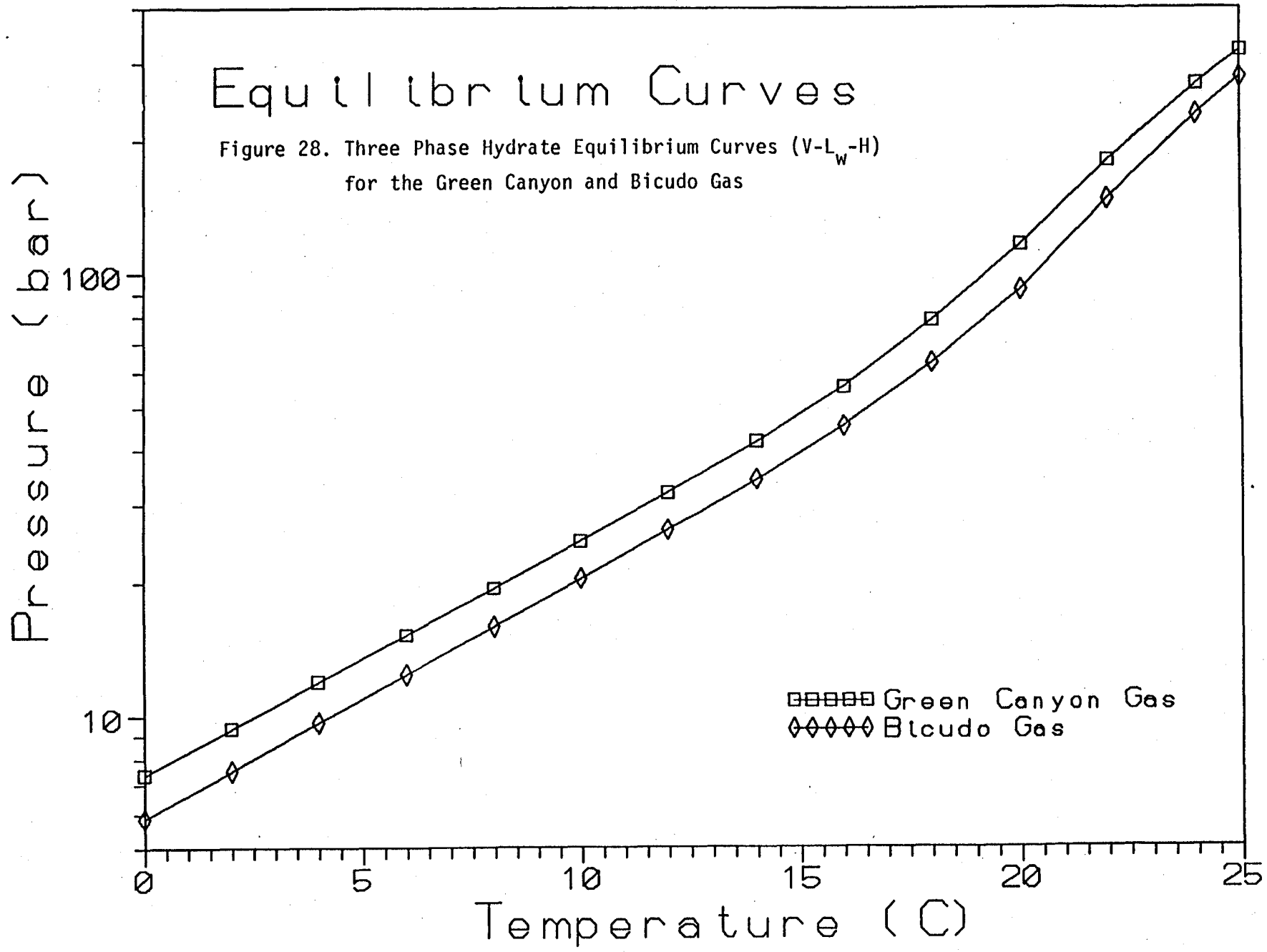

Figure 28. Three Phase Hydrate Equilibrium Curves (V-L_w-H) for the Green Canyon and Bicudo Gas

Figure 29/

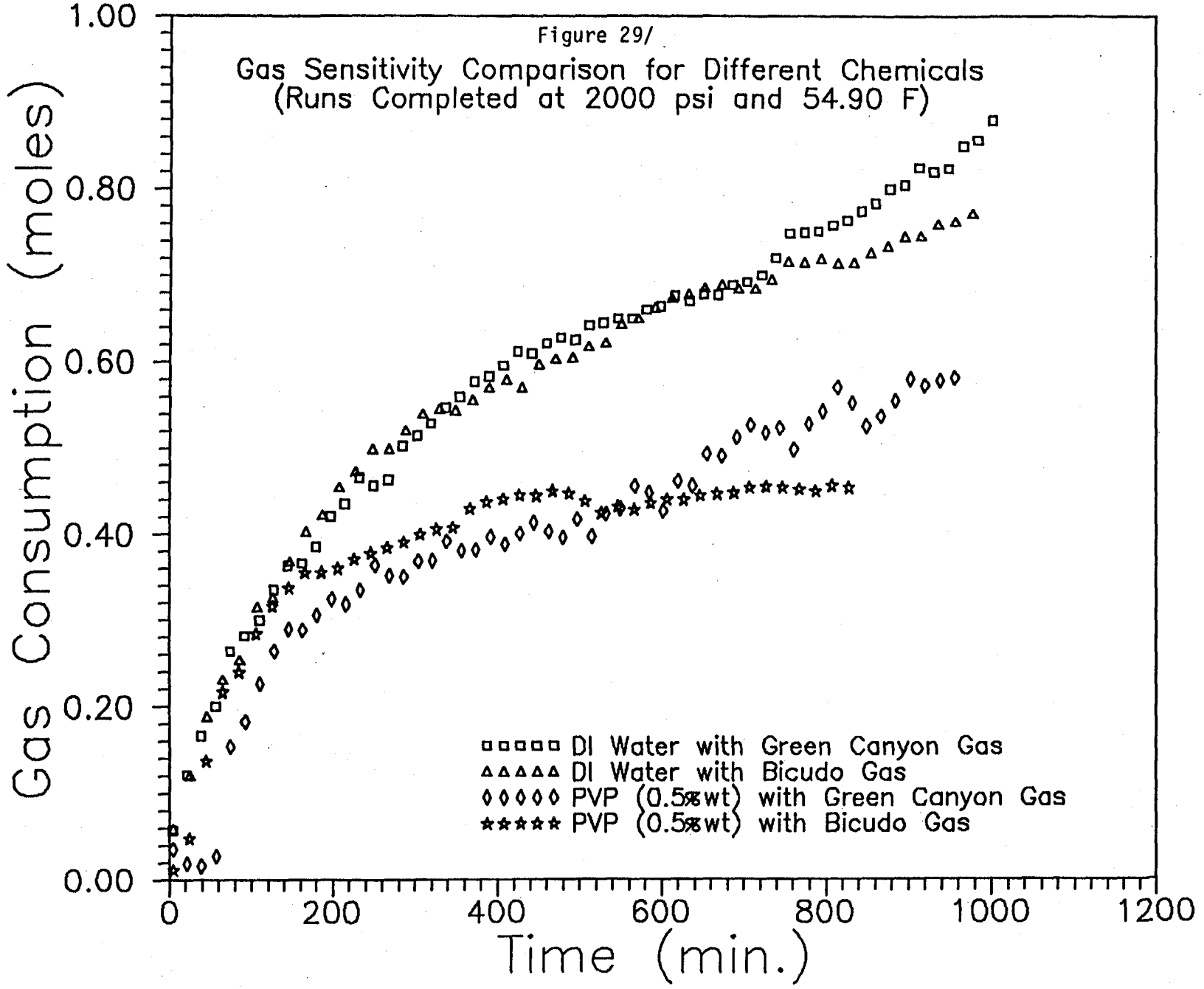
Gas Sensitivity Comparison for Different Chemicals
(Runs Completed at 2000 psi and 54.90 F)
Gas Consumption (moles)
1.00
0.80
0.60
0.40
0.20
0.00
0
200
400
600
800
1000
1200
Time (min.)
DI Water with Green Canyon Gas
DI Water with Bicudo Gas
PVP (0.5%wt) with Green Canyon Gas
PVP (0.5%wt) with Bicudo Gas

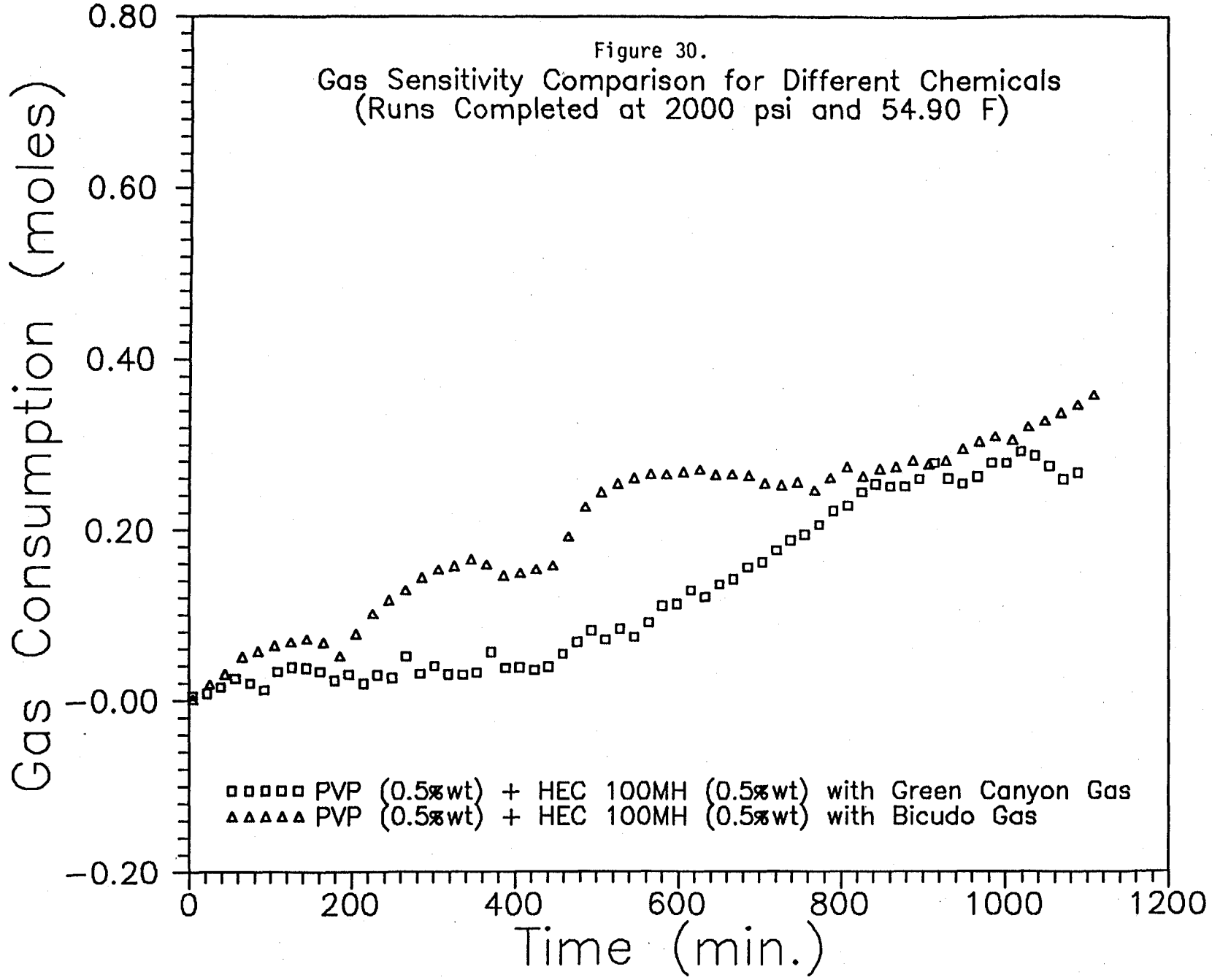
Figure 30.
Gas Sensitivity Comparison for Different Chemicals
(Runs Completed at 2000 psi and 54.90 F)
Gas Consumption (moles)
0.80
0.60
0.40
0.20
-0.00
-0.20
0
200
400
600
800
1000
1200
Time (min.)
PVP (0.5%wt) + HEC 100MH (0.5%wt) with Green Canyon Gas
PVP (0.5%wt) + HEC 100MH (0.5%wt) with Bicudo Gas

For simplicity, decane was used as a model hydrocarbon condensate. The n-decane was obtained from Aldrich Chemical Co. with a density of 0.73 g/ml and 99.0^{+}% purity. Three different systems were studied as follows:

a. Methane + D.I. Water + N-Decane,

b. Natural Gas + Pure Water + N-Decane, and

c. Natural Gas + Sea Water + N-Decane.

For each system, 4 or 5 different oil/water ratios were studied. Pure de-ionized (D.I.) Water and ASTM synthetic sea water were used in the experiments. Both 99.9% pure methane and the Green Canyon Gas indicated in Section IV.B.1. were used as supplied by Matheson.

Figure 31 is a schematic diagram which shows the operating conditions for the system. For pure methane, the operation condition was at 40.2° F and 700 psig with an equilibrium pressure of 590 psig. The over pressurization was about 110 psig and subcooling was about 3.2°F. The operation condition for the natural gas system is at 40.2°F and 700 psig with an equilibrium pressure of 180 psig, giving an over pressurization of about 520 psig or a subcooling of 20.6°F.

The tabulated experimental results are given as follows:

(a) Table-9, for pure methane + D.I. Water + n-Decane,

(b) Table-10, for natural gas + D.I. Water + n-Decane, and

(c) Table-11, for natural gas + Sea Water + n-Decane.

A typical temperature trace is given in Figure 32. For each sample, more than one experiment was performed to check reproducibility. The gas consumption was computed by total gas

Figure 31.

EQUILIBRIUM PURE GAS-WATER-HYDRATE PHASE DIAGRAM

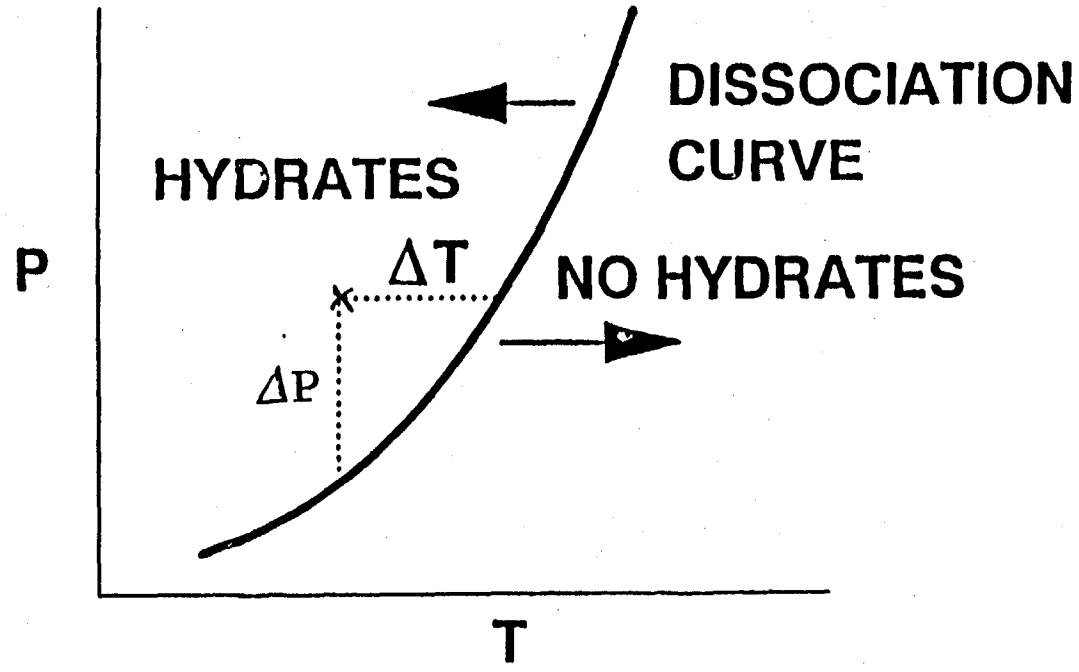

Table 9.

Date: July 29 of 1992 | Summary of Runs in HP Apparatus | DECANE-1

Directory: D:\HYDRATE\DRUN

Chemical: X ml DI Water + Y ml DECANE + Methane | Equilibrium Pressure at 40.2°F is 590 (psi)

RUN CODE	C10/H2O y//x(ml	P/T (psi)/(°F)	Induc. Time (min)	Stdev (min)	Gas Consump. Total (moL)	STDEV (mol)	Final Temp. Diff. (°F)	Reproducbility No. of Total Runs
D01	0//120	700/40.2	15.9	10.5	0.387 (hyd) 0.387	0.081	0.225	4 of 4
D02-1	10//110	700/40.2	59	13	0.543 (hyd) 0.524	0.141	0.337	3 of 3
D02-2	10//110	750/40.2	6.4	4.1	0.337 (hyd) 0.318	0.025	0.185	3 of 3
D03	40//80	700/40.2	9.1	3.5	0.235 (hyd) 0.158	0.073	0.123	3 of 4
D04	80//40	700/40.2	256	71.8	0.409 (hyd) 0.255	0.066	0.28	2 of 2
D05	100//20	700/40.2	318.3	48.5	0.307 (hyd) 0.115	0.079	0.11	2 of 2
			Solubility Data From Peng_Robinson Prediction					

Avg. Induct. Time -

Standard Deviation -

Avg. Gas Consump. -

Facts Compiled by:

Jinping Long and Amadeu Sum

Table 10.

Date: July 29 of 1992

Summary of Runs in HP Apparatus

DECANE-2

Directory: D:\HYDRATE\DRUN

Chemical: X ml DI Water + Y ml DECANE + Nat. Gas					Equilibrium Pressure at 40.2°F 180 (psi)			
RUN CODE	C10/H2O y//x(ml	P/T (psi)/(°F)	Induc. Time (min)	Stdev (min)	Gas Consump. Total (moL)	STDEV (mol)	Final Temp. Diff. (°F)	Reproducbility No. of Total Runs
E01	100//20	700/40.2	28.02	8.5	0.311 (hyd)0.053	0.07	0.103	3 of 3
E02	80//40	700/40.2	25	5	0.48 (hyd) 0.274	0.013	0.46	3 of 3
E03	40//80	700/40.2	0	0	0.351 (hyd) 0.248	0.033	0.185	3 of 3
E04	20//100	700/40.2	0	0	0.372 (hyd) 0.32	0.08	0.55	2 of 2
E05	0//120	700/40.2	0	0	0.273 (hyd) 0.273	0.082	0.29	1 of 2

Avg. Induct. Time -

Avg. Gas Consump. -

Facts Complied by:

Standard Deviation -

Jinping Long and Amadeu Sum

Table 11.

Date: Aug. 2, of 1992

Summary of Runs in HP Apparatus

DECANE-3

Directory: D:\HYDRATE\FRUN

Chemical: X ml Sea Water + Y ml DECANE + Nat. Gas					Equilibrium Pressure at 40.2°F 180 (psi)			
RUN CODE	C10/H2O y//x(ml	P/T (psi)/(°F)	Induc. Time (min)	Stdev (min)	Gas Consump. Total (moL)	STDEV (mol)	Final Temp. Diff. (°F)	Reproducbility No. of Total Runs
F01	0//120	700/40.2	0	0	0.258 (hyd)0.258	0.043	0.29	2 of 2
F02	20//100	700/40.2	0	0	0.188 (hyd) 0.136	0.044	0.15	2 of 2
F03	40//80	700/40.2	0	0	0.231 (hyd) 0.128	0.05	0.26	2 of 2
F04	80//40	700/40.2	33.3	0	0.296 (hyd) 0.09	0	0.1	1 of 1
F05	100/20	700/40.2	>517 (min)	0	0.207 (hyd) 0.0	0	0.12	1 of 1

Avg. Induct. Time -

Avg. Gas Consump. -

Facts Compiled by:

Standard Deviation -

Jinping Long and Amadeu Sum

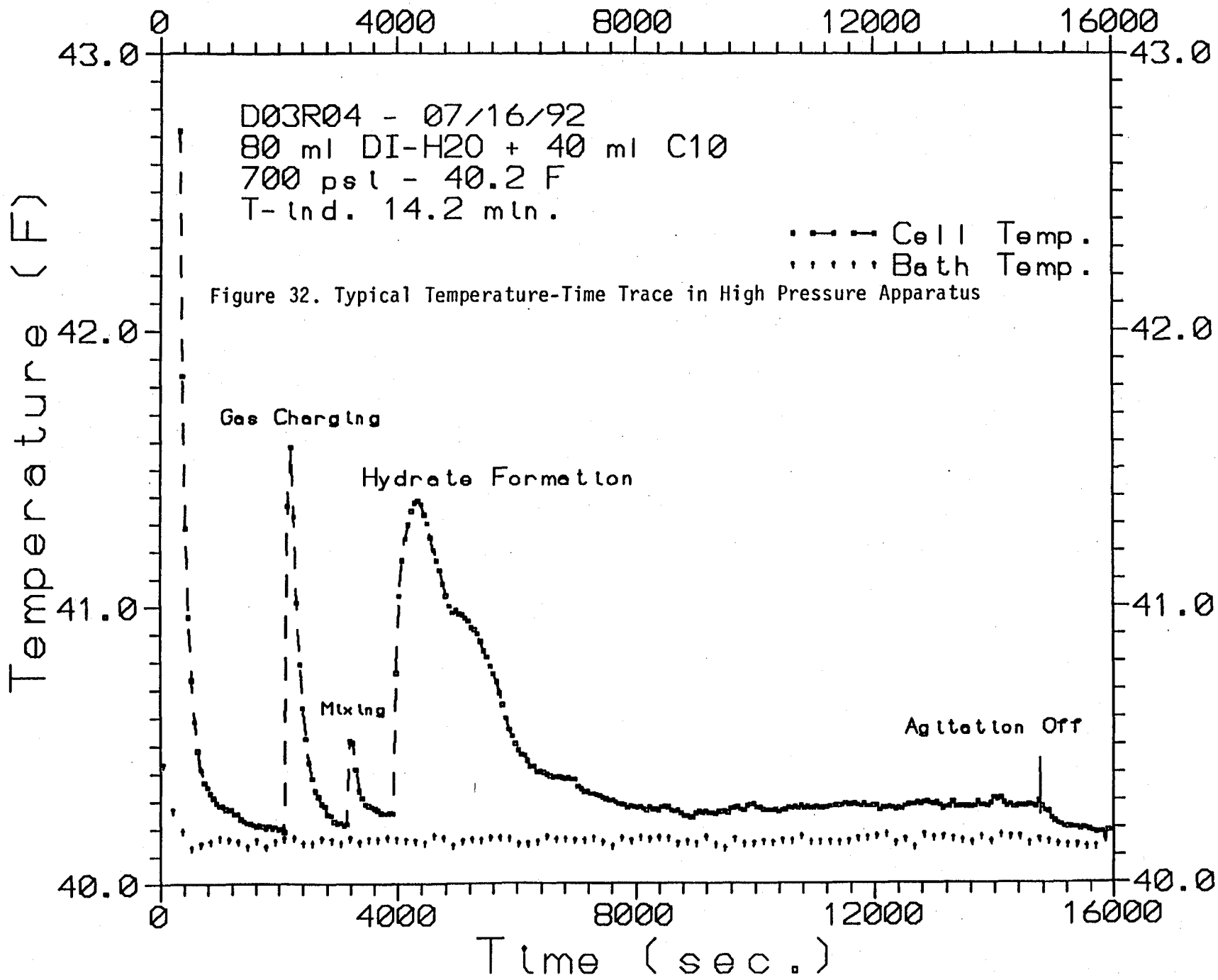

Figure 32. Typical Temperature-Time Trace in High Pressure Apparatus

consumption minus the gas consumption due to solubility effects, as calculated with the Peng-Robinson prediction program PHASE_88. The final cell temperature difference with and without agitation was also measured; this quantity was correlated with the gas consumption upon hydrate formation.

From Tables 9-11, we conclude that the gas consumption can be reproduced within 25%, and induction time can be reproduced to within 30%. A major cause of inaccuracy is our pressure control, which is only good to ± 50 psig.

Liquid n-decane has a significant influence on hydrate formation kinetics. The induction time of hydrate formation for the three systems in Tables 9-11 are shown in Figure 33-35. From these three figures we can conclude that larger oil/water ratios have longer induction times. Natural gas with sea water at the highest oil/water ratio never formed hydrates in 12 hours. There are two reasons for such phenomena:

(1) the n-decane dissolves heavy natural gas components selectively and thus shifts the equilibrium to a higher pressure. Eventually this reduces the driving force for hydrate formation.

(2) due to the immiscibility of n-decane and water, the liquid hydrocarbon may act as mass transfer barrier. Gas molecules dissolved in liquid n-decane require a longer time to transfer to the water phase.

Gas consumption was also found to be a strong function of the oil/water ratio as shown in Figures 36-38. The gas consumption was composed of two parts: (1) gas consumption due to solubility, (which is not insignificant in n-decane solution) and

Figure 33. **Induction Time vs. Volume Percent D.I. H2O + Decane + Methane**

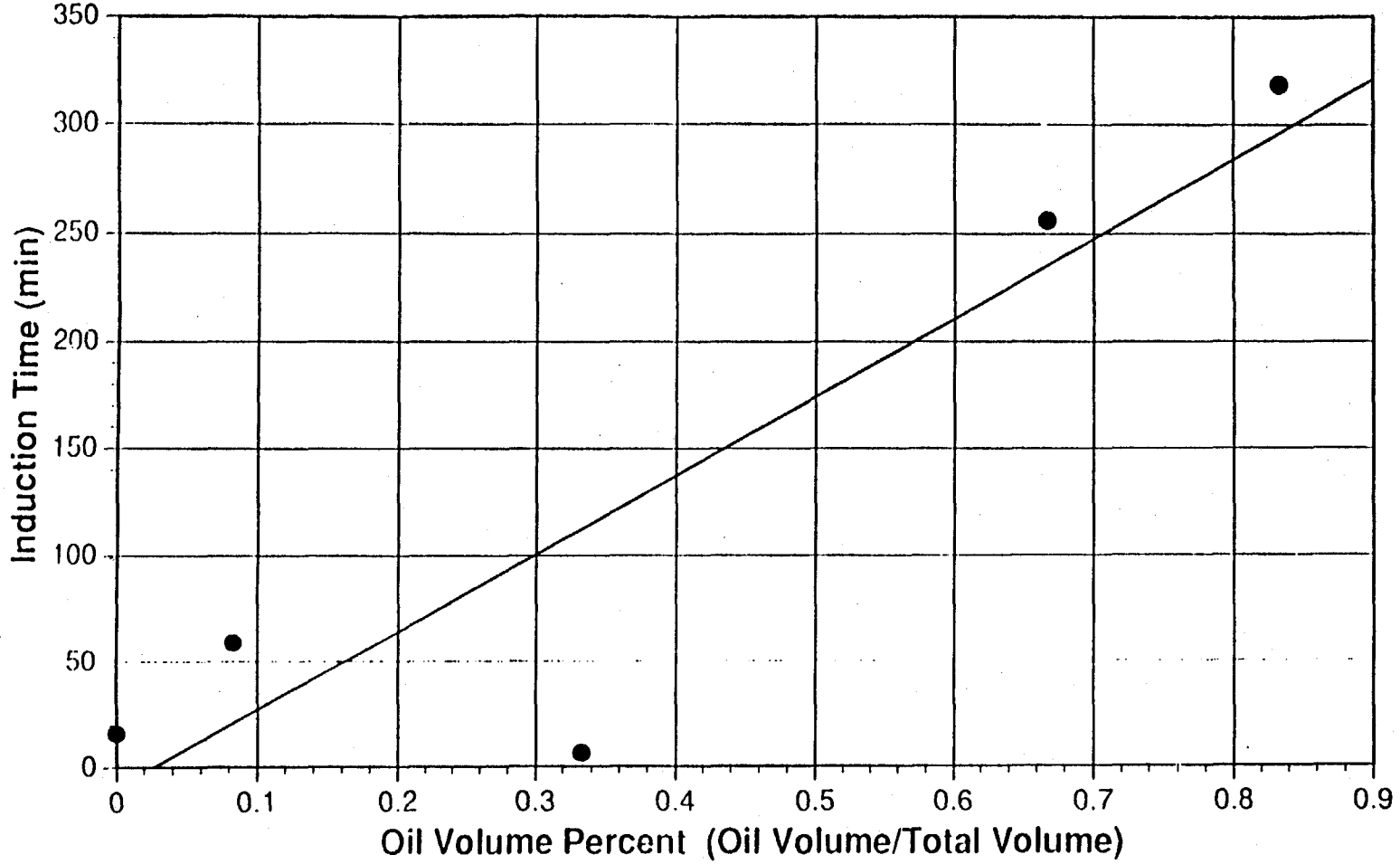

Volume Percent	0	0.083	0.333	0.833	5
INDUCTION TIME	15.9	59	6.4	256	318.3

Equilibrium pressure at 40.2 deqree F is 591 (psi). The overpressurization is about 110 (psi)

Figure 34.

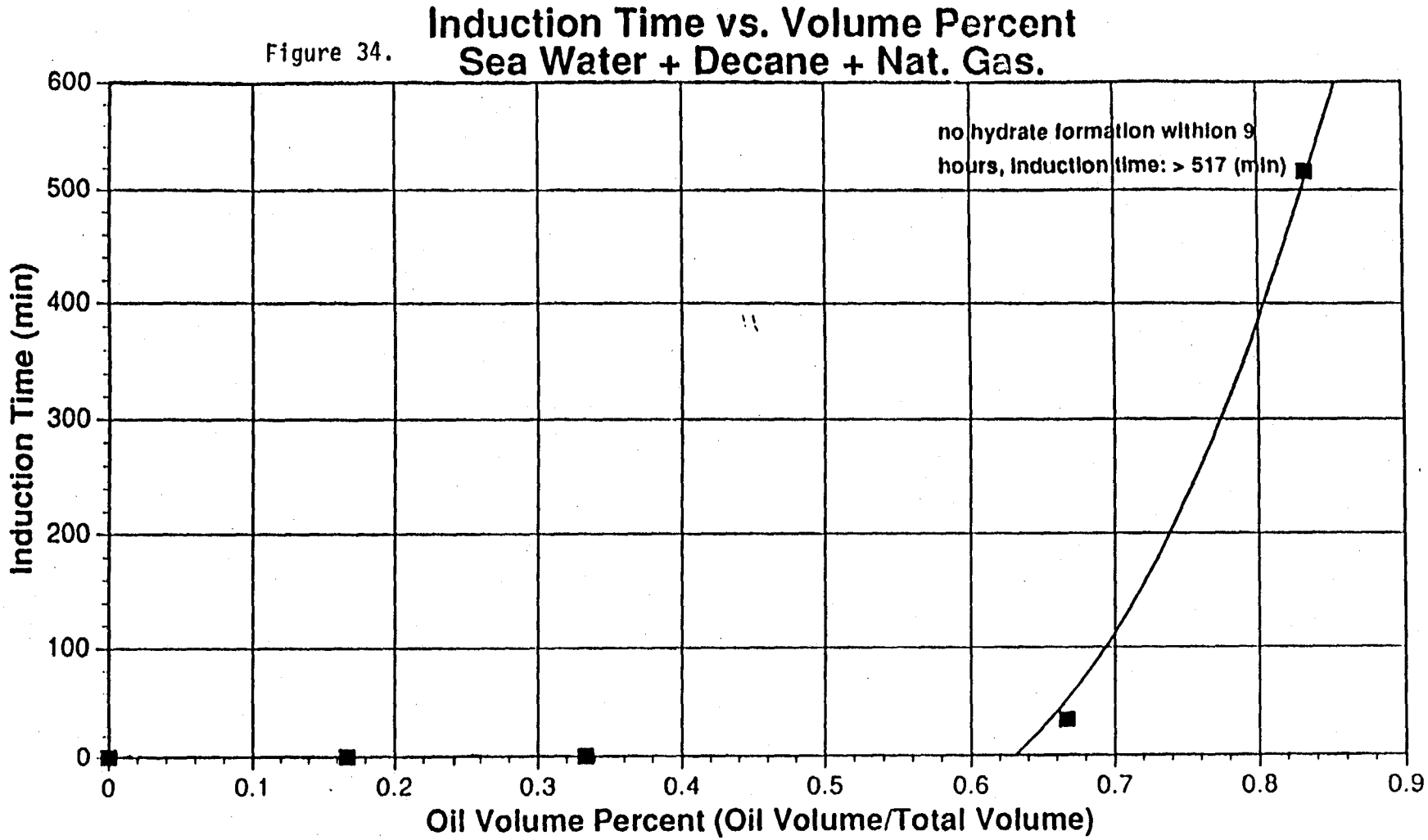

VOLUME PERCENT	0	0.167	0.333	0.667	0.833
INDUCTION TIME	0	0	0	33.3	>517

Equilibrium Pressure at 40.2 degree F is 180 (psi). Overpressurization is about 520 (psi)

Figure 35. **Induction Time vs. Volume Percent D.I. Water + Decane + Nat. Gas.**

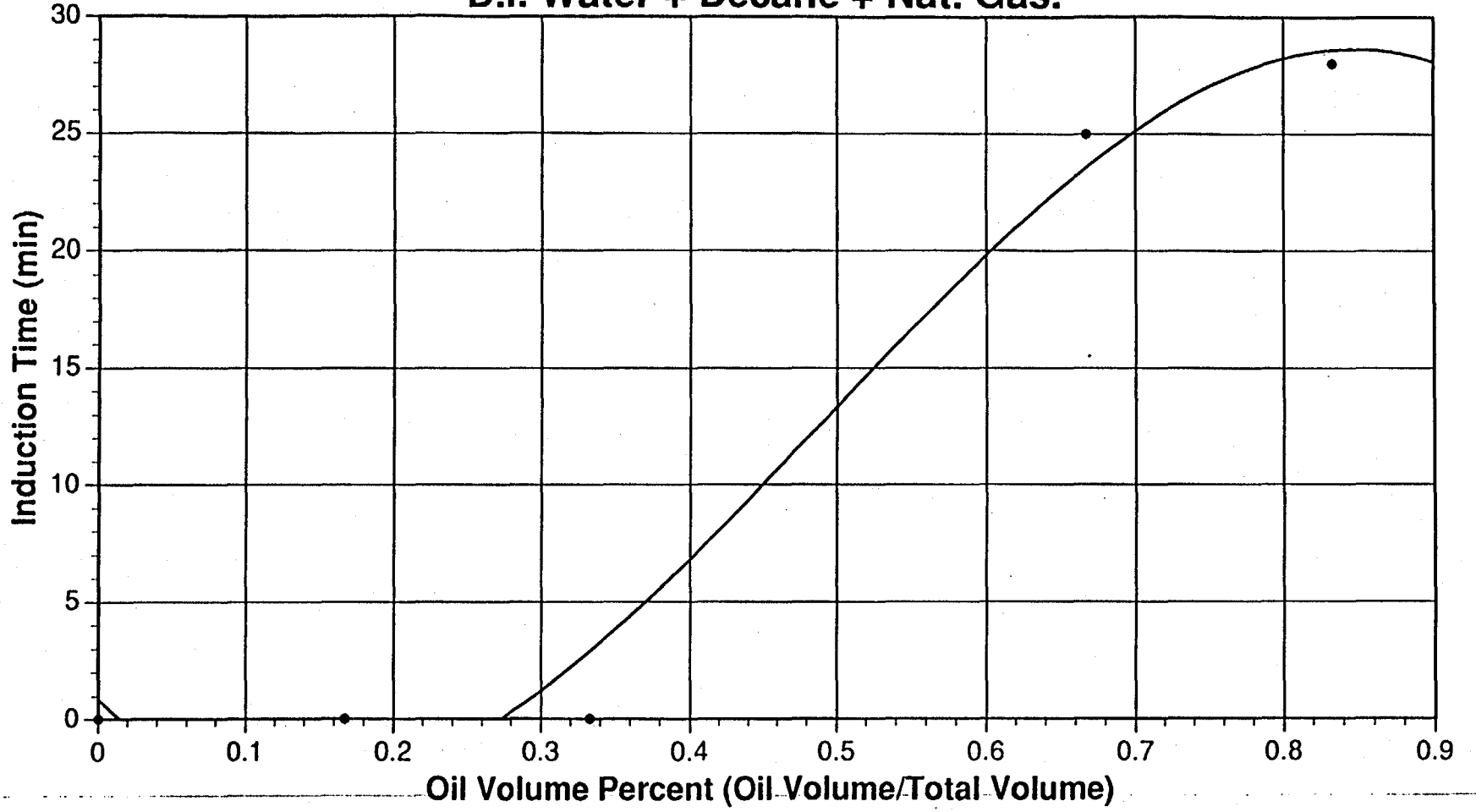

VOLUME PERCENT	0	0.167	0.333	0.667	0.833
INDUCTION TIME	0	0	0	25	28.3

Equilibrium Pressure at 40.2 degree F is 180 (psi). Overpressurization is about 520 (psi)

Figure 36. Gas Consumption vs. Water Volume Percent
D.I. Water + Decane + Methane

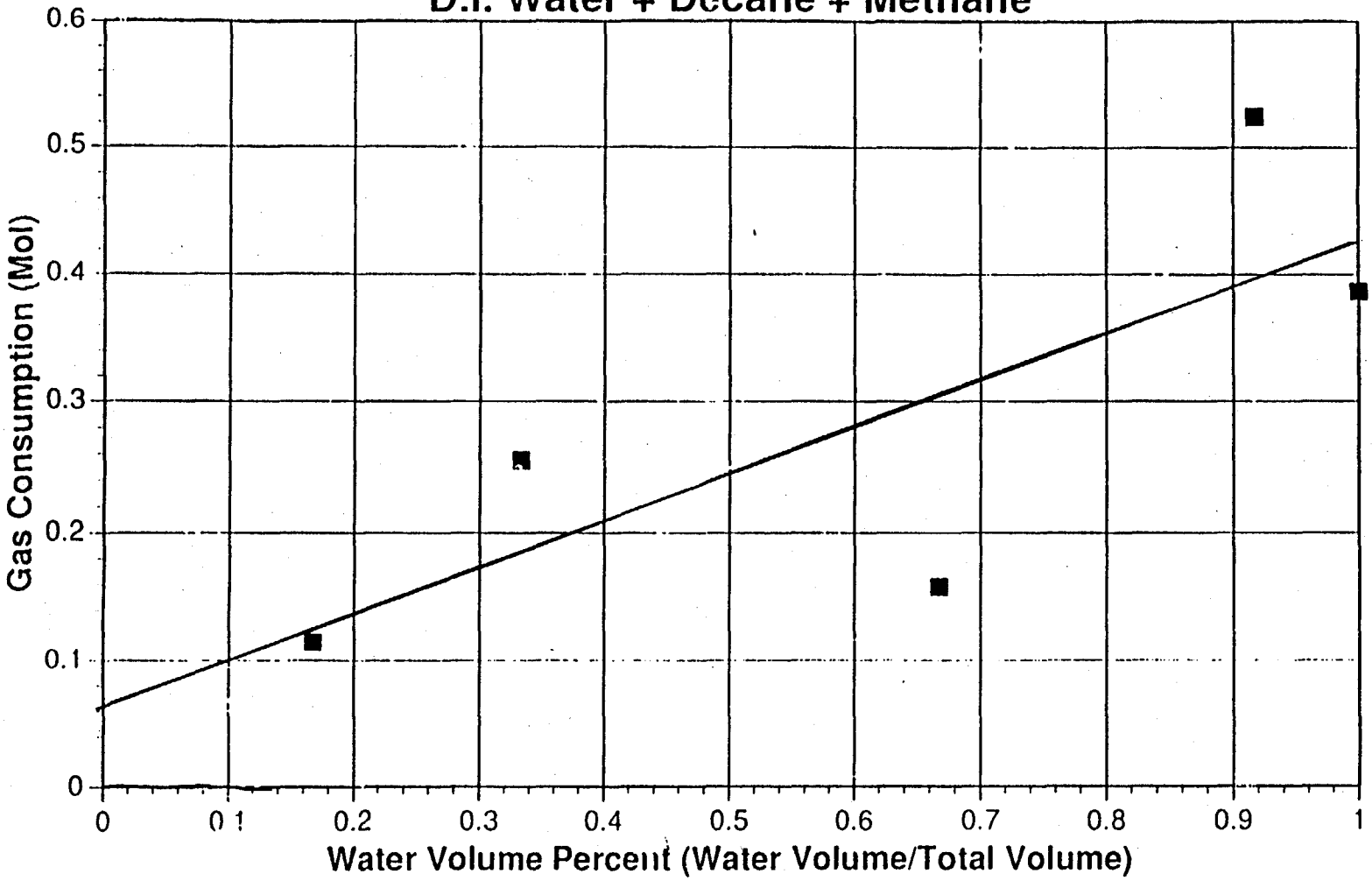

Volume Percent	1	0.9167	0.667	0.333	0.167
GAS CONSUMP. (MOL)	0.387	0.524	0.158	0.255	0.115

Equilibrium pressure at 40.2 degree F is 590 (psi). The overpressurization is anout 110(psi)

Figure 37. **Gas Consumption vs. Water Volume Percent**
D.I. Water + Decane + Nat. Gas

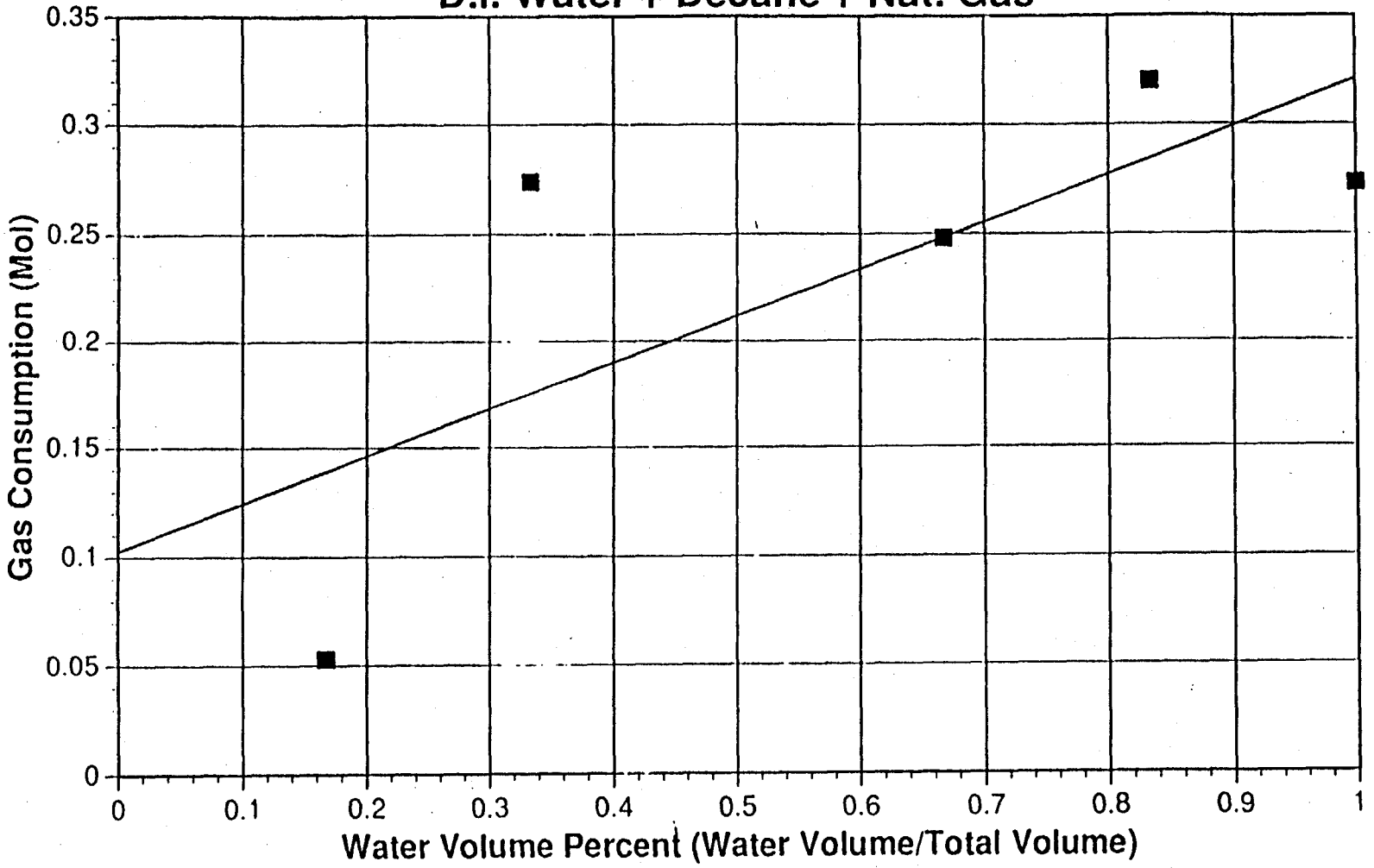

Volume Percent	1	0.833	0.667	0.333	0.167
GAS CONSUMP. (MOL)	0.273275	0.32	0.248	0.274	0.053

Equilibrium pressure at 40.2 degree F is 180 (psi). The overpressurization is anout 520 (psi)

Figure 38 Gas Consumption vs. Water Volume Percent
Sea Water + Decane + Nat. Gas

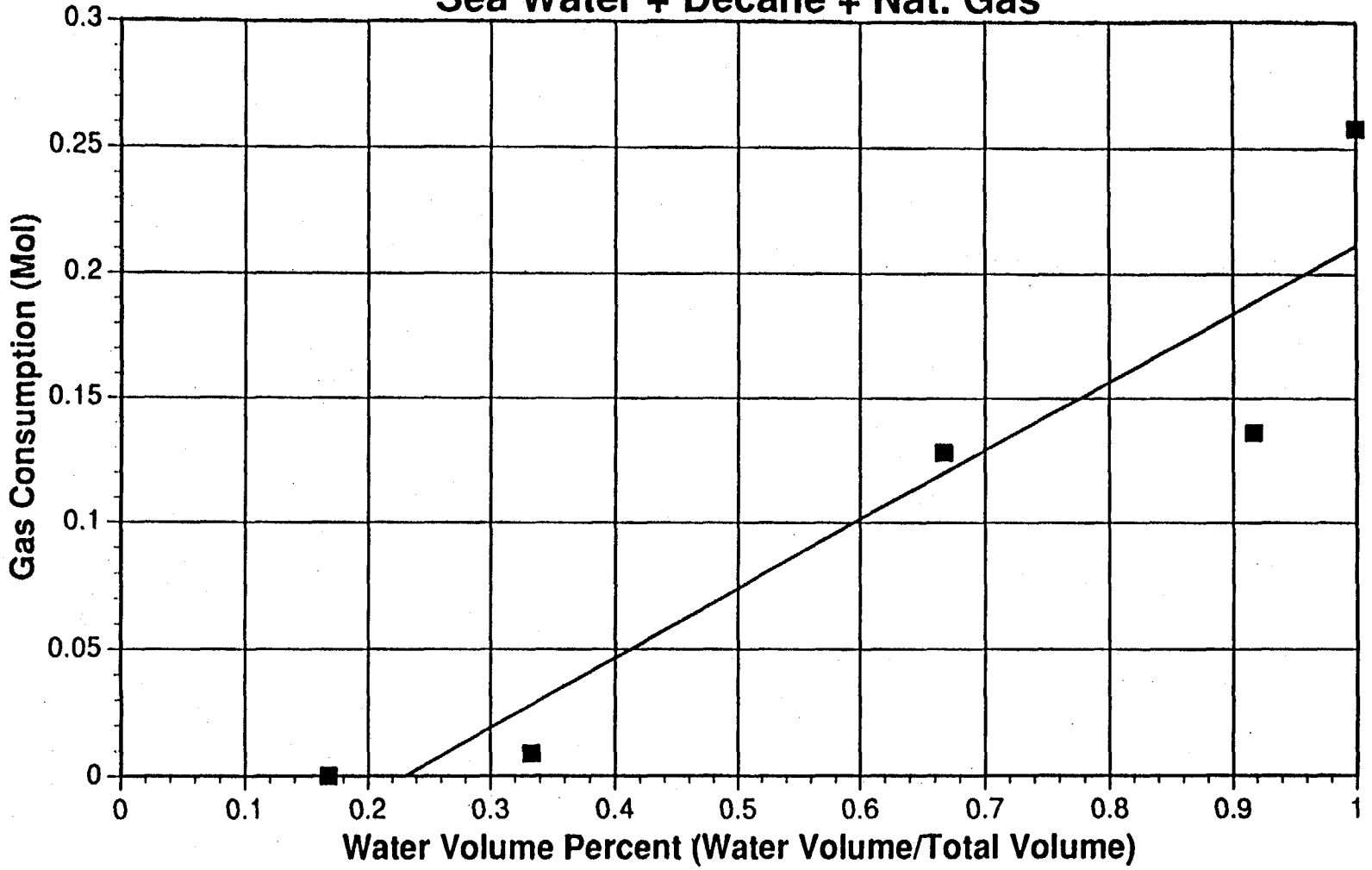

Volume Percent	1	0.9167	0.667	0.333	0.167
GAS CONSUMP. (MOL)	0.258	0.136	0.128	0.009	0

Equilibrium pressure at 40.2 degree F is 180 (psi). The overpressurization is anout 520 (psi)

(2) hydrate formation. The amount of gas forming hydrates will decrease as the oil/water ratio is increased. One of the reasons for this is that the absolute amount of water differs. A second reason is that the oil/water ratio may also determine the phase distribution (internal or external) of oil and water.

An separate video tape study was conducted with a glass test tube to examine such phase distribution with mixing. At an impeller revolution of 1000 rpm, the oil/water solution was well mixed, so that it was not possible to visually identify the internal or external phases; it appeared homogeneous. The gas consumption at high oil/water ratios suggests that water is the internal phase. The possibility of gas and water contact is significantly decreased in such systems.

The final cell temperature difference between agitation and no agitation is depicted in Figure 39 for the three systems with decane (listed in Tables 9-11). This temperature difference ΔT is caused by viscous heat dissipation. The ΔT quantity can be qualitatively correlated with the amount of hydrate formed. If the solution were homogeneous, we might be able to obtain the viscosity. However we do not have knowledge of the hydrate morphology in the system, and thus it is difficult to use this information further. The other point is that this temperature difference is too small ($<0.5\ ^{\circ}F$) in our system to quantify inhibitor performance.

This part of the work established the baseline for the system in the presence of n-decane. A more extensive study of inhibitor performance with condensate will follow.

IV.C. Simulation of Hydrates and Inhibition

IV.C.1 Simulating a Hydrate-Water Interface

Since the phenomena of hydrate formation occurs on a molecular level, it would be very useful to be able to see what actually happens at this small scale. Unfortunately, it is not possible to conduct laboratory experiments with a limited number of molecules, and observe these microscopic phenomena. Computer simulation provides a means of modeling systems with a few hundred or a few thousand molecules and following their behavior over time.

In the annual report for 1991, it was proposed to set up solid - liquid interfaces between solid structure I and structure II hydrate crystal and liquid water saturated with a hydrocarbon. Earlier work by Karim and Haymet (J.Phys.Chem.,6889,88,1988) set up an ice - water interface and thus provided the basic model for this work. The Karim and Hamet work was duplicated, and then extended to solid hydrates. Interface simulations have been completed for both structure I and structure II hydrates.

Figure 40 shows the ice - water interface, and Figures 41 and 42 show the structure I and structure II interfaces respectively. When regarding these figures, it is important to remember when that these three dimensional figures represent boxes containing the molecules. However, the ordered structure of the crystal solid becomes much more clear when one looks

Figure 39. Comparison Between Natural Gas Hydrates in D.I. Water and Sea Water, Methane hydrates in D.I. Water

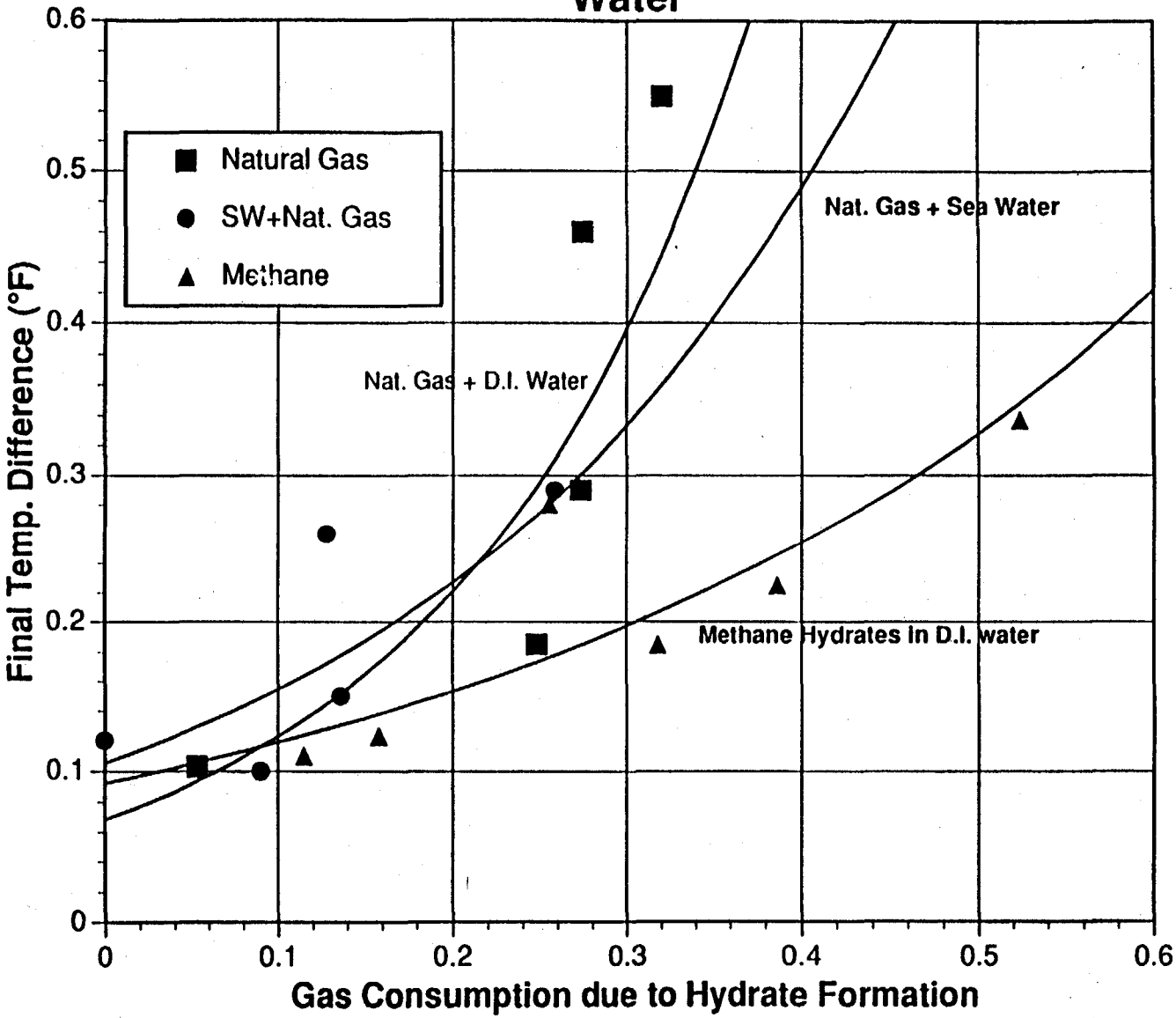

orthogonally at the parallelepiped; i.e., when the front of the box and the back of the box exactly line up.

Our interface models began with the parallelepiped entirely in the solid state. The box was then arbitrarily divided into three equivalent sections along the vertical (long) axis. At this point, all of the molecules in the top and bottom sections were artificially constrained to be fixed in their lattice positions. The temperature was then raised by increasing the translational and rotational motion of the unconstrained molecules, located in the middle section of the box, with the effect of melting the solid crystal. The motions of the molecules increased to the point that they break out of their lattice positions, and their configurations take on the random nature of a liquid.

At this point, it is necessary to allow sufficient time for residual ordering from the previous solid state to totally dissappear. When the central portion of the box has completely melted and is in the liquid state, the system is cooled back down and the artificial constraints that had been placed on the top and bottom sections are removed. It is also necessary to remove the tremendous excess of non polar molecules from the middle section; otherwise they would be rejected from the melted water phase (the hydrocarbon solubility in water is very low). Of the 64 "guest" hydrocarbon molecules now distributed randomly in the liquid, 62 of them are removed from the system, leaving only two in the liquid water. With the artificial constraints removed, the system is allowed to re-equilibrate, and after a sufficient

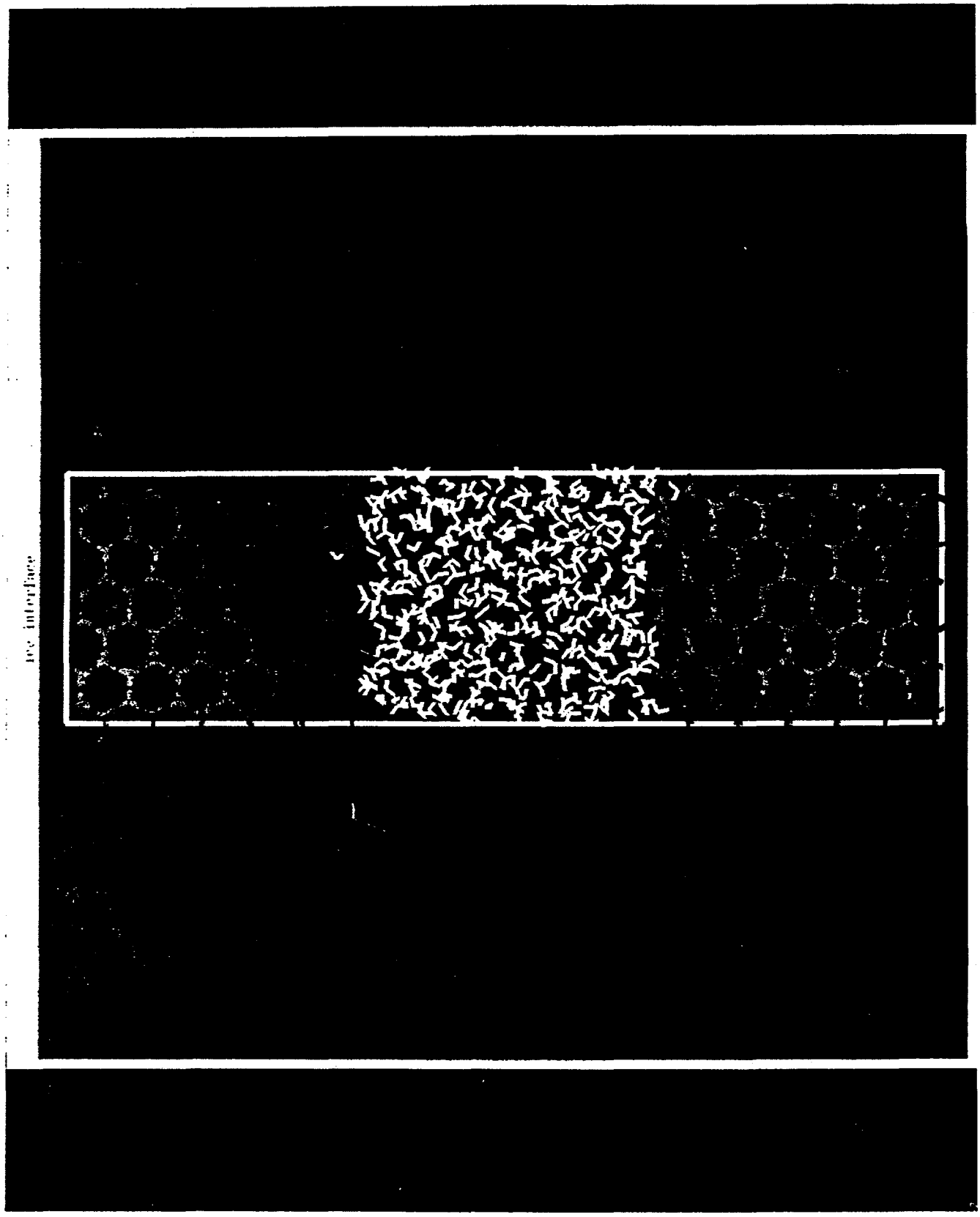

Figure 40. An Ice-Water Sandwich

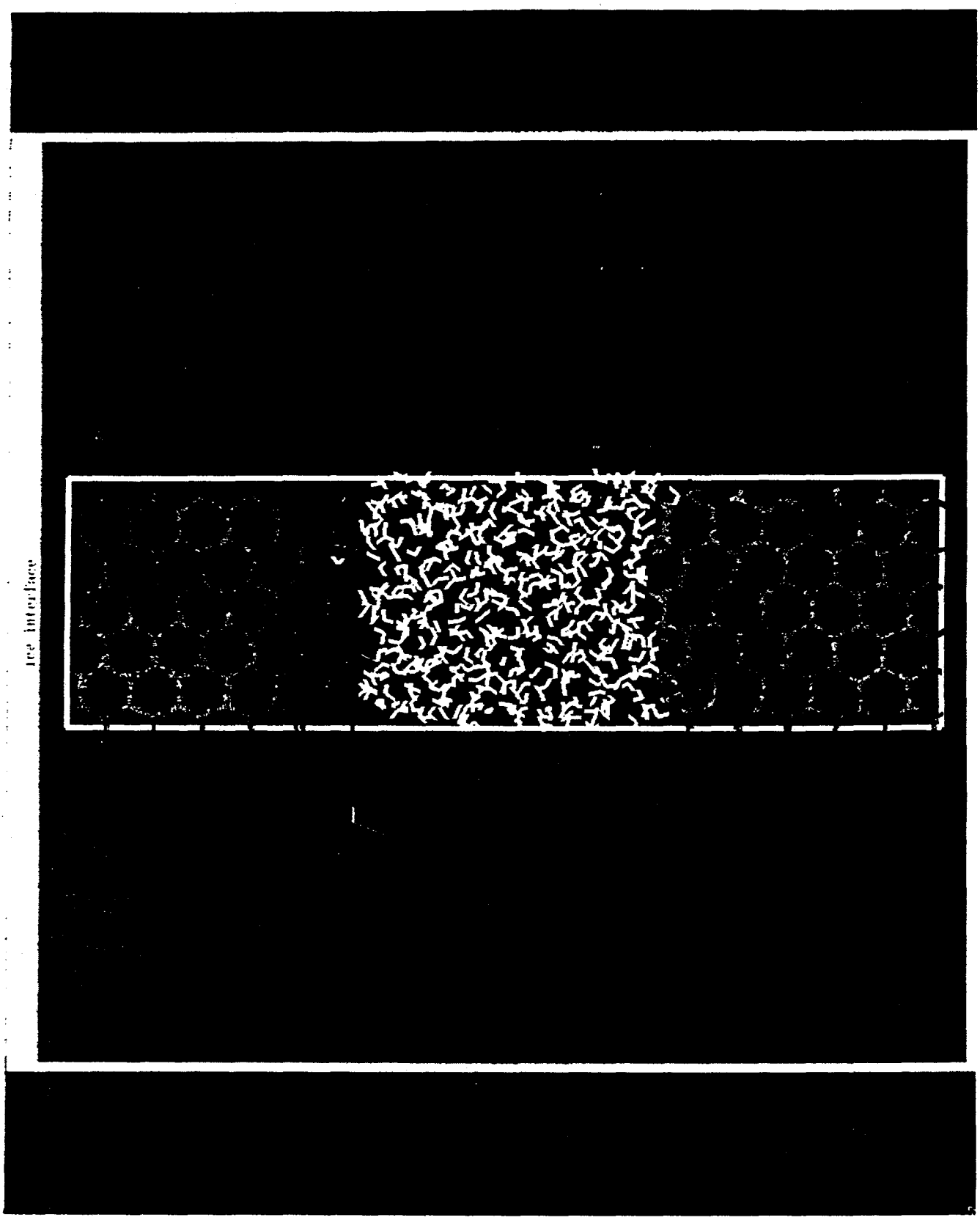

Figure 40. An Ice-Water Sandwich

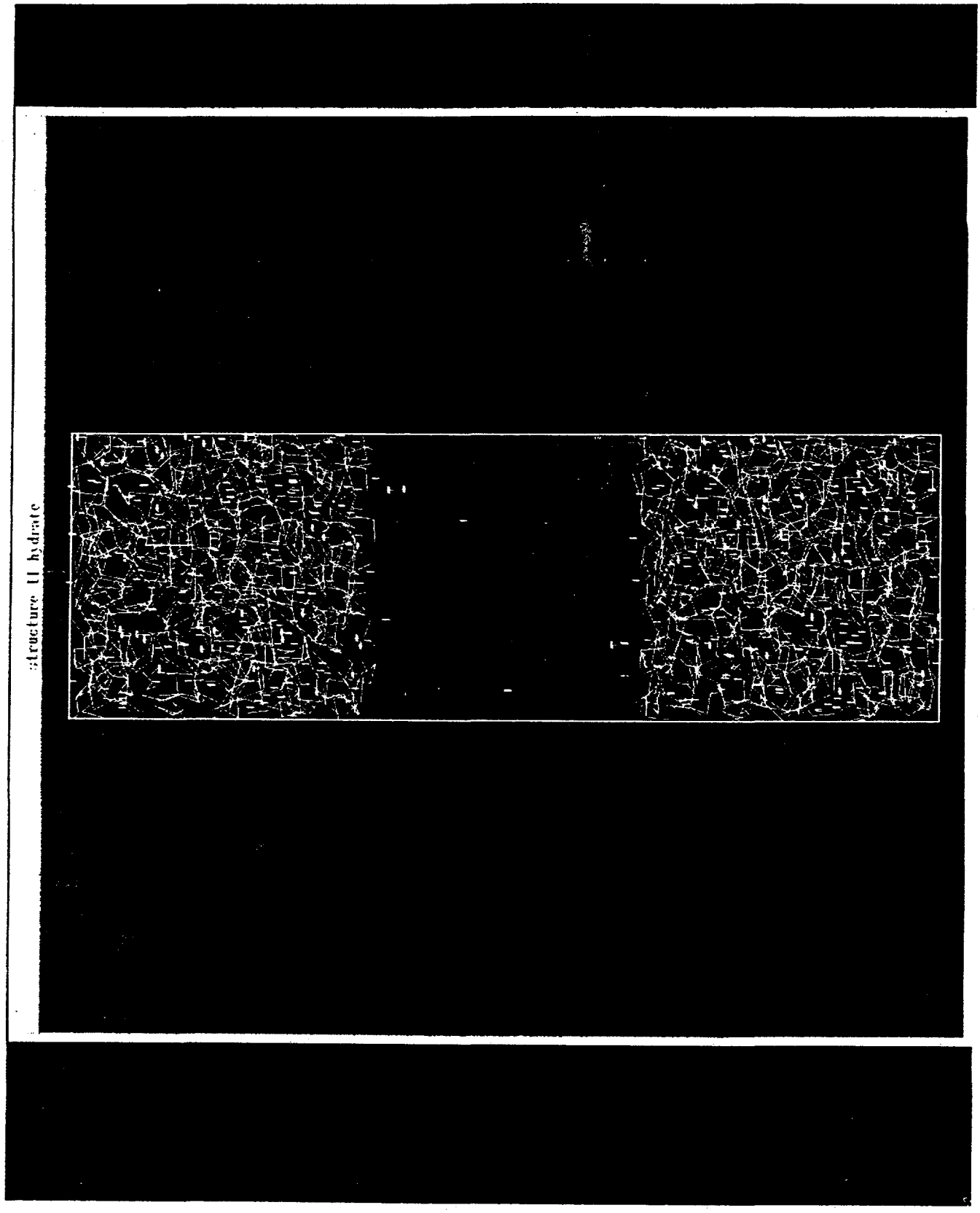

Figure 42. A SII - Water Sandwich Simulation Result

length of time, the solid - liquid interface has been established.

Ideally, as a result of performing these interface simulations, we would like to be able to observe hydrate crystal growth, i.e., we would like to be able to gradually lower the temperature of the system by reducing the kinetic motion of the molecules, and observe growth along the interface. Unfortunately it has not been possible to observe such crystal growth. Inherent in computer simulations is the constraint to work with very small time spans. For example, a run which takes up to a week to run on our IBM RISC Model 570 computer, only covers about 40 pico-seconds of real time. This time period is not sufficient to observe the growth of an ordered crystal from bulk liquid water. As one lowers the temperature of the system, the liquid molecules simply freeze into a glass; they freeze into random liquid configurations.

It is possible to observe property changes as one moves from the bulk water towards the interface and from the bulk solid toward the interface. From Figures 40-42, one can observe that the solid structure becomes less "perfect" as one moves toward the interface. By dividing the box in thin slices, each slice parallel to the interface, one can calculate molecular properties such as mean square displacements. One indeed observes that the transition from solid to liquid is somewhat gradual, i.e. effects can be observed a few angstroms on either side of the interface.

It was also mentioned in the last annual report, that we wish to use these interface simulations as a means of observing

the effect of various polymers and surfactants. Specifically, we wished to place an inhibitor molecule, such as a polymer or a surfactant at the interface, to observe how this molecule could prevent hydrate growth. Since it is not possible to simulate hydrate growth, we are restricted to observing the interactions between the inhibitor molecule and a static face of solid hydrate. To do this realistically would involve a tremendous use of computer time, and it has been decided in the meanwhile to consider the use of a commercially available software package for molecular modeling, to continue these investigations as molecular docking studies.

IV.C.2. Beginning Chemical Docking Studies

With the aid of Shell Oil as an industrial partner, we have obtained SYBYL, a commercial program marketed by Tripos Associates in St. Louis. We currently have a demonstration version of SYBYL which we have evaluated for about two months, and we feel it is suitable for continuing our molecular studies. An important feature of SYBYL is that we can use the molecular configurations generated by the previously discussed interface simulation programs as input to SYBYL. SYBYL also facilitates the building of polymer chains and monomers of specified length, configuration, and tacticity. It is a reasonably smooth transition to model the effects of kinetic inhibitors and solid hydrates.

Thus far, conclusive studies have been carried out with the aid of SYBYL concerning various monomers. We have initially

studied various "docking" configurations for each atom of monomer portions of inhibitors such as PVP with the atoms in a pentagonal hydrate face. As a result of these initial studies, we conclude that no orientational configuration of the monomer to the pentagonal face is preferred.

It is anticipated that the inhibiting effect of certain polymers and surfactants is due not to characteristics of the monomers, but due to the effect of long molecular chains. As of now, no preference of inhibitors can be observed, based on monomeric models. It is felt that we need to continue these studies with larger polymer units, and such studies are currently underway.

IV.D. Raman Spectroscopic Studies

In order to understand how hydrates form, from a molecular point of view, we need a means of determining the microscopic structure as well as intermolecular and intramolecular interactions. Raman spectroscopy has proven to be a successful analytical tool to obtain such microscopic information. In more common FTIR spectroscopy, the spectra of the water interferes with some of the hydrate spectra.

Based on the screening studies in our group, we chose tetrahydrofuran (THF) for our hydrate former, as an analog to natural gases. THF hydrates have the following attributes which aid in experimental viability: (1) THF hydrates form at

atmospheric pressure, (2) the melting point of the THF hydrates is 278 K, (3) the complete miscibility between THF and water.

IV.D.1. Experimental Method.

We used an Ar+ laser as our source to excite the molecules in Raman spectroscopy and a double dispersion spectrometer to measure the Raman scattering. The wavelength of the laser line was 514.5 nm. Under most situations, the laser power used was 170 MW and the slit width of spectrometer was 400 micron. A custom glass cuvette water jacket was used as our sample container. Methanol was our coolant.

In our experiment, we first cooled the THF+H2O mixture to -10°C, to provide enough supercooling to initialize the crystallization process. After we formed hydrates, we slowly warmed it back to just below the melting point, and allowed the system temperature to become stable before performing the measurements.

Different THF to H2O ratios were used to determine the sensitivity of the spectral response. The results of these spectra are given in Figures 43, 44, and 45. Concentration differences introduce very fine changes in the peak position of the C-O-C stretch mode and the interaction coupling peak position. The convoluted peak shape of the O-H stretching band involves very complicated coupling between hydrogen-bonded water molecule and non-hydrogen-bonded water molecule. These spectra were obtained under the same temperature and pressure.

We also studied the temperature effect for three cases: (1)

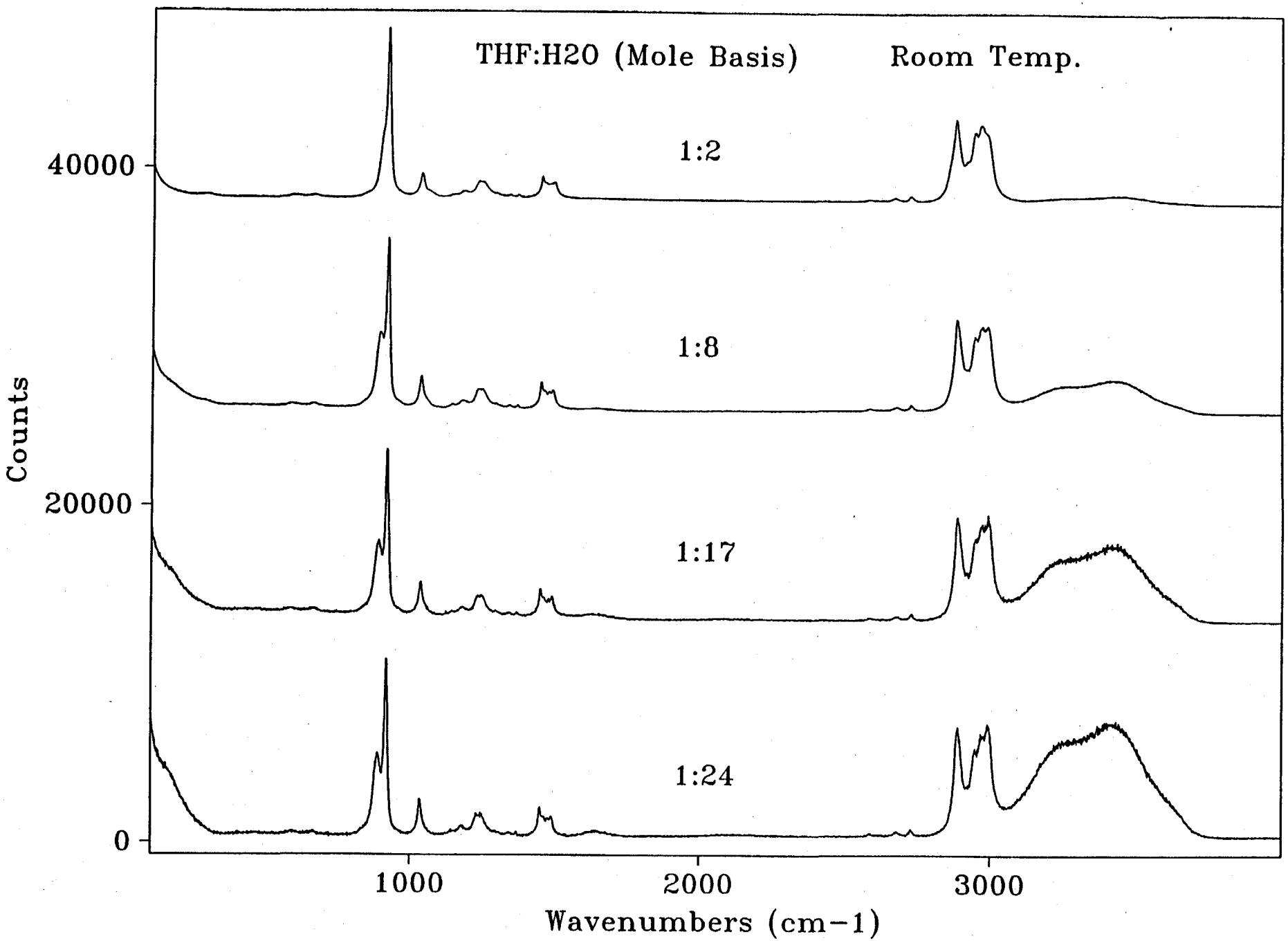

Figure 43. Raman spectra of THf+H20 solu. at diff. THF concentration

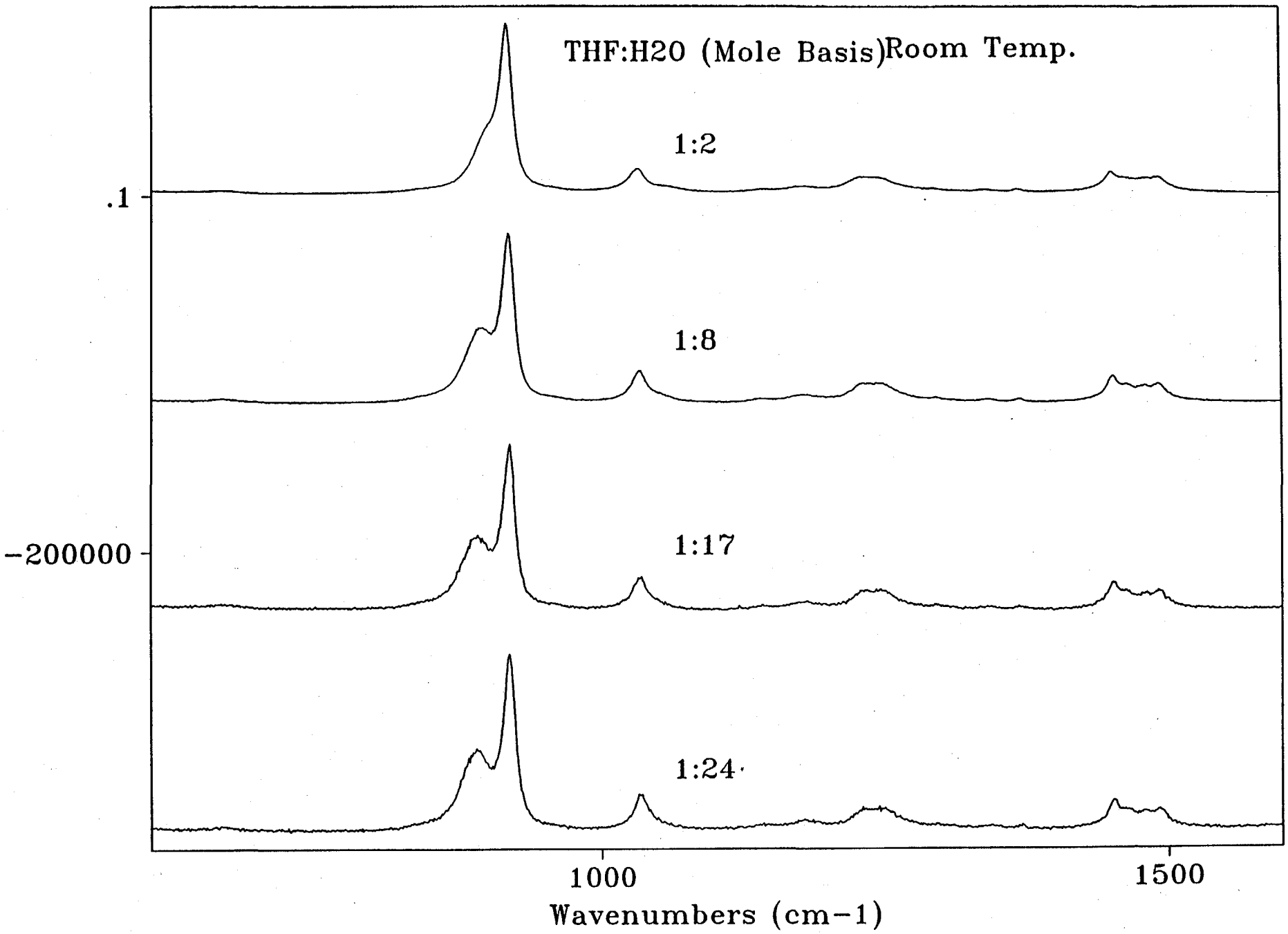

Figure 44. Raman spectra of THf+H20 solu. at diff. THF concentration

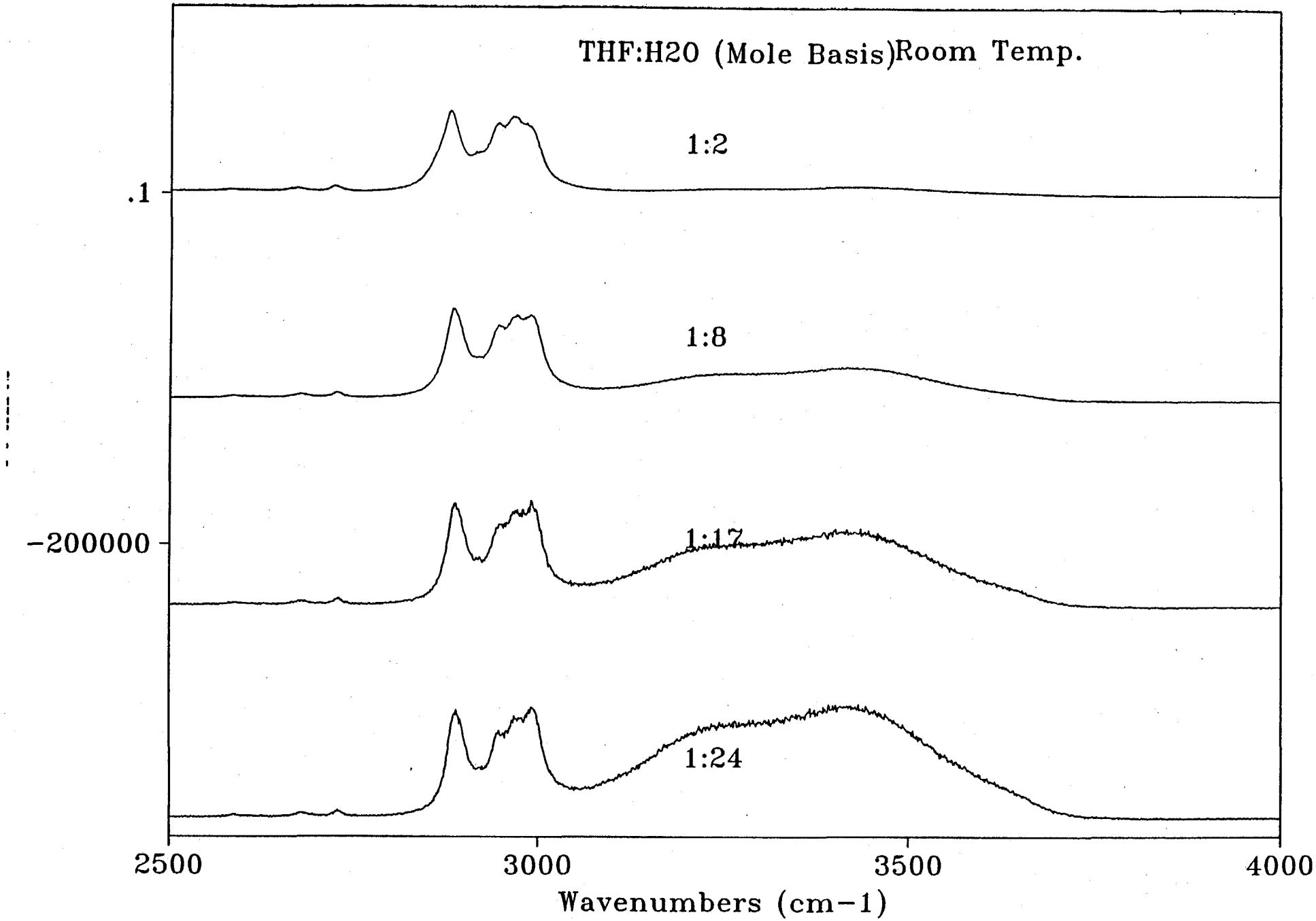

Figure 45 Raman spectra of THf+H20 solu. at diff. THF concentration

the pure THF solution, (2) the solution composed of 1 mole THF to 17 moles water, and (3)THF hydrates. As seen in Figure 46, 47, and 48, the effect of temperature has a strong effect on the degree of hydrogen bonding which effects the O-H stretching band region (3200 to 3700 cm^{-1}). The peak position of C-O-C symmetric stretching (~913 cm^{-1})is not a strong function of temperature.

We also performed polarization ratio and temperature effect experiments to determine the depolarization ratio of C-O-C symmetric and O-H stretch band.

IV.D.2. Experimental Results.

Our spectra demonstrate that when the THF+H2O solution crystallizes to form hydrates, there are obvious changes in both the vibration frequency of O-H stretching mode and the C-O-C symmetric stretching mode as shown in Figures 49 and 50 at 3200 to 3700 cm^{-1} and ~913 cm^{-1} respectively.

The hydrophilic interaction between THF and water in the liquid state induces very strong coupling interaction between hydrogen bonding of water with itself and hydrogen bonding of water with THF. The balance between hydrophobic interaction and hydrophyllic interaction encourages metastability before hydrate formation is initialized.

Once hydrates ar formed, the THF molecule is no longer bonded as strongly to water. Inside the cage the THF molecule can rotate similar to the free THF molecule in the pure liquid state rather than hydrogen bonded THF molecule in a liquid water mixture. There are very obvious features of lattice motion at

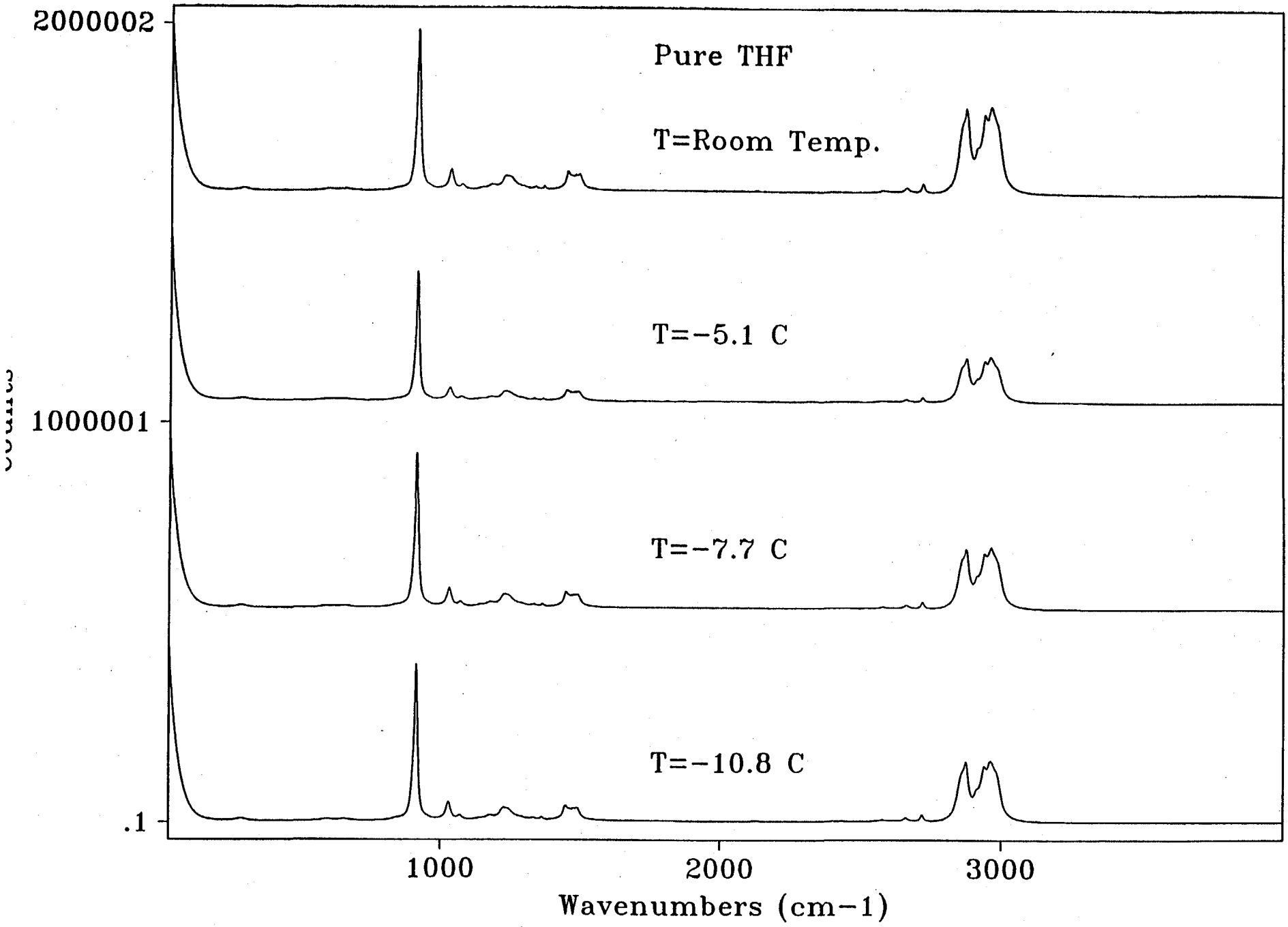

Figure 46. Raman spectra of pure THF at different temperatures

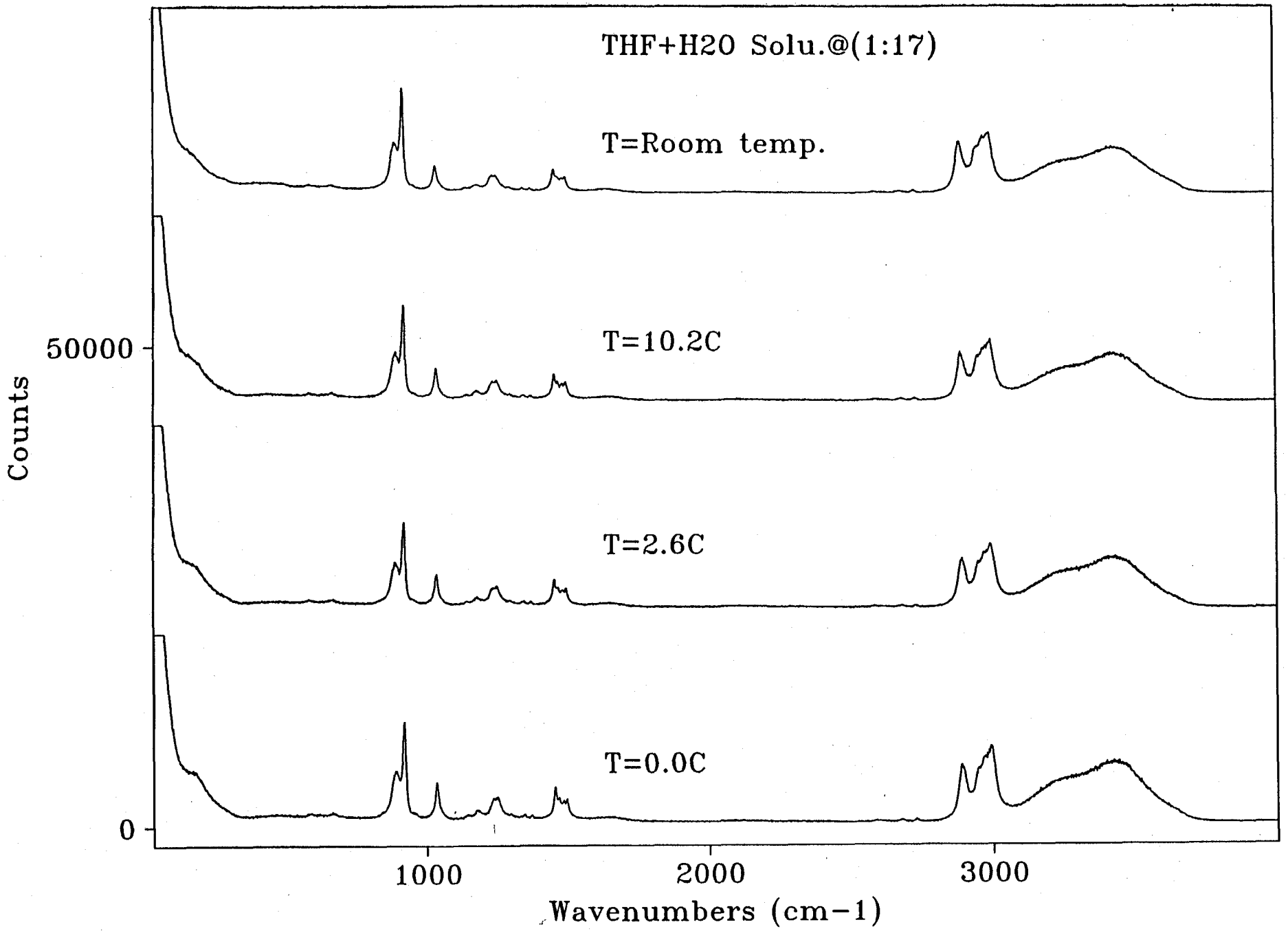

Figure 47. Raman spectra of THF+H20 solu. at diff. temp.

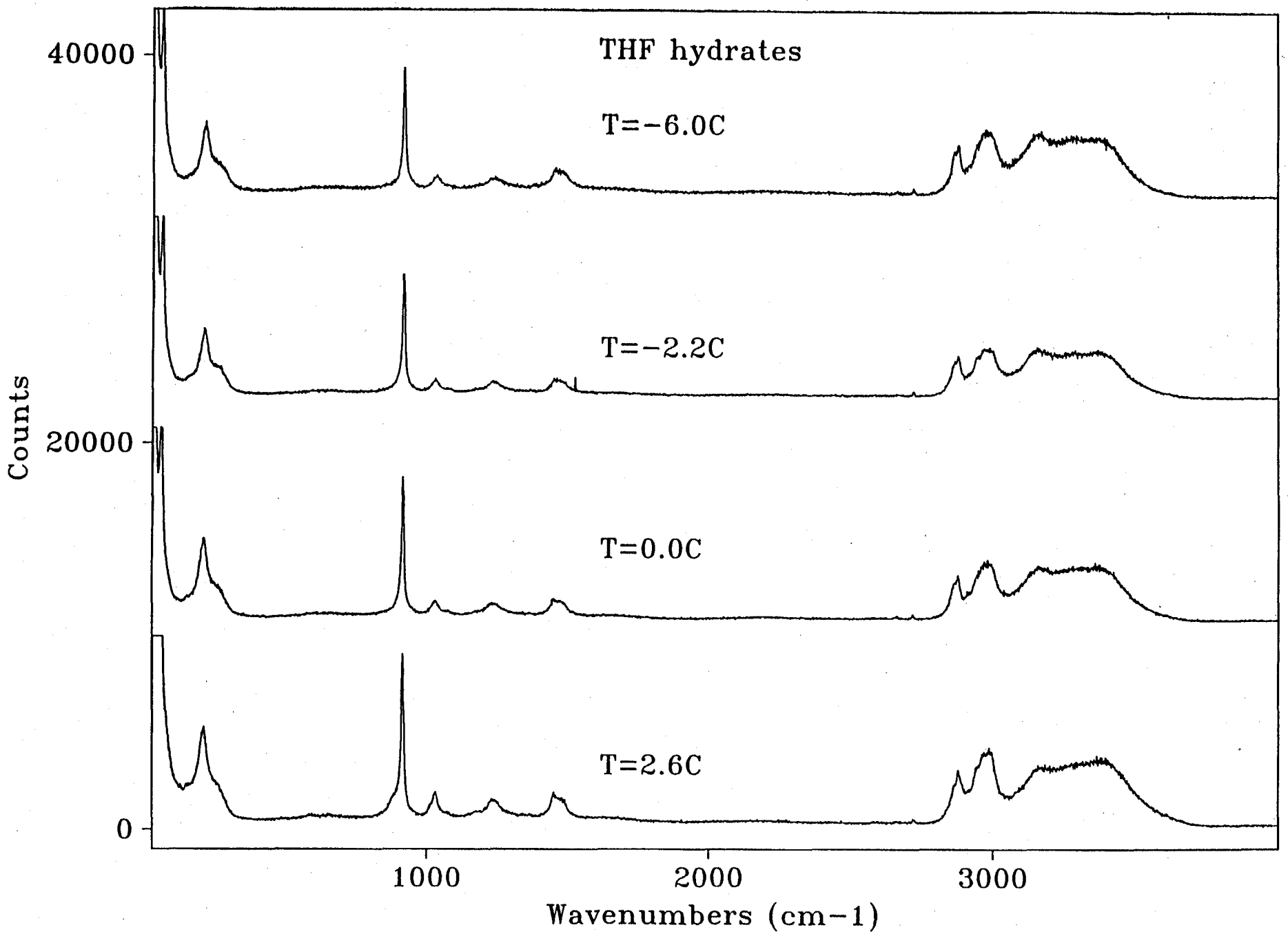

Figure 48. THF hydrates at different temperature

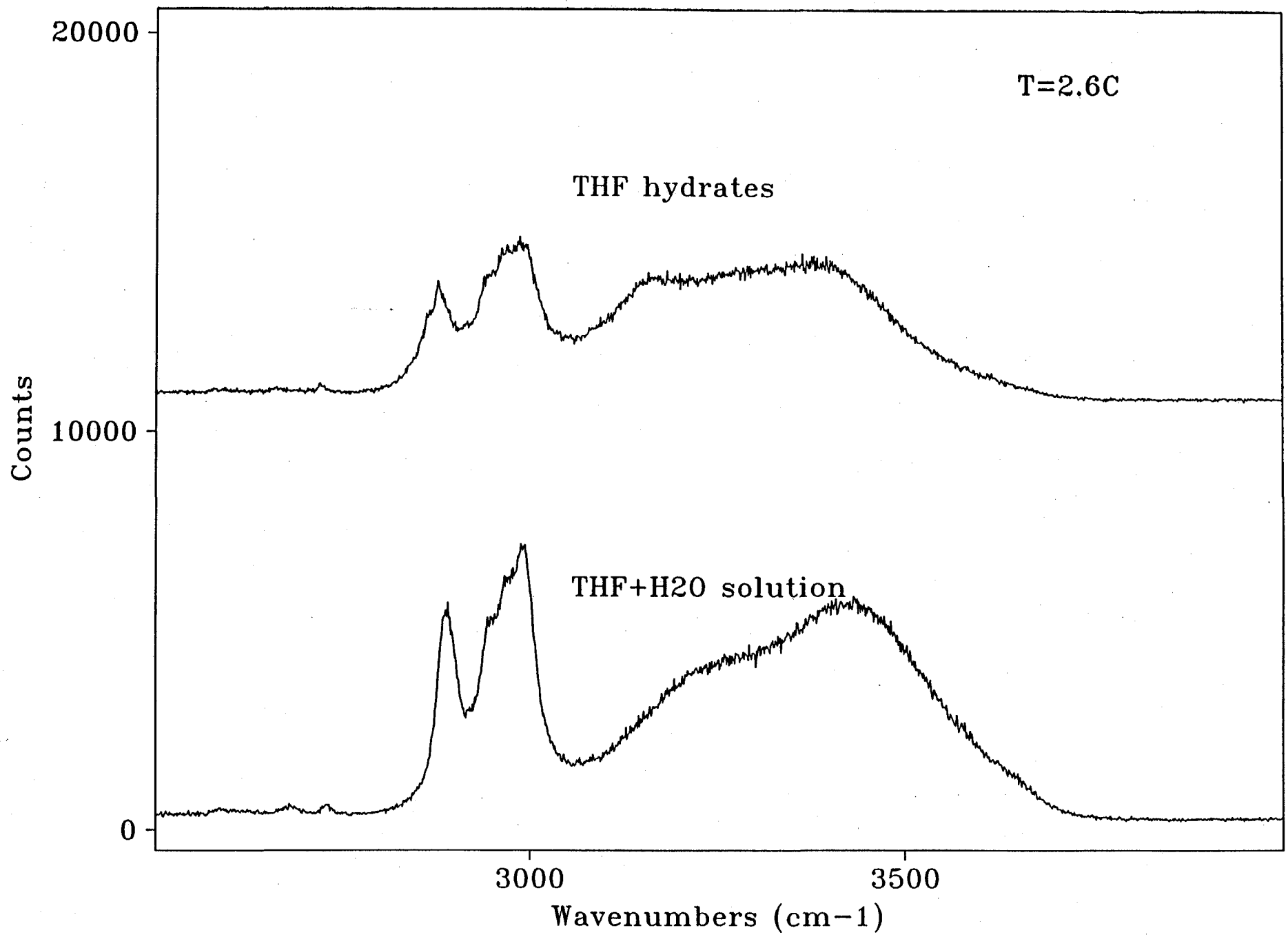

Figure 49. Intramolecular O-H stretching mode for both THF hydrates and THF+H20 solution

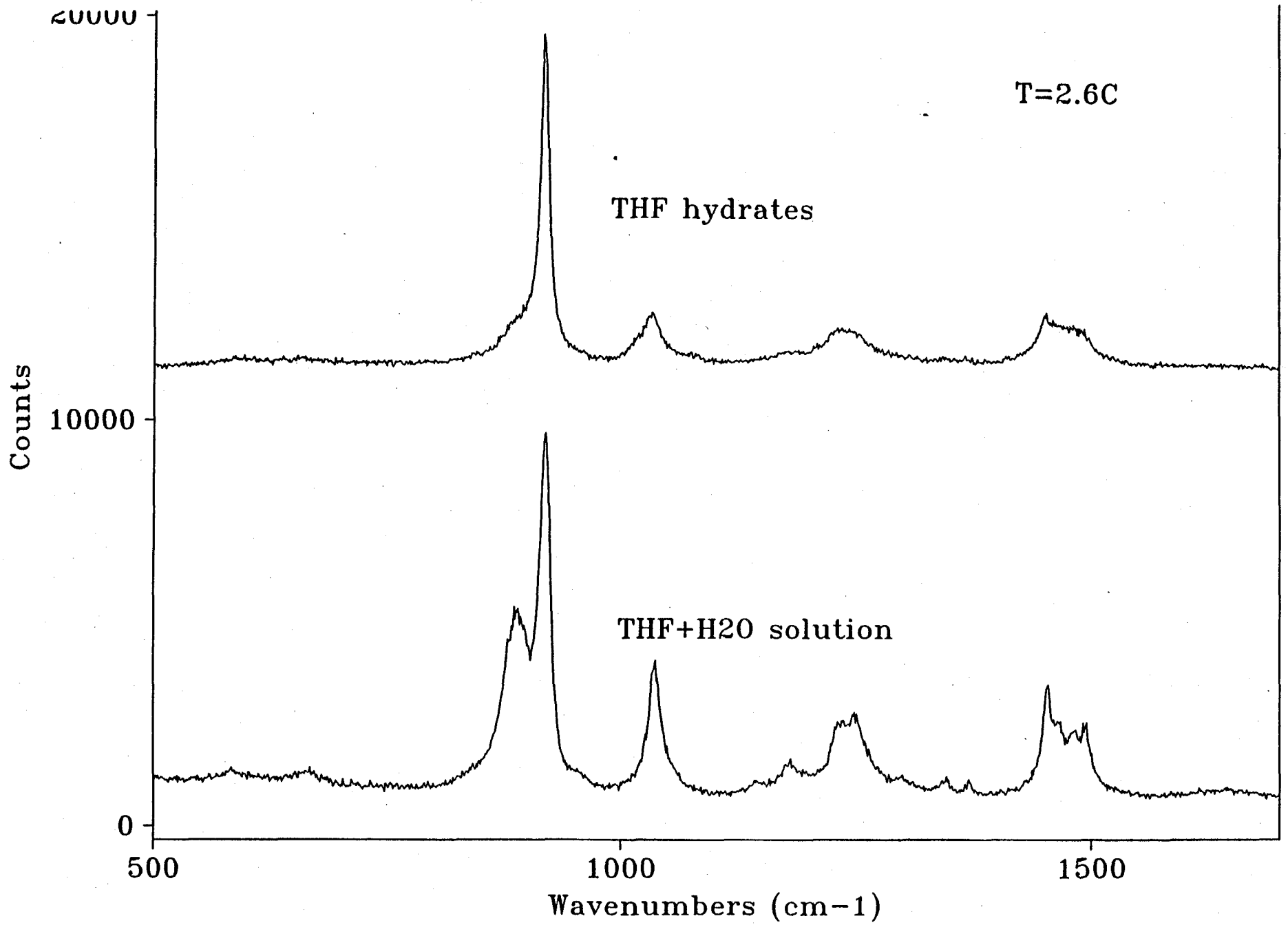

Figure 50. THF C-O-C stretching mode for both THF hydrates and THF+H20 solution

lower wavenumbers in Figure 51 which are shown around 67 cm^{-1} and 220 cm^{-1}.

Next we performed precise time measurements of the THF hydrate nucleation process. By using a fast scan Raman spectroscopy technique, we obtained what appears to be the first measurements of spectra during hydrate formation. Figure 52 shows the disappearance of a shoulder (at about 500 cm^{-1}) to the left of the largest intensity peak. Each of the 100 spectra in Figure 52 were obtained at intervals of 5 seconds, as hydrates form with a decrease in temperature from 5° to -5°C. These spectra suggest a quantifiable phenomenon as THF begins hydrate formation. These spectra were just performed at year's end and will be extended and fully interpreted in the imminent future. We will proceed to define THF hydrate formation spectra with inhibitors like PVP, as well as Raman spectra for methane, and perhaps Green Canyon gas hydrates.

V. PROJECTIONS FOR 1993

V.A. Continuing Work for Screening and High Pressure Testing

In order to understand PVP's inhibiting mechanism, we will test vinylpyrrolidone monomer and make the ring density the same as that in the polymer. In addition testing structure similar to PVP but without the ring is indicated by the behavior of PVP as a good inhibitor. From testing these chemicals, and a series of

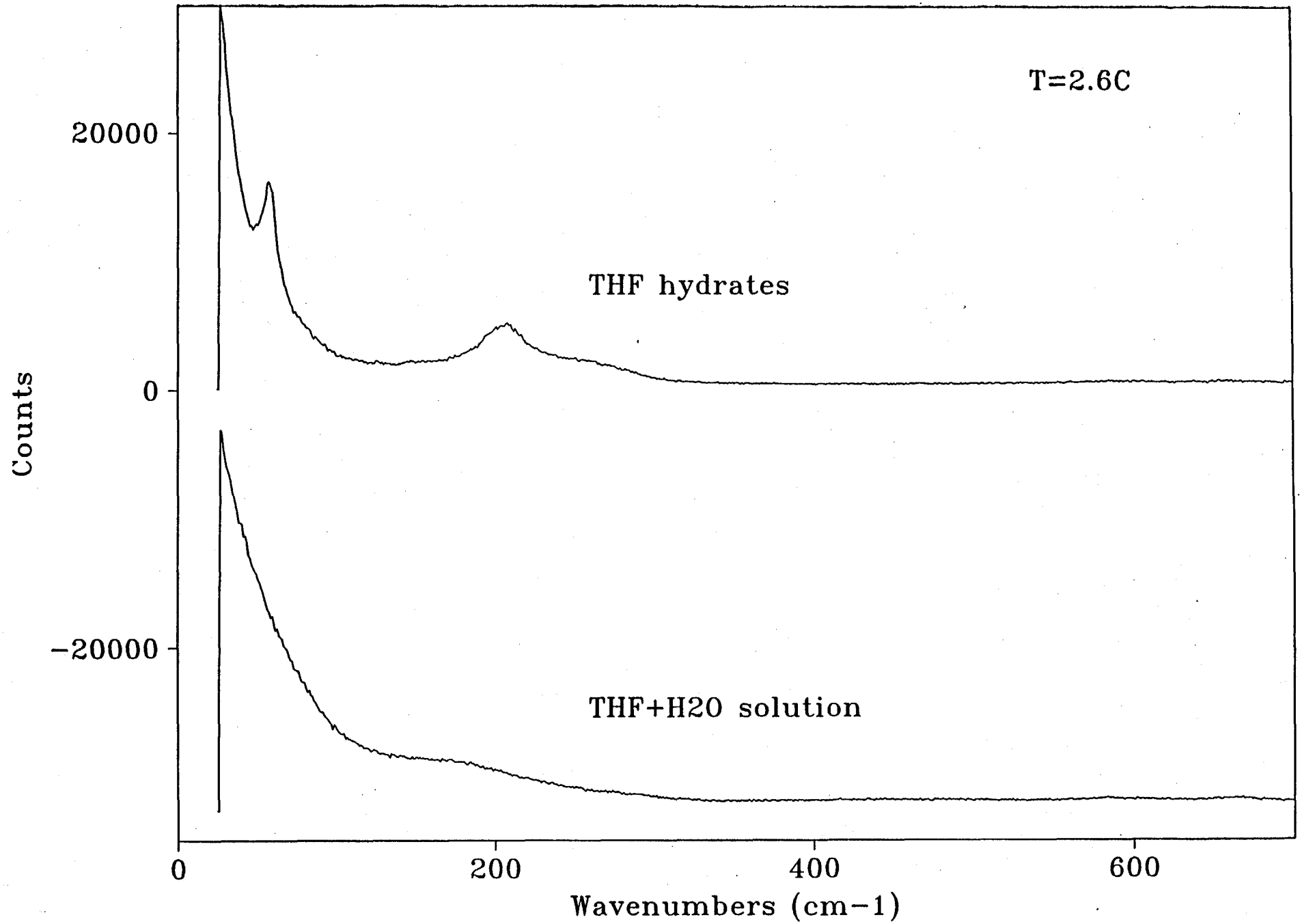

Figure 51. Intermolecular H--O--H stretching and bending mode both THF hydrates and THF+H20 solution

3D plot of THF+H2O system from THF solution to THF hydrates.

100 spectra at time interval=5 seconds

Figure 52. Time-Dependent Spectra for Formation of THF Hydrates on a Kinetic Scale

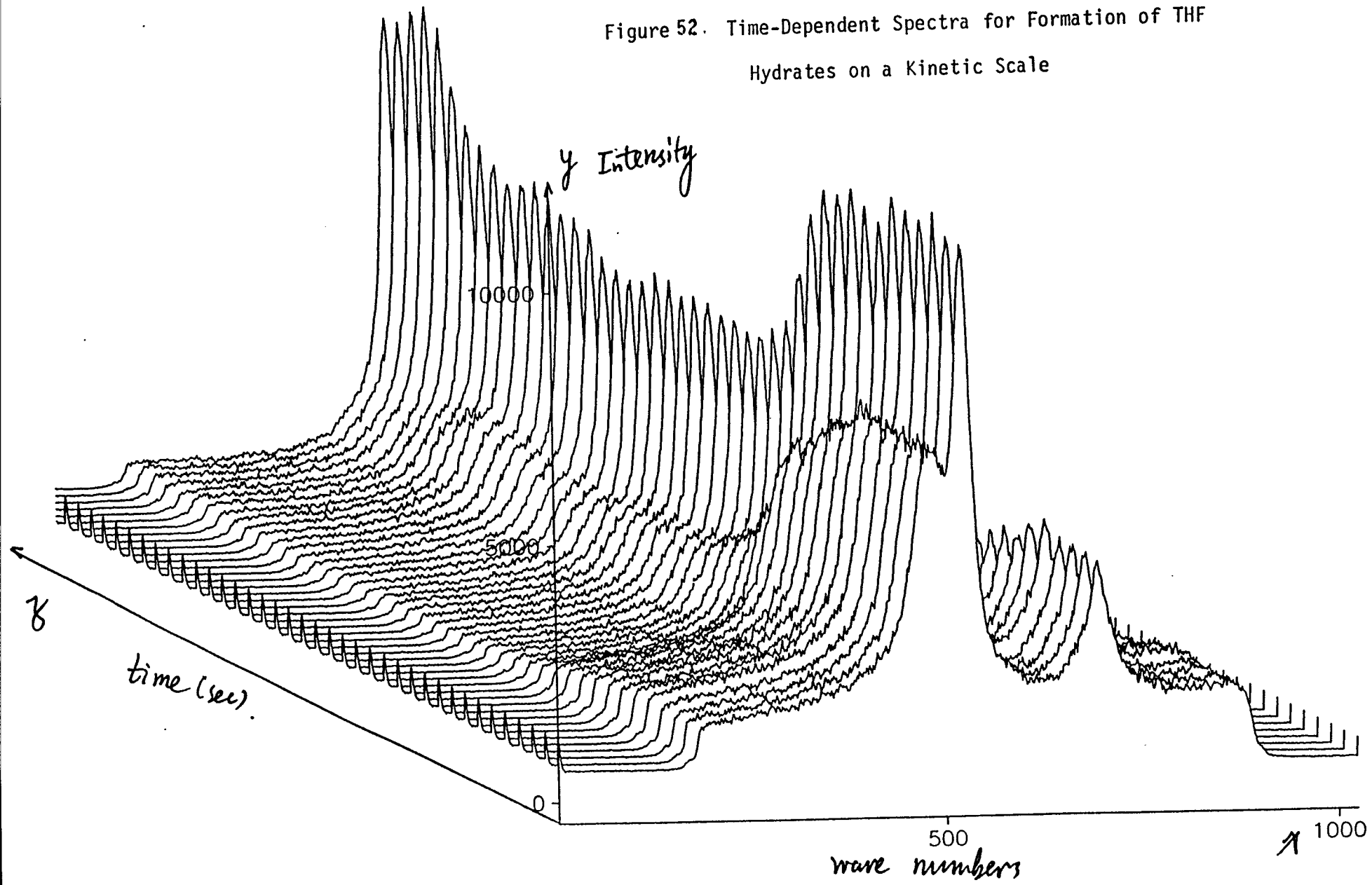

co-polymers, we can better determine the inhibition mechanism. After we finish testing the above chemicals, we can design some chemicals and perhaps synthesize some chemicals with specific structures.

During the coming year we intend to test many more chemicals both in the screening apparatus and the high pressure apparatus. The screening tests to date have given us three foundations for future tests, namely:

(1) the probability that there are a number of chemicals which can serve as good inhibitors,

(2) some general characteristics of good inhibitors, such as a five or six-member ring-substituted structure, as outlined in the screening apparatus section (IV.A.2.b), and

(3) the idea that success in the multiple reactor screening apparatus is necessary but not sufficient for success in the high pressure screening apparatus.

It is therefore our intention to define and obtain chemicals which will lead to a global optimum performance in kinetic inhibition. We will do this in concert with the advice of representatives from the Consortium, perhaps with the help of a chemical synthesis expert.

V.B. Simulation and Modeling of Inhibition Mechanisms

The combination of the multiple reactor screening apparatus and the chemical interfacial studies using computer simulation (see Section IV.C.) will enable us to determine hypotheses for

the mechanism of chemical inhibition. Once these hypotheses are stated, we can then probe them using both experimental and calculational techniques. The result will be the formulation of a set of heuristics for good inhibitor performance, perhaps stated in some mathematical model of an inhibition scheme.

V.C. Spectroscopic Measurements

It is our intention to extend and confirm the Raman spectroscopic experiments into the time-dependent regime for both THF and for methane hydrates during the coming year. We also have begun a set of FTIR experiments, which we hope to bring to fruition during the coming year. In addition Appendix B contains results from the Canadian National Research Council on NMR measurements for hydrate formation.

Of the three spectroscopic results on hydrate formation, it appears that the Raman instrument bears the most promise, and so should be pursued most diligently.

V.D. Other Possible Experiments

Since most of the high pressure experiments have been done in a blind cell, we have begun the construction of a sapphire, visual high-pressure cell. Visual observation may provide further information about the nucleation process.

To more closely simulate industrial situations, we are in the planning stages of constructing a 1 inch flow loop about one hundred feed long. The loop may be designed and constructed in such a way to simulate an industrial situation. In addition Exxon has graciously agreed to test the best chemicals from our system in their flow loop at Friendswood, just outside Houston. This will be done in parallel to the field tests indicated in the below section.

V.E. Field Tests and Reporting

During the 1992-1993 winter, many of the best chemicals indicated here will be tested in the field by several member companies. With two exceptions, every member company has agreed to such a test, perhaps done jointly with another company, and the results to be jointly shared. The two exceptions are (1) Shell, which wishes to participate via help with purchase of SYBYL, the chemical docking package (see Section IV.B.C.2) and (2) Exxon who will participate through the use of their flow loop in Friendswood, as indicated above.

While the majority of the work in this laboratory and its funding will not be affected by these field tests, the consortium meeting will be a convenient venue for the dissemination of results in the field to determine successful applications in various pressure and temperature regions.